Geoarchaeological investigations at Tiryns and Stymphalia (Peloponnese, Greece)

Dissertation

Zur Erlangung des Doktorgrades der Naturwissenschaften (Dr. rer. nat.) der Mathematisch-Naturwissenschaftlichen Fakultät der Christian-Albrechts-Universität zu Kiel

vorgelegt von

Thomas Birndorfer, M. Sc.

Kiel, 2021

Dekan: Prof. Dr. Frank Kempken

Erster Gutachter: Prof. Dr. Ingmar Unkel

Zweiter Gutachter: Prof. Dr. Hans-Rudolf Bork

Tag der Mündlichen Prüfung: 20.05.2021

Acknowledgements

First of all I would like to thank my first supervisor Ingmar Unkel, without whom this great project would not have been possible. I would like to thank you for your support and assistance to develop this research project. Thank you for giving me enough space to develop my ideas and guiding me in the right direction. I couldn't have wished for a better supervisor. Our numerus joint research trips to Greece in the last years were a great experience for me, thank you very much for that. I would also like to thank Hans-Rudolf Bork as my second supervisor for his excellent support during the field campaigns. Through your enormous wealth of knowledge, I now see the landscape and excavation sites with different eyes. I will miss our joint research trips and our dinners together at the tavern. Thank you both to meet always at eyelevel you were great colleagues.

A special thanks also goes to Sophia Dazert, who supported me during the lab work and who was always helpful with questions. I would also like to thank Kay Adam for the great collaboration and idea development when working and experimenting with the lab equipment. I would also like to thank Svetlana Khamnueva-Wendt for the great professional talks, the support and good cooperation during the field campaigns. Further thanks goes to Doris Kramer for the excellent pictorial illustrations that enriched my work. I would also like to thank our colleagues at Patras University Pavlos Avramidis, Alexandros Emmanouilidis and Eleni Zagana for the good cooperation. Furthermore, I would also thank Prof. Maran, who made it possible for us to work at Tiryns and was very kind in welcoming us to his excavation. Thank you for the great cooperation.

My last and special thanks goes to my family, without whom this work could never have been done. First and foremost my life partner Johanna Wischka, thank you for giving me so much strength and encouragement and Anton Wischka, only with your love and happiness I was able to accomplish this huge project. I would also like to thank my parents Brigitte and Josef Birndorfer who always support me on my way and made this great experience in my life possible.

Abstract

The imposing heritage of the Mycenaean culture and subsequent cultural periods is being studied in great detail through archaeological excavations in Greece. Statements about human-environment interactions are often made through written sources (Linear-B) from the respective periods. The analysis of geoarchives directly at or in the immediate vicinity of archaeological excavation sites represent the exception until today. Through geoarchaeological investigations in early settled landscapes it is possible to reconstruct the interventions of humans in the natural environment and to depict the natural development that has occurred as a result of these interventions. Accordingly, the investigations offer an enormous extension of the interpretation possibilities of a settlement context in former societies.

One of the most important Mycenaean fortresses is the palace of Tiryns, which can be considered as a central site in southern Europe already in the 3rd millennium BC. Archaeological excavations at the palace allowed to reconstruct economic and trade relations as well as the settlement system of the Mycenaean culture. Ongoing archaeological excavations on the related lower city of Tiryns also show settlement activity in the area while all other palaces in the eastern Mediterranean disappeared in the Late Bronze Age (Late Helladic Period). Another peculiarity was revealed during the excavations under the city area, river gravels were found in the inner courtyard of the houses. One of the aims of this dissertation is to reconstruct the environmental conditions and human-environment interactions in the Argolid region during the Late Bronze. The reconstruction of sedimentary conditions was carried out through sediment analysis and the attribution of fluvial architectural elements. The stratigraphy under the walls of the city showed cultural horizons and single flood periods, which were interrupted by phases of human activity. In addition to the reconstruction of a 150 years long period of river dynamics during the Late Helladic III period, the geoarchaeological investigations also made it possible to detect anthropogenic interventions in which a foundation was laid for the construction of the lower city.

Why the great palaces disappeared in the Late Bronze Age is still unclear. However, it is certain that the palace centres were supplied with agricultural

products from the surrounding countryside. Another aim of this thesis is to investigate the effects of land use, which lasted for thousands of years, on the soils of the north-eastern Peloponnese in the wider vicinity of important ancients sites like Mycene, Tiryns, Nemea and Corinth. For this purpose the valley of Stymphalia was intensively investigated as an exemplary study. A geomorphological and pedological survey was carried out in a raster covering the entire valley, in which the topography and the topsoils were analysed and classified. The evaluation of the soil quality was done by creating a classified soil quality index. The soil quality index includes the soil parameters of particle size distribution, organic matter, pH value, stone content, C/N ratio and the concentrations of calcium, potassium and magnesium. In order to record the soil genesis and degradation phenomena, selected soil profiles were analysed in detail. Large differences in soil quality were found, which can be attributed to degradation, triggered by human land use, as well as to geological conditions. High soil quality is especially evident in the centre and terraced sites of the valley. Except for the soils of the agricultural terraces, the investigations show a general decrease in soil quality with increasing depth. An average quality is shown by the soils in the east at Kaliani, while the quality of the topsoil in the west at Kastania is the lowest. The results show that in models for reconstructing the land use of prehistoric societies, soils have to be considered in a much more differentiated way and with a stronger weighting. Not only climatic extremes, social unrest or earthquakes can be responsible for a decline or demise of once advanced civilizations, but also soil degradation and exploitation have to be included in these considerations.

Zusammenfassung

Die imposanten Hinterlassenschaften der Mykenischen Kultur und darauffolgender Kulturepochen wurden und werden in Griechenland in großem Umfang durch archäologische Ausgrabungen detailliert untersucht. Aussagen über Mensch-Umwelt Wechselwirkungen werden oft durch schriftliche Überlieferungen (Linear-B) aus den vergangenen Epochen abgeleitet. Die Untersuchung von Geoarchiven im unmittelbaren Kontext zu archäologischen Ausgrabungen an frühen Siedlungsstandorten stellen in Griechenland aber bis heute die Ausnahme dar. Durch geoarchäologische Untersuchungen in frühen Siedlungslandschaften können die Eingriffe des Menschen in den Naturraum rekonstruiert werden und die naturräumliche Entwicklung, die sich seit der anthropogenen Landschaftsveränderung vollzogen hat, besser dargestellt werden. Die Untersuchungen bieten demnach eine enorme Erweiterung der Interpretationsmöglichkeiten des Siedlungskontextes in früheren Gesellschaften.

Zu den bedeutendsten Mykenischen Palästen zählt der Palast von Tiryns, der bereits im 3. Jahrtausend v. Chr. als Zentralort in Südosteuropa anzusehen ist. Durch die Ausgrabungen am Palast konnten Wirtschaftsweisen und Handelsbeziehungen sowie das Siedlungswesen der Mykenischen Kultur erfasst werden. Archäologische Ausgrabungen in der dazugehörigen Unterstadt von Tiryns zeigen eine fortwährende Nutzung des Areals, während alle anderen Paläste im östlichen Mittelmeerraum in der Späten Bronzezeit (Späthelladische Zeit) bereits im Niedergang waren. Eine weitere Besonderheit zeigte sich bei den Ausgrabungen in der Unterstadt, wo man im Innenhof einiger Häuser Flussschotter oberflächig anstehend antraf. Ein Ziel dieser Dissertation ist es anhand dieser Flußablagerungen, die in der Unterstadt von Tiryns dokumentiert wurden, die Umweltverhältnisse in der Späten Bronzezeit zu rekonstruieren. Dies erfolgte durch detaillierte Sedimentanalysen sowie der Zuweisung von fluvialen Architekturelementen. Die Stratigraphie unter den Mauern der Stadt zeigt Kulturhorizonte und einzelne Überschwemmungsphasen, die unterbrochen wurden von Nutzungsphasen. Neben der detaillierten Rekonstruktion einer 150 Jahre umfassenden Sedimentationsphase des Flusses in der Unterstadt während der Späthelladischen Periode (LH-III), war es durch die geoarchäologischen

Untersuchungen zudem möglich, anthropogene Eingriffe zu fassen, bei denen ein Fundament zur Errichtung der Unterstadt angelegt wurde.

Warum die großen Paläste in der späten Bronzezeit untergingen ist bis heute unklar. Sicher ist jedoch, dass die Palastzentren aus dem Umland mit landwirtschaftlichen Erzeugnissen versorgt wurden. Welche Auswirkungen die über Jahrtausende andauernde Landnutzung auf die Böden in der nordöstlichen Peloponnes in der Nachbarschaft zu bedeutenden antiken Städten wie Mykene, Tiryns, Nemea und Korinth hatte, ist ein weiteres Ziel dieser Dissertation. Dazu wurde das Tal von Stymphalia als Fallstudie im Detail untersucht. Es erfolgten einerseits bodenkundlich-geomorphologische Aufnahmen des gesamten Tales, in denen in einem Raster die Oberböden dokumentiert und anschließend analysiert wurden. Um die Bodengenese und Degradationserscheinungen zu erfassen, wurden andererseits an einigen ausgewählten Standorten Bodenprofile dokumentiert und analysiert. Eine anschließende Bewertung der Bodenqualität erfolgte durch die Erstellung eines klassifizierten Bodenqualitätsindexes. Der Index beinhaltet die Bodenparameter zur Korngrößenverteilung, organischen Substanz, pH-Wert, Steingehalt, C/N Verhältnis sowie den Konzentrationen an Kalzium, Kalium und Magnesium. Dabei wurden große Unterschiede der Bodenqualität festgestellt die sowohl auf Degradationserscheinungen, ausgelöst durch anthropogene Nutzung, als auch auf die geologischen Gegebenheiten zurückzuführen sind. Eine hohe Bodenqualität zeigt sich vor allem in der Mitte und an den Terrassenstandorten des Tales. Bis auf die Böden der Ackerterrassen zeigen die Untersuchungen eine generelle Abnahme der Bodenqualität mit zunehmender Tiefe. Eine durchschnittliche Qualität weisen die Böden im Osten bei Kaliani auf, während die Qualität des Oberbodens im Westen bei Kastania am geringsten ist. Die Resultate zeigen, dass in Modellvorstellungen zur Rekonstruktion der Landnutzung prähistorischer Gesellschaften die Böden wesentlich differenzierter und mit einer stärkeren Gewichtung betrachtet werden müssen. Es sind nicht nur Klimaextreme, gesellschaftliche Unruhen oder Erdbeben, die für einen Zusammenbruch einst blühender Kulturen verantwortlich sein können, ebenso müssen die Bodendegradation und Überbeanspruchung der Böden in diese Überlegungen miteinbezogen werden.

Table of contents

List of figures

List of tables

List of appendices

List of abbreviations

Ap	plough horizon
a.s.l.	above sea level
Bht	humus and clay accumulated in subsoil horizon
BC	Before Christ
BP	Before present
Bt	clay accumulated in subsoil horizon
Bv	weathered brownish subsoil horizon
Ca	calcium
cC	carbonate rich subsoil horizon
C/N	Carbon / Nitrogen Ratio
DFG	Deutsche Forschungsgemeinschaft
Fe	iron
K	potassium
LH	Late Helladic
LOI	loss on ignition
OSL	optically stimulated luminescence
PCA	principal component analysis
ppm	parts per million
pXRF	portable x-ray flourescnce
Rb	rubidium
Sr	strontium
TC	total carbon
TIC	total inorganic carbon
TN	total nitrogen
TOC	total organic carbon
Zr	zircon

1 Introduction

A decisive change in the development of the Greek culture occurred around 1.200 BC at the end of the Late Helladic (LH) IIIB phase, which brought about enormous societal changes in early Greece. The Mycenaean palace centers were destroyed and palatial political constructs no longer existed. The reasons for the decline of this advanced civilization are sought and discussed in dramatic climatic changes, political unrest and earthquakes (Drake, 2012; Maran, 2009). However, another possible driving factor, the aspect of land management, over-exploitation and soil degradation, is less frequently discussed. It is still unclear today whether the collapse of the Mycenaean culture as an economic system coincided with the collapse of the agricultural system (Isager & Skydsgaard, 1992). It is clear that the Mycenaean palaces were supplied with agricultural goods by the surrounding settlements (Knitter et al., 2019).

How much cultivated land was needed to supply the Mycenaean population in the Argolid with agricultural products was addressed by the work of Knitter et al. (2019).

While the palaces of Mycenae and Argos were destroyed in the Late Helladic period in Tiryns, a completely different development can be seen with the northern lower town being built and expanded (Maran, 2008). In order to build the lower town, a river was diverted, which had previously flooded the construction area. Until today it is still unclear to what spatial extent and how often floods occurred, how the people reacted to the floods and changed the landscape to use the area for settlement. It is currently assumed that one extreme flooding has occurred in connection with earthquake events (Zangger, 1994).

The excavations in the lower town enabled a close intersection of excavation findings and the investigation of a geo archive, as the fluvial sediments were uncovered directly below the walls of the city. In this work, the stratigraphy of the river sediments were presented and the paleoenvironment conditions during the Late Bronze Age will be reconstructed.

Preliminary work on land use and erosion processes was done by Fuchs et al. (2004) at Phlious, southwest of Corinth. In order to illustrate the effects of several millennia of land use, the polje of Stymphalia was investigated. The former city of

Stymphalia, next to Phlious, had its largest expansion and highest population in Hellenistic times. Several thousand people lived there during this cultural period, which shows the importance of the city. Detailed analysis of the soil quality in this old settlement landscape has not yet been carried out. This thesis shows the agricultural supply potential of the region at Stymphalia in order to serve Mycenaean palace centers beyond its own demands.

1.1 Aims and research questions

Initial geoarchaeological investigations in the vicinity of the acropolis of Tiryns were carried out by E. Zangger in 1994. The investigations showed that the lower city of Tiryns lay under several meters thick flood sediments. According to Zangger (1994), these deposits were formed by a single catastrophic flash-flood event, which served as a trigger for the people of the Late Bronze age to erect the dam of Kofini with a large artificial channel to redirect the river to the south of Tiryns. However, the results of the lower town excavation in the northern area of Tiryns indicate settlement continuity during the supposed flooding (Maran & Papadimitriou, 2006). The aim of the investigations in Tiryns is the reconstruction of the environmental conditions in the context of settlement activity during the Late Bronze Age. In the focus are the analysis of the fluvial depositional conditions and the elaboration of the stratigraphic sequence under the lower town of Tiryns. The reconstruction of the depositional conditions will be performed on the basis of sedimentological investigations and generally valid allocation of fluvial architectural elements. In order to determine possible effects of floods, the present work addresses the following questions:

- What was the extent of the floods? Is it possible to reconstruct the runoff behaviour, i.e. can sedimentation and erosion phases be identified?
- How was the floodplain area prepared for the building development? Have any special measures been implemented to take advantage of the floodplain?

The modelling on land use and required agricultural products at the former palaces of the Argolis, as well as the studies on soil erosion caused by land use in the neighbouring polje of Phlious, include hardly any studies on soil quality and yield capacity. The aim of the thesis is furthermore to investigate the effects of land use activities in the Stymphalia polje. In order to determine the consequences of long-term land use, the soil quality was assessed. Therefore, the following questions should be answered:

- How can the recent soil quality and thus yield potential be classified?
- In which condition are the soils after thousands of years of continuous land use activity by humans, i.e. are degradation characteristics visible?
- What potential does the region possess to produce beyond its own demand of agricultural products and to support Mycenaean palace centers?
- In this context, what is the significance of the terraced sites? Are there differences in soil quality at different sites?

1.2 Thesis outline

The first chapter describes the relevance of the research, its aims and research questions. Chapter 2 contains an overview of the natural environmental conditions of both study areas Argolid and Stymphalia, including the geological setting, climate, pedology as well as the vegetation and land use of the areas. Chapter 3 is divided into two main parts: the first one focuses on the settlement history in the Argolid, with a special focus on the lower town of Tiryns, the dam of Kofini, the late quaternary alluviation and soil erosion processes. The second part describes ancient Stymphalos, and gives an overview on the general context of agriculture practices and agricultural terraces in Greece. The fourth chapter is dedicated to the methodology of the study. The field work in which a geomorphologic survey was conducted at Stymphalia is described as well as, the special sampling procedure at Tiryns. Furthermore, the laboratory methods and the compilation of

the soil quality index are explained. In chapter 5 the results from Tiryns and Stymphalia are presented. The stratigraphic sequence of the fluvial sediments under the lower town and the anthropogenic application horizon are presented. In the second part of the results chapter, the soil profiles documented and sampled in Stymphalia are presented. Subsequently, three transects were illustrated that were created in the polje. A combination of the soil profiles with the sediment samples of the topsoil in the polje as well as the classification of soil fertility and degradation status will follow. In chapter 6, in the results from Tiryns are interpreted and discussed with special respect to the environmental conditions in the postpalatial period. The second part of the discussion is dedicated to the evaluation of soil quality and degradation phenomena in Stymphalia. In particular, the soil profiles and samples of the soil sediments of the polje are evaluated with regard to their condition. This is followed by a description of limiting factors such as soil reaction, soil nutrients and soil degradation that affect soil fertility. The last part of the discussion focuses on how soil properties can be integrated in modelled land use scenarios at Archaic and Hellenistic times from a geoarchaeological point of view. Chapter 7 provides a summary of the conclusions.

2 Geographic setting

Tiryns is located in the southern Argolid, the shallowest part of the Argive Plain on the Eastern Peloponnese (figure 1). The Argolid is divided into three different physiographic units: the northern part is characterized by hills consisting of massive limestones. The second part is built of alluvial fans lying at the foot of steep bedrock slopes, which surrounding the entire plain. The third part of the alluvial plain spreads from the coastline up to the alluvial fans surfaces (Pope & van Andel, 1984; Zangger, 1993). The second research are the polje of **Stymphalia** is located in the north-eastern part of the Peloponnese in the mountainous region. The polje lies on the south side of the Mt. Kyllini/Ziria limestone massif, with its hydrological catchment ranging from 2.257 m a.s.l. to the level of the lake at 600 m. a.s.l. The topography is orientated southwest to northeast. Steep slopes are situated in the south of the polje, while in the north the terrain is only slightly sloping (Morfis & Zojer, 1986; Walsh et al., 2017).

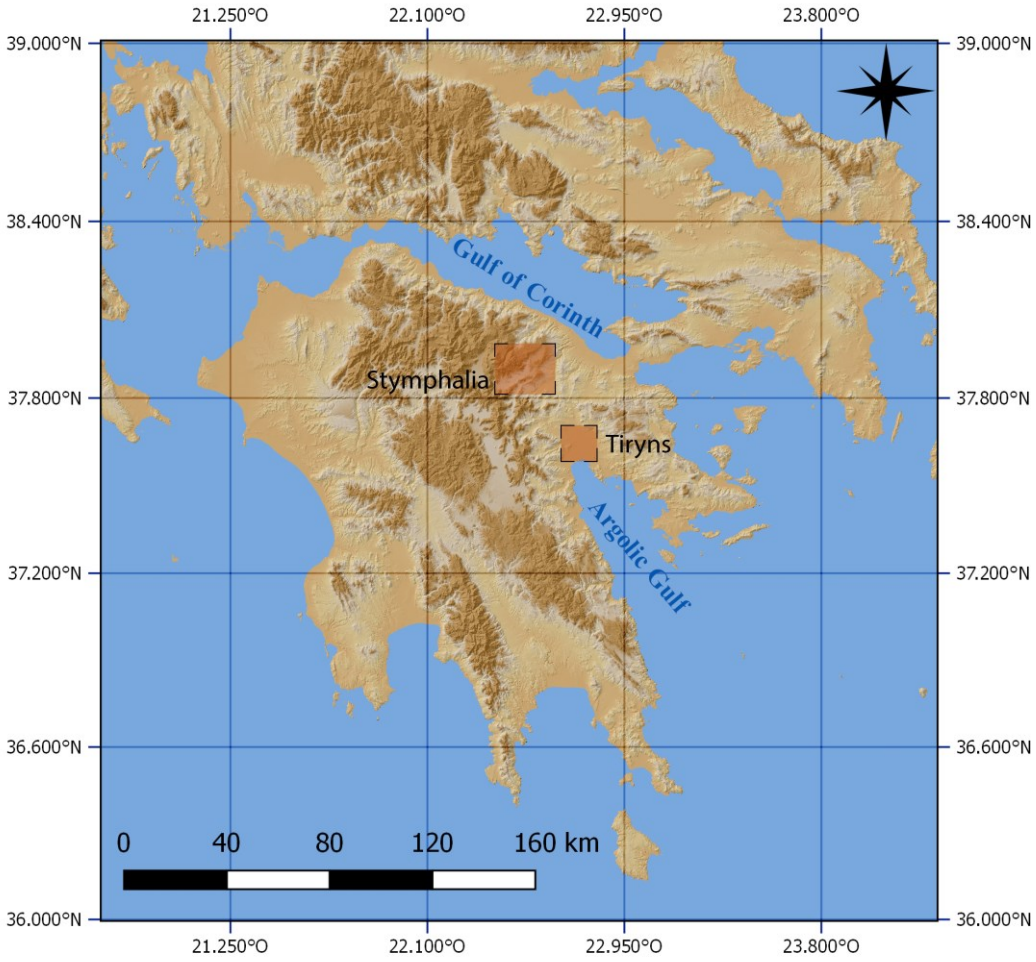

Figure 1: Research areas at Tiryns and Stymphalia on the Peloponnese.

2.1 Geological structure

The **Argolis** was formed by several tectonic events: Mesozoic rifting, passive margin evolution, ophiolite emplacement by middle Cenozoic-to-present normal faulting and arc volcanism (Robertson et al., 1991). These tectonic events are related to the movements of the Eurasian and African Plate. The subduction of the African Plate below the Eurasian and the Aegean Plate resulted in the tectonic deformation in the region (Kokinou et al., 2005). The geological structure consists of folded and tectonically fractured thrust sheets stacked during the Alpine orogeny. The stratigraphy shows at the bottom a basal 1.700 m thick Upper Triassic-Upper Jurassic Lower Unit, which is composed of Pantokrator Limestone (ca. 1.000 m thick), overlaid by the Kimmeridgian to Tithonian greenschist facies of the Potami Formation (ca. 700 m thick). The Middle Unit is built of Albian-Cenomanian to Paleocene Middle Eocene carbonate sequence (ca. 100 m thick) overlaid by post-Early Eocene continental flysch deposits (< 200 m thick). The Upper Unit is composed of an Upper Jurassic ophiolitic melange (< 100 m thick) capped by a Middle Cenomanian to Middle Maastrichtian carbonate sequence (ca. 300 m thick), covered by Middle Turonian to Middle Maastrichtian ca. 40 m thick pelagic sediments (Hinojosa, 2016; Photiades, 2017). The outcropping bedrock in the western Argive Basin (figure 2) is dominated by folded tectonically fractured and highly weathered limestones and continental flysch deposits (Hinojosa, 2016, Tataris et al., 1970). During the Pliocene, the first sedimentation on the basis of seasonal river flows started. As a result, conglomerates and sandstones, sandy marl and consolidated marls were deposited (Maroukian et al., 2004; van Andel, Zangger, & Perissoratis, 1990). The Quaternary deposits include a solidified Pleistocene sequence of more than 20 m thick marine clays, sands, silts, and gravels followed by alluvial terraces (Hinojosa, 2016).

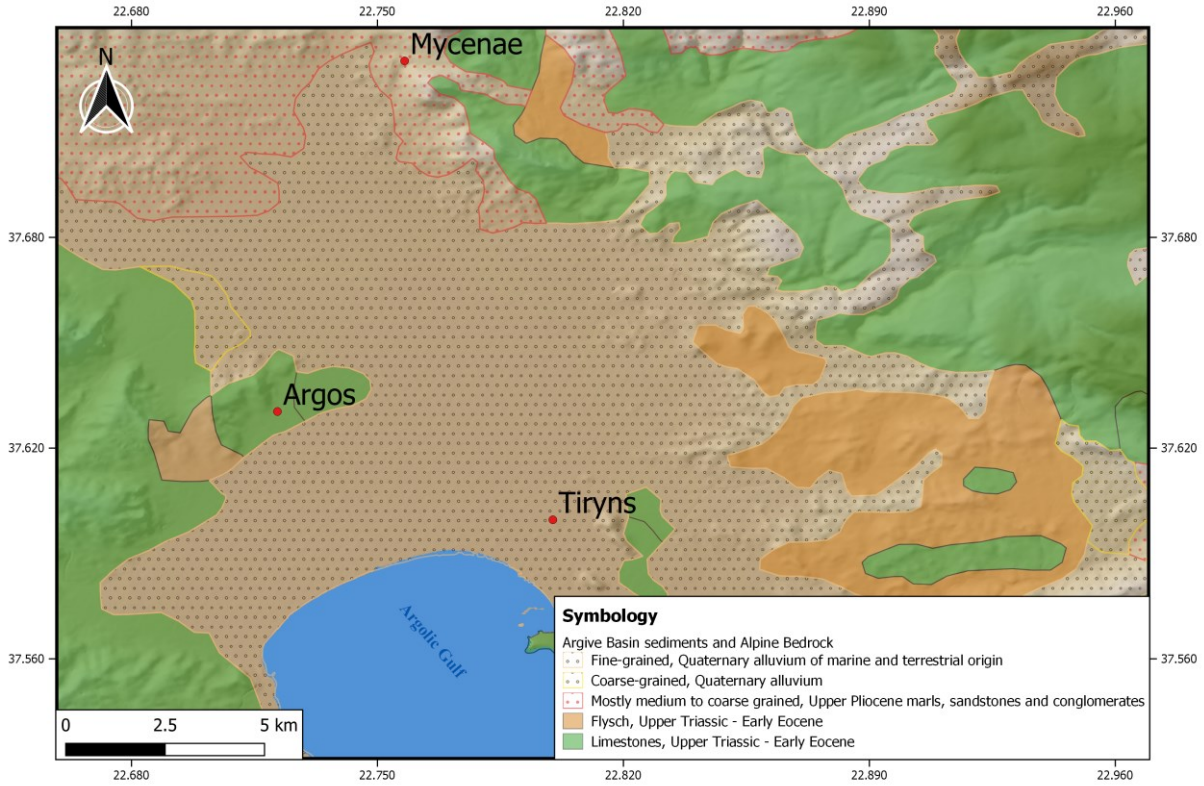

Figure 2: Simplified geological map of the Argolis (after Tataris et al., 1970).

Four geological units characterize the **Stymphalia** region (figure 3). A Phyllite-Quarzite unit, which consisting of very compact quarzites and mica schists. This unit is overlaid by the Tripolis nappe, which can be divided into phyllites and schists from the Tyros layer. Near Kastania these phyllites are often accompanied by andesites were they can reach a thickness of about 200 m. The following Tripolis limestone was deposited during the Upper Trias until the Eocene. These massive light grey to blackish limestones are well karstified (Morfis & Zojer, 1986; Vött et al., 2009). The last geological sequence, the Tripolis flysch, consisting of calcareous marls (formed until the Miocene). The uppermost geological nappe is the Olonos-Pindos unit, which contains pelagic sediments (limestones, radiolarites and marls) of the Middle Triassic to the Eocene age. The northern and eastern areas of Mount Ziria are covered by fluviatile and lacustrine conglomerates of the Plio-Pleistocene age. The conglomerates, which reaching a thickness about 500 m at Kefalari (Cornithia), consist mainly of limestone gravels grouted by calcareous cement.

Such conglomerates are also found near Drosopigi, although it is not clear whether they were formed jointly. The last unit are Late Pleistocene and Holocene deposits representing the filling of the polje. They reach a thickness of about 150 m, containing red, grey and greenish lacustrine clays (Morfis & Zojer, 1986).

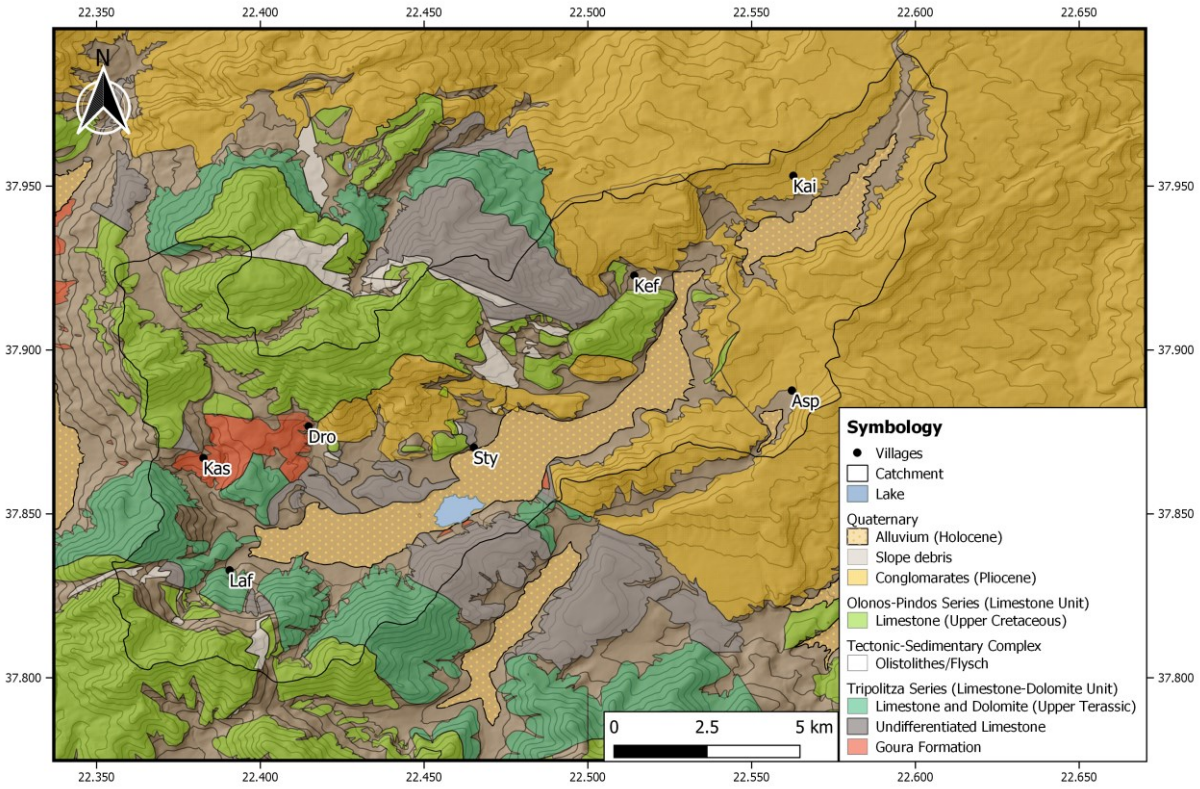

Figure 3: Geological map of the Stymphalia polje (Peloponnese, Greece) depicting the catchment and villages of the area. Villages: Kas = Kastania, Dro = Drosopigi, Sty = Stymphalia, Kef = Kefalari, Kai = Kaisari, Asp = Asprokampos (adapted after Morfis & Zojer, 1986).

2.2 Climate

The Peloponnese is located in the subtropical climate zone, whose periphery reaches the arid areas of North Africa as well as the area of Southern Europe, which is dominated by the west wind drift (Xoplaki et al., 2003). The subtropical winter rain climate is characterized by two ecological stress factors: an excessive summer drought and a pronounced precipitation variability (Xoplaki et al., 2003). The Eastern Mediterranean climate is affected by the South Asian Monsoon during summer and the western Russian/Siberian High Pressure System in the winter (Roberts et al., 2012). Additionally influenced by the topography, Greece can be divided into four climate regions: the central mountain area, Northern Greece, the West coast and the Eastern and Aegean islands (Morfis & Zojer, 1986). The North Atlantic Oscillation (NAO) affects the precipitation and temperature during winter periods in (Southern) Greece. If there occurs a positive NAO, it will by cooler and drier. A negative NAO leads to warmer and wetter conditions. The implications from the NAO on temperatures during the winter in Greece occur on a decadal scale (Finné et al., 2014).

The precipitation on the Peloponnese decreases from west to east and from north to south (Xoplaki et al., 2000). The mean annual precipitation ranges from 400 mm in Athens to 1352 mm at Kérkira. The precipitation reaches its maximum in the western part of Greece, triggered by moist air advection from the west and orographic uplift mechanisms due to the Pindos mountain chain and the Peloponnese mountains. The winter precipitation is at its maximum at most stations in November and December. The lowest precipitation values are recorded in the leeward rain shadow, on the eastern Greek islands, and the Ionian Sea (Xoplaki et al., 2000, Haversath J. -B., 2004).

The mean annual precipitation measured at the meteorological station at Driza-Stymphalia (figure 4) is about 618 mm, which is based on the data recorded form 1950 until 2011 (Seguin et al., 2019).

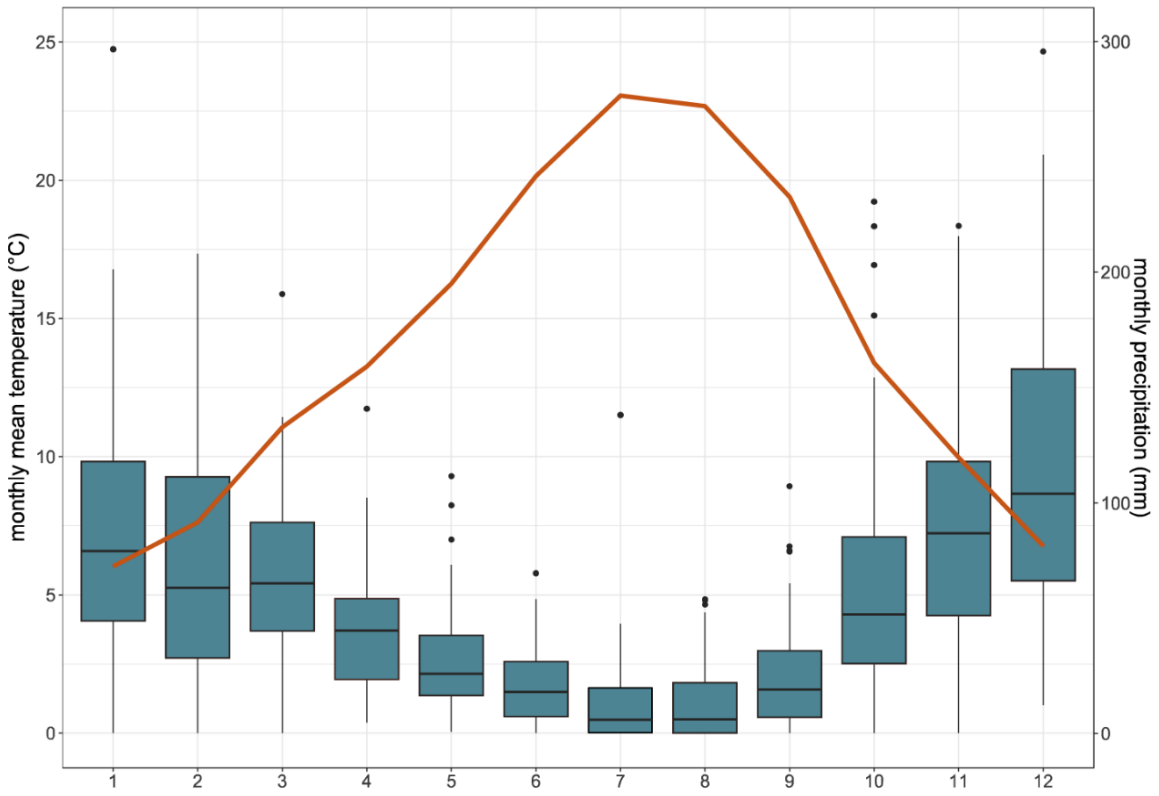

Figure 4: Climate diagram of the weather station Driza-Stymphalia for the period 1950-2011. The mean monthly temperature (orange line) and the precipitation (boxplots) shown form January (1) to December (12) (source: adapted after Seguin et al., 2019)

2.3 Soils

Due to climatic and geological conditions, the following soils may predominate in the study area: Soils developed on hills and mountains can be subdivided into soils on Mesozoic limestones, soils on schists and soils on flysch. Colluvial soils are dominating, as well as soils on artificial terraces, soils on alluvial deposits and soils developed on clay deposits and conglomerates. According to the classification of the world reference base for soil resources Leptosols, Fluvisols, Luvisols and Regosols (table 1 and 2) are prominent in the research area today (Panagos, 2006; Yassoglou et al., 2017).

The genetic horizons of soils developed on limestones in their climax stadium are on top the organic horizon under forest, Al-organic matter-enriched mineral surface horizon, Ae-eluvial horizon, Bt-illuvial horizon and C-semi-decomposed limestone parent material and R-undecomposed limestone rock. The

characteristically red coloured Bt-horizon identifies these soils as Rhodoxeralf (formerly known as "Terra Rossa")(Yassoglou et al., 2017). In Greece, there were formed two type of red soils: the autochthonous and the soils formed on soil sediments, which are linked to the thermos-Mediterranean, meso-Mediterranean and sub-Mediterranean bioclimatic zones. The Bt-horizons of these soils having the highest amounts of dithionite extractable iron oxides, whereas the soils formed on sediments on Pleistocene and Late Pliocene terraces having the lowest amounts (Yassoglou et al., 1997). The clay distribution reaches its maximum in the B-horizons and the pH value ranges from the slightly acid to neutral. The favourable pH and high organic matter content in the A-horizons as well as the availability of plant nutrients (total N, extractable P, Fe, Zn and Cu, exchangeable K, and Mg) indicate that these soils can be very fertile (Boero & Schwertmann, 1989; Yassoglou et al., 2017).

Soils on mica schist are very loamy and sandy loamy in texture and therefore having a greater water retention capacity. Their pH, base saturation and the horizontal development depend mainly on the influence of carbonates originating from the neighbouring marble and limestone. Soils on mica schist are moderate in their potential biomass productivity and therefore suitable as forestlands, on steeper slopes and as controlled pasture on lower slope open lands (Nakos, 1979; Yassoglou et al., 2017).

Due to its parent material soils on flysch are highly susceptible to erosion. The soil characteristics are depending on the composition thickness or proportion of the layers in the parent rock. The soil texture on slate appears as sandy clay loam or clayey. The climax soil derived from flysch and developed an Alfisol (Luvisol) with chromic argillic horizons. Above 1.000 m a.s.l. a argillic horizon can develop with a dystric character belonging to leaching bases (Yassoglou et al., 2017).

Soils developed on Tertiary or Quaternary clays and conglomerates are usually classified as Inceptisols (Cambisols). These soils are showing a moderate fine (clay loam, sandy clay loam) or fine (clay, silty clay) texture and developed moderately deep (soil depth 60-100 cm) to very deep (soil depth > 150 cm). They often include inorganic carbonates in the whole soil profile, but this is not the case for soils in which pedogenic processes were active for a long period. Yassoglou et al. (2017) point out that soils developed on clay deposits and conglomerates are presenting

moderate to severe limitations for agricultural use. As the most limiting factors the soil depth, presence of rock fragments and the slope gradient are described and characterized as moderately productive soils.

Soils developed on Holocene Alluvia represent the most productive soils. In Greece, soils on alluvial deposits are separated by their formation time into soils formed up to 2.000 years ago and soils formed in the last 2.000 years (Yassoglou et al., 2017). The most wide-spreading soil types in this context are Fluvisols or Xerofluvents. These soils are characterized by a fine texture, friability and a good hydraulic permeability. Furthermore, they are highly susceptible to weathering processes, solid and produce enough organic matter (Yassoglou et al., 2017).

Soils on artificial terraces are distributed on hillslopes, where they are protected by erosion. They formed on residual soils as well as soil sediments. The soil genesis is often difficult to comprehend, because the soil sediment was transported from surrounding areas, mixed and artificially placed into the terraces. Properties and soil-forming factors depending on the age of the terrace, the type of vegetation and the land management practices. The last point in particular involves a lot of uncertain and variable effects on these soils for example the planting of certain crop species, adding how much and which kind of fertilizer, and the amount of irrigation (Yassoglou et al., 2017). More detailed explanations of agricultural terraces are given in chapter 3.

Table 1: Attribute table of the mapping units of the 1:500.000 soil association map of Greece (Yassoglou et al., 2017)

Soil reference group	SMU	Dominant soil typological unit STU	Associated STU	Soil quality	Desertification vulnerability	Sustainable agronomic uses	Restrictions for non-agronomic uses
Leptosols	2	Calcaric Leptosol (PLca)	Calcaro-leptic Regosol; Calcaro-petric Cambisol; Rock outceops	Low	Very high	Wild nature	Weak
Regosols	9	Calcaric Regosol (RGca)	Calcarochromic Cambisol; Calcaric Leptosol; Rhodic Luvisol	Low	Very high	Forest, controlled pasture, wild nature	Moderate
Fluvisols	19	Calcaric Fluvisol (FLca)	Calcaric Cambisol, inclusionsof Solonchak in some cases	Very high	Low	Agriculture	Very strong
Luvisol	36	Chromic Luvisol (LVcr)	Haptic Calcisol; Calcaric Regosol	High	Medium	Controlled agriculture and pasture, forest	Moderate

Table 2: Soil association map of Greece (Yassoglou et al., 2017)

Soil order	Soil mapping unit (SMU)	Dominant soil typological uni (STU) FAO	Associated STU FAO	Dominant soil taxonomic unit (Soil Taxonomy)	Associated taxonomic units	Parent material
Lithosols	2	Calcaric Lithosol (Ic)	Calcaric Regosol (Rc), Caclcarochromic Cambisol (Bcc)	Lithic Xerorhtents	Lithic Xerochrepts	
Regosols	9	Calcaric Regosols (Rc)	Calcaric Cambisol (Bcc); Calcaric Lithosol (Ic); Rhodochromic Luvisol (Lcr)	Typic Xerorthents	Typic Xerochrept; Lithic Xerorthents; Typic Rhodoxeralfs	Limestone
Fluvisols	19	Calcaric Fluvisol (Jc)	Fluvi-calcic Cambisol (Jkf)	Typic Xerofluvents	Fluventic Calcixerollic Xerocherpts; Calcixerollic Xerochrepts	Holocene alluvium
Luvisols	36	Chromic Luvisol (Lc)	Calcic Cambisol (Bk); Calcaric Regosol (Rc)	Rypic Haploxeralfs	Calcixerollic Xerochrepts; Vertic Xeralfs	Unconsolidated Tertiary deposits

2.4 Vegetation and land use

Both the Argolid Plain and the Stymphalia basin having an exceptionally high agricultural use, which is due to the prevailing fertile soils. The original forest cover before the onset of human land-use activity depended on the climatic conditions. On the one hand, xeromorphic plants grow on them, on the other hand the climate allows evergreen plants growing (Haversath, 2004). In the Stymphalia polje the lake is covered by dense reed beds of *Phragmites australis*, only few parts of open water are left. Near wetter areas the tree species, *Silax alba* and *Populus alba* are present (Papastergiadou et al., 2007). On many slopes Phrygana shaping the landscape, species like *Quercus coccifera*, *Pistacia lentiscus* and *Cistus spp.*, and on the boreal areas endemic species like *Abies cephalonica* are dominating (Papastergiadou et al., 2007). On the other hand, the vegetation on slopes and plateaus is formed by *Pinus halepensis*, *Pinus pinea* and *Cupress sempervirens* (Haversath, 2004). Due to the relatively cool climatic conditions related to an altitude above 600 m a.s.l., neither wine, olives nor citrus fruits can be cultivated in the Stymphalia basin. Mainly cereals such as oats are grown, but also walnuts, onions, tomatoes, potatoes, almonds and honey are cultivated. This contrasts to the alluvial plain of the Argolis, where citrus fruits are mainly cultivated due to suitable climatic conditions.

3 Research History

3.1 Tiryns

Tiryns is located in the shallowest part of the Argive Plain. The acropolis of Tiryns lies about 1.8 km from the present coast of the Bay of Nauplion on top of a rocky outcrop (figure 6).

3.1.1 The settlement history in the Argolid

The Mycenaean culture appeared first in the late Bronze Age with the beginning of the prepalatial period (Late Helladic - I/II, ca. 1650/1600-1400 BC; table 3). It flourished in the palatial period (LH IIIA/B, ca. 1400-1200 BC) and had its decline after the postpalatial phase (LH III C, ca. 1200-1050 BC) (Hinojosa, 2016; Mühlenbruch, 2009). The beginning of the Mycenaean cultural development is marked by the shaft grave round A exposed in the year 1876 by H. Schliemann. Hence, Mycenae located in the north-eastern part of the Argive plain, become eponymous for the culture spread throughout central and southern Greece (Ruppenstein, 2012). In the period from 1.400 to 1.200 BC (LH IIIA/B), the Argolis was the centre of the Mycenaean culture with the concentration of palace centers like Mycenae, Tiryns, Argos and Midea (Brysbaert, 2015). As many archaeological sites also the Acropolis of Tiryns was repeatedly chosen for settlements locations. The settlement history already began in middle Neolithic Times (ca. 5.900-5.400 BC). Due to earlier excavations and partial destruction of the find complexes, it is not clear today how long Tiryns was inhabited (Cline, 2012). The excavations of many years revealed a complex building architecture and different phases of the palace (Hinojosa, 2016; Kilian, 1983, 1988; Maran & Papadimitriou, 2006; Schliemann, 1886). These complexes contain the Lower Citadel in the north, the Upper Citadel in the center of which the Great Megaron is located, and the East and South Galleries built on the eastern and southern flanks of the ridge (Hinojosa, 2016).

The proximity to the sea, but also evidence of trade relations underline the importance of Tiryns as a major Mediterranean harbour during the Bronze Age. Furthermore there are three periods during which Tiryns had an outstanding

significance: during the later part of the Early Helladic II period (EH II, ca. 2.500-2.200 BC) and during the Mycenaean Palatial (ca. 1.400-1.200 BC) and postpalatial periods (ca. 1.200-1.050 BC) (Cline, 2012). While after 1.200 BC all the other former palace centers shrank or have been abandoned, in Tiryns there are impressive aspects of attempts to entrench a central political power and of rebuilding processes, even expansion (Maran, 2008).

Table 3: Cultural chronology of southern Greece (chronologies based on Bintliff, 2012; Demoule & Perlès, 1993; Manning, 2010; Parker, 2014; Perlès & Monthel, 2001).

Time (BC/AD)	Period		Event	Abbreviation	
AD 1204–1460	Byzantine and Frankish/Late Medieval		Start: Frankish conquest of Constantinople.	B, F	
AD 641–1204	Byzantine/ Medieval		Start: Death of Emperor Heraclius and the collapse of the Late Roman political order.	B	
AD 300–641	Late Antiquity/Late Roman		Start: Founding of the city of Constantinople and the parting of ways between the Western and Eastern parts of the Roman Empire.	LR	
146 BC–AD 300	Roman (Early, Middle)		Start: Destruction of Corinth and end of Achaian war.	R (ER, MR)	
323–146 BC	Hellenistic		Start: Death of Alexander	H	
479–323 BC	Classical		Start: Greek victory over the Persians in the battle of Plataea; Persian invasion of Greece repelled.	C	
750/700–479 BC	Archaic		Start: The first literary sources.	A	
900–750/700 BC	Early Iron Age	Geometric	Start: end of Mycenaean culture.	EIA	G
1075–900 BC		Proto-Geometric			PG
1700–1075 BC	Late Helladic / Mycenaean		Periodization modeled on Minoan Crete, which in turn was modeled on the Old, Middle and New Kingdom of ancient Egypt.	LBA	LH I-III
2100–1700 BC	Middle Helladic			MBA	MH I-III
3100–2100 BC	Early Helladic			EBA	EH I-III
4500–3100 BC	Neolithic	Final Neolithic	Start: Introduction of a farming economy in Greece.	N	FN
5450–4500 BC		Late Neolithic			LN
5950–5450 BC		Middle Neolithic			MN
6800–5950 BC		Initial and Early Neolithic			IN, EN

3.1.2 The lower town of Tiryns

The settlement remains of the Mycenaean post-palatial period lie near the urban area of modern Nea Tiryns either directly under the present surface, or they have already been eroded by natural or anthropogenic factors (Maran & Papadimitriou, 2006). Between 2013 and 2018 the German-Greek excavation in the north-western lower town of Tiryns has brought to light the close interrelationship between the palace and settlement of the post-palace periods (figure 5). The aim of the excavation was to understand the construction planning at the onset of the post-palatial period. Shortly after the destruction of the palace, the northern area in front of the Acropolis was systematically used for construction. The development of the area followed a building scheme consisting of rectangular modules of equally aligned courtyards and houses, which were maintaining basic features in two building horizons of the 12th century BC (Maran et al., 2019). This pattern is well-known from other areas of the northern lower town, in which buildings were grouped around courtyards. During this period, which did not last more than 70 years the structure of the settlement however, did not remain static, rather the arrangement of the buildings were repeatedly changed, which resulted in a continuous change in the boundary and use of the area (Maran et al., 2015).

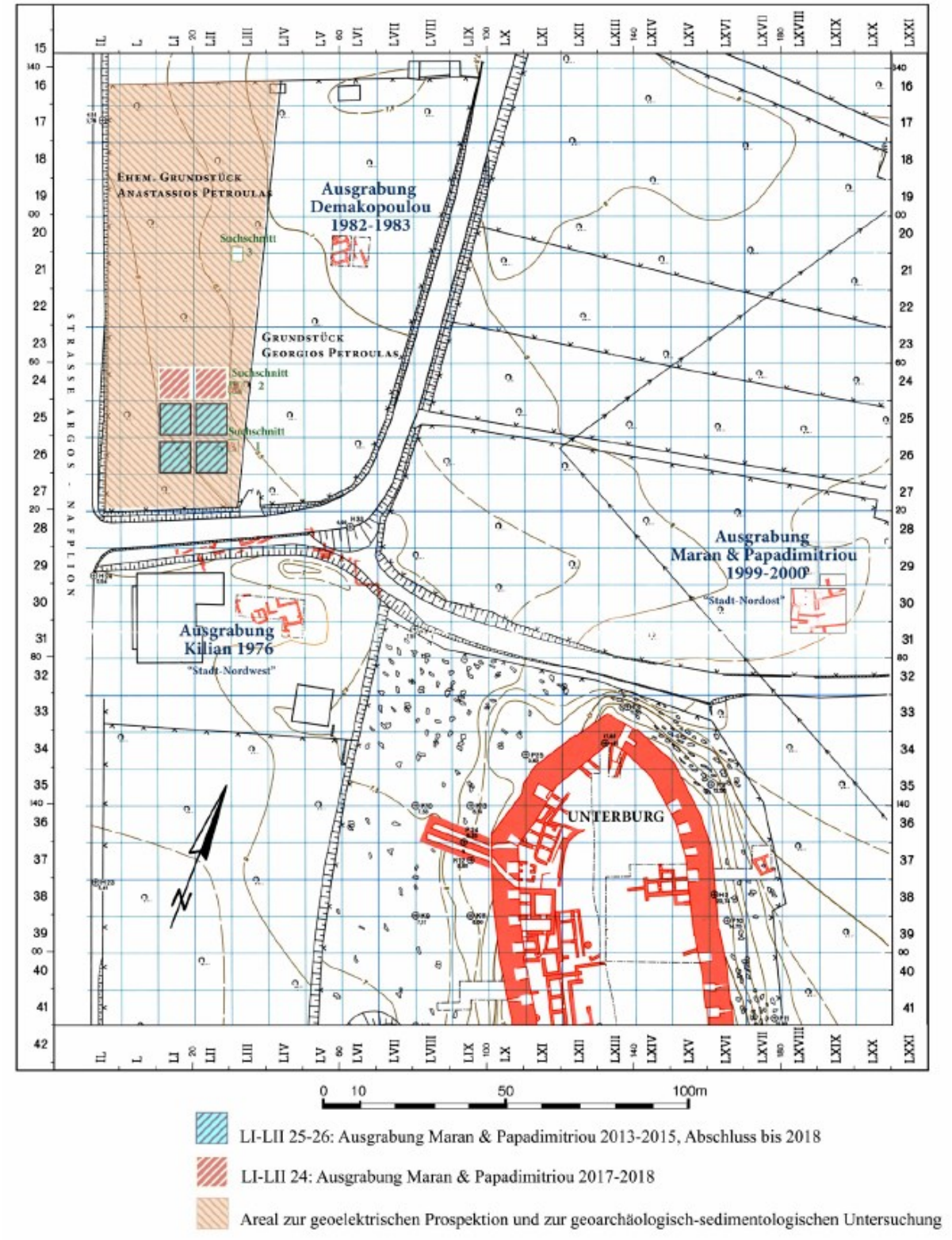

Figure 5: Plan with location of the excavation in the north-western lower town. Blue hatched: quadrants 2013-2018; red hatched: quadrants 2017-2018 (plan M. Kostoula after A. Rieger and W. Böser)(Maran et al., 2019).

3.1.3 Late quaternary alluviation and soil erosion processes

Already in 1960, C. Vita-Finzi constructed a general model of the late Quaternary alluviation history of the Mediterranean region. His model includes two stages of alluviation, the Older and Younger Fills, each followed by a phase of denudation. According to Vita-Finzi (1969), the Older Fill characterized by its full red colour should date into the late Pleistocene, while the brown-greyish Younger Fills were assigned to a late Roman to early Modern date and both due to climate causes (van Andel et al., 1986).

After the Argolid Exploration Project in 1979, directed jointly by M. H. Jameson and Tj. H. van Andel, seven alluvial events were recorded during the late Quaternary in the Southern Argolid. The project showed that these phases can be separated either by periods of landscape stability, characterized by soil formation, or by periods characterized by quick alluviation (Pope & van Andel, 1984; van Andel et al., 1986).

In the Argolis, three different forms of deposition can be distinguished. The first are debris flows, confused beds of unsorted, largely angular boulders, cobbles and pebbles, surrounded by a matrix of finer sediments. Denudation, due to the reduction of the plant cover, persisted drought, fire or clearing, causes debris flows, which are overlying the entire valley floor with a single unit of several meters thickness (van Andel et al., 1986; van Andel, Zangger, & Demitrack, 1990).

The second types are stream flood deposits, which are showing lenticular formed beds including well-sorted gravels and sands (Miall, 1985). These deposits originate from increased runoff through line type erosion in the form of gullies, probably due to heavy rain events. The most prominent alluvial deposits after van Andel et al. (1986) are sandy overbank loams, usually in combination with thin pebble layers, which were formed during flood stages and referred to distal areas of alluvial fans. The stratigraphy of the southern Argolid shows that all alluvial units are covered by overbank loam, which builds the surface for soil formation also interpreted as post-depositional intervals of stability (Pope & van Andel, 1984; van Andel et al., 1986; van Andel, Zangger, & Demitrack, 1990).

Due to the extensive and persistent settlement history in the Argolid, increased soil erosion occurred at different periods. The anthropogenic soil erosion was

mainly triggered by clearing, farming, deforestation, overgrazing and fires. The latest with the Final Neolithic, but especially during the Early Bronze Age, the thick woodland soils on slopes and some valley floors in the Southern Argolid were influenced by human activity (van Andel, Zangger, & Demitrack, 1990).

3.1.4 Geoarchaeological research

With the Argive Plain Project in 1984, the first geoarchaeological investigations in the Argolid were carried out. The aim of the project was to determine the late Quaternary environmental history driven by climate and tectonic processes and sea level fluctuations and to compare it with historic landscape changes by human impact. A special focus was on the investigation of fluvial that were found at the project frame. The Manessi river traversed the alluvial plain and passed the Upper Citadel of Tiryns from the Neolithic to the early LH IIIB period in the south (1) and then in the north during the LH IIIB period, around 1.200 BC (2). Zangger (1993) hypothesised that these deposits may have been caused by a single catastrophic flash-flood event, which served as a trigger for the people of the late Bronze Age to erect the dam of Kofini with a large artificial channel to redirect the river (3) to the south of Tiryns (figure 6).

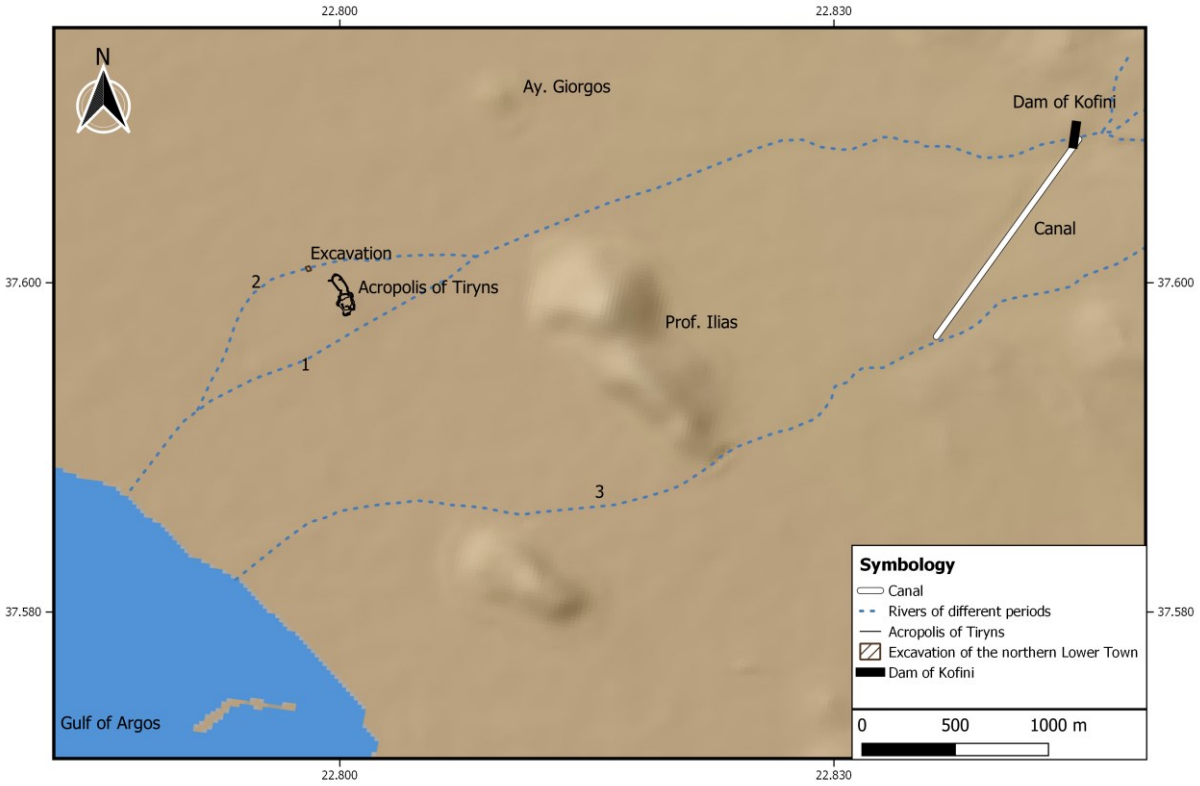

Figure 6: Map showing the course of the Manessi River 1) from the Neolithic to LH IIIB2; 2) during the natural diversion in LH IIIB2/C; and 3) after the artificial redirection. (adapted after Zangger, 1994).

The Dam of Kofini and the Manessi River

The Dam of Kofini is located about 1.25 km to the north of modern Agios Adianos and more than 4 km east of the Mycenaean acropolis of Tiryns (figure 6 and 7). Three major streams from the eastern mountainous edges converge and flow westward as one grater stream (Balcer, 1974). The original channel of Megalo Rema, has an E-W direction and is still traversing on the west side of the dam. The north-south oriented dam has a length of 80-100 meters, a total height of 10 m and a mean base width of about 60 m. The core of the dam is built by natural red sediments while on both eastern and western sides two protective walls have been constructed (Maroukian et al., 2004).

Figure 7: Photograph of the dam of Tiryns, southwest view (H.-R. Bork 2018).

During the excavation in 1987 (carried out by the Nauplion Ephoria) in the north-western part of Tiryns, about 50 m beyond the corner of the citadel the trench Pa was documented. It shows an EH II (Early Helladic) site at the bottom at 5.45-6.0 m depth directly above a red Pleistocene palaeosoil. The upper surface of the cultural layer consisted of a soil A-horizon (at 5.2-5.45 m) which is attributed to intense human activity. Between 5.20 and 3.95 m below ground level, natural alluvial deposits and Early Helladic pottery fragments were found. Between 3.95 and 2.80 m follow undisturbed, interlayered stream and floodplain deposits. The uppermost 2.80 m of the trench profile consist of reworked soil material associated with a variety of Mycenaean and Geometric pottery. The present stratigraphic evidence therefore shows that the former lower town (dating to the Early Helladic period) is buried under 6 m thick deposits. During the Early Helladic period (3.100-2.100 BC) the Manessi River, which deposited several meters of overbank loam, was located in the south of Tiryns (figure 7) (Maroukian et al., 2004; Zangger, 1994, 1993).

Through further excavations by Killian in March and April 1976, three overlaying building horizons were found northwest of the citadel. The building horizons date to the Early to Middle LH III period. These buildings were arranged around a courtyard as in the lower castle. At the bottom, the stratigraphy shows a Pleistocene palaeosoil documented until 4.35 m (Zangger, 1994, 1993). Above this soil, an alluvial layer is documented between 2.25 and 3.25 m. It shows two phases interrupted by two A-horizons containing LH III B1 sherds (2.65 to 2.8 m) and Neolithic pottery. The oldest of these construction horizons has been founded on sterile gravel and sand deposits of 1.20 m thickness deposited by the Manessi River (Maran & Papadimitriou, 2006). The texture (poor sorting and rounding) and structure (cross bedding) of these sediments characterize them as river deposits. Furthermore four sediment cores were drilled at the east side of the citadel (Zangger, 1993). Furthermore, four sediment cores were drilled at the east side of the citadel. The borehole transect extends from the main entrance of the citadel about 300 m in easterly direction. It shows a three-part stratigraphy consisting of a Pleistocene palaeosoil about 6 m below the present surface. The palaeosoil is covered by a Neolithic to Late Helladic soil, which was interpreted as a period with no colluvial soil development at this area. The most prominent horizon of the profile, however, is the 4.90 m thick and poorly sorted alluvium. Due to the accompanying fact that a large number of sherds were found in one of the 4 cores in the transect (-core 104), Zangger attributes this layer to a singularly occurring event in LHIIIB2 (Zangger, 1993).

Table 4: Late Bronze Age Chronologies (after Shelmerdine, 1997).

Period	High	Low	Modified
LH I	ca. 1680-1600/1580	1600-1510/1500	
LH IIA	1600/1580-1520/1480	1510/1500-1440	
LHII B	1520/1480-1425/1390	1440-1390+	
LH IIIA1	1425/1390-1390/1370	1390+-1370/1360	1390+-ca. 1370
LH IIIA2	1390/1370-1340/1330	1370/1360-1340/1330	1370-1310/1300
LH IIIB	1340/1330-1190/1180	1340/1330-1185/1180	1310/1300-1190/1180
LH IIIC	1190/1180-1065/1060	1185/1180-1065	1190/1180-1065

3.1.5 Fluvial deposits and cultural layers as geoarchives at the Lower Town

Dotterweich (2008) points out that for large river systems several methods have been developed to reconstruct Holocene river activity in high resolution. Therefore, it is possible to show long-term variations between forcing and response between land use, climate an river activity at a regional scale. However, it is not always clear how Holocene river floods had an impact on human settlements and land use or to what degree the land cover in a river catchment must change to either amplify or reduce the climate signal recorded in fluvial deposits, and whether the location of changing the landscape is important in this regard (Dotterweich, 2008; Macklin et al., 2006).

Koutsoyiannis et al. (2012) point out that analyses of palaeofloods often not provide appropriate estimates of the hydrological regime, because palaeofloods are strongly linked with changes in the catchment vegetation or land use. This factor becomes more important the further back in time such floods occurred. Especially in the Mediterranean region, there have been enormous changes in vegetation over thousands of years (Macklin et al., 2002).

The reconstruction of flood magnitude-frequency relationships in the past can be supported by micro-XRF analysis. Several element rations have previously been used as proxies for grain-size in the palaeo-environmental interpretation of sediment sequences including Si/Al, Ti/Al, Zr/Al, Zr/Ti and Zr/Rb (Calvert et al., 2001, 1996; Dypvik & Harris, 2001; Oldfield et al., 2003). The Zr/Rb and Zr/Ti ratios are particularly suitable for reconstructing flood events. During fluvial transport Zr, Rb and Ti become concentrated in particular grain-size fractions attributed to the varying resistance of the minerals in which these elements generally appear. While Zr can accumulate in the fine sand and coarse silt fractions, Rb is often concentrated in the fine silt and clay-sized fractions. (Dypvik & Harris, 2001; Rothwell & Croudace, 2015).

Cultural layers and buried soils

Of particular importance is the archive function of soils, in the context of environmental and cultural history (Krebs et al., 2017). Soils provide information on environmental conditions and processes over the time of their formation. However, the change in soil properties due to recent overprinting must be taken into account. Former soils can either be covered by younger sediments and undergo pedogenetic processes, or they can be found due to erosive processes at the surface. In archaeological research, buried soils are generally referred to as former soils preserved under building remains, or over colluvial or alluvial deposits (French, 2003).

To differentiate areas where human activities took place from those which were unaffected the study of Entwistle et al. (2000) is useful. They investigated a former settlement area at Greaulin (Isle of Skye) and showed that the spatial variability of soil properties like the concentration of K, Rb, Th, Cs, and Sr differ in terms of settlement activity.

The investigation of heavy metals has also a great potential with regard to the identification of use-of-space-patterns in former settlements (Gauss et al., 2013). For example, increased concentrations of Fe, Cu and Hg indicate workshops, craft, or ceremonial actions and are often associated with wall paints. For example, the wall paintings of the palace of Nestor from the Late Bronze age including iron-based pigment for the red, yellow and brown hues, a manganese-based pigment for the black colour, while calcite is the major material used for the white coloration (Kokiasmenou et al., 2020). Furthermore, increased values of Fe, Sn, Zn and Cu indicate possible metal processing sites (Alexandrovskaya & Panova, 2003; Gauss et al., 2013; Khamnueva, 2017). According to Entwisle et al. (2000), settlement and land use activity and especially cultivation lead to enrichment of the soil in certain elements like K, Ca, Sr and P through the entry of shell-sand, bones and fish refuse.

3.2 Stymphalia

3.2.1 Stymphalia: an ancient Arcadian town

First traces of settlement in the Stymphalia polje in the form of agricultural point to the Early Neolithic. Very few findings were made for the Mesolithic, Neolithic and the Bronze Age in the polje (Walsh et al., 2017; Williams & Gouley, 2005). The ancient town of Stymphalos lies on the north shore of Lake Stymphalia about 600 m a.s.l. A fortified wall extending 800 x 800 meters surrounded the city (figure 8). The rising masonry was built of mud-bricks, while the foundation shows a 2.5-4.5 m wide stone base. In between, semi-circular and rectangular towers and overlap style gates were erected (Williams, 2003). Beyond to the surrounding city wall, the acropolis, the propylon, the Athena sanctuary, the temple and the fountain house are the main features of the archaic cityscape. The acropolis of the town is located along the north bank of the lake. The city flourished in Archaic to Middle Hellenistic times (600 – 250 BC) (Williams, 2003). Williams and Gouley (2005) estimate that the city could accommodate more than 2500 people and 500 in the surroundings based on the town dimensions known so far (figure 8).

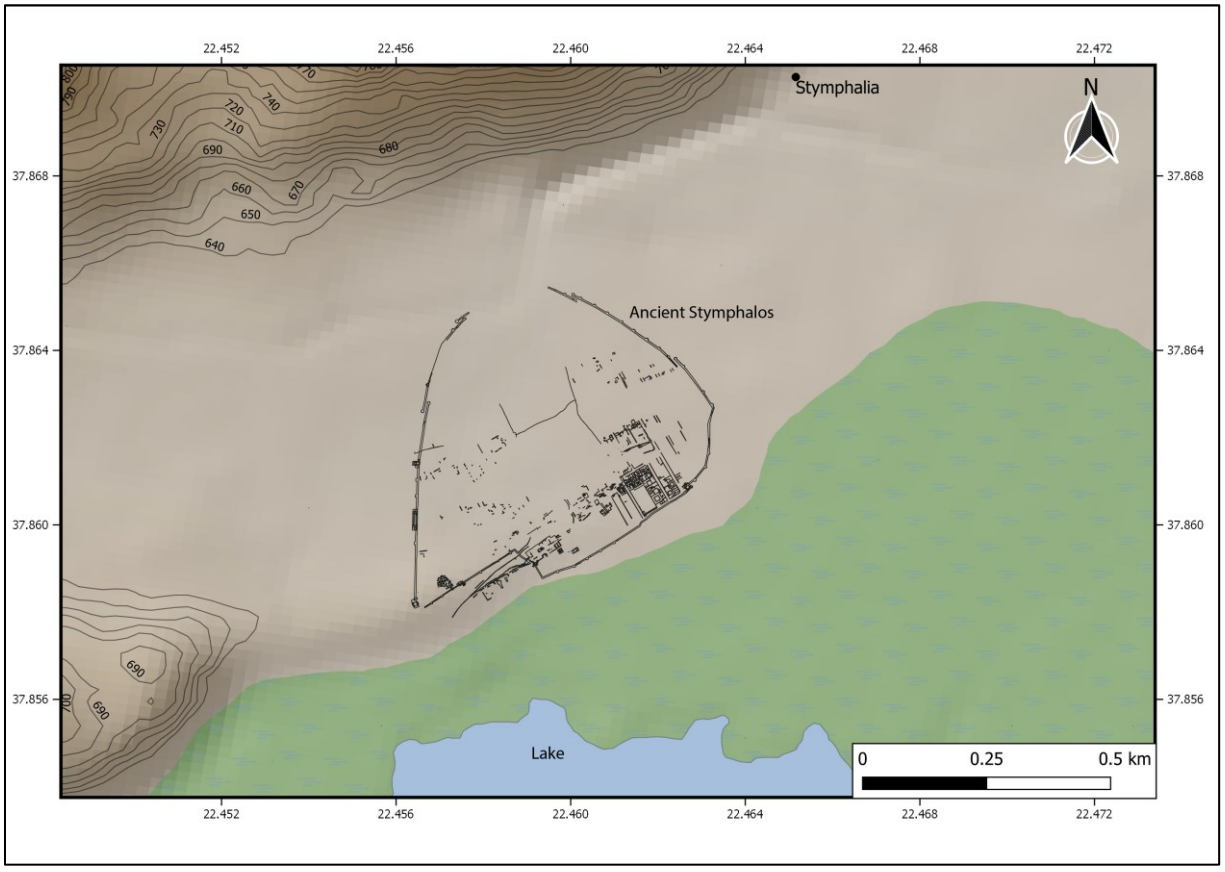

Figure 8: Plan of the site of ancient Stymphalia (adapted after Williams et al., 1998).

3.2.2 Ancient agriculture in Stymphalia

Due to the local climatic and topographic conditions, there several different agricultural systems have established. Agriculture during the Classical period stands out by labor-intensive, small homestead farms, in addition to more traditional transhumance, fallow-cropping and nucleated settlement (Hanson, 1992). Typical land use management was achieved by small-scale mixed farming, combining intensively managed gardens with small fields and limited animal husbandry. Field cultivation systems focused on localized, risk-buffering strategies, where food production was carefully managed, and the risk of crop failures of one income could be compensated by another (Weiberg et al., 2019). Traditional Mediterranean farming practices include seasonal pastures of sheep and goats accompanied by wheat or barley fields, which were sown on a two-year fallowing cycle (Halstead, 1987). Cultivated crops include wheat (*Triticum dicoccum, Triticum vulgare or cereal and hordeum*), millet (*Panicum miliaceum*), broad bean (*Vicia faba*), pea (*Pisum sativum*), lentil (*Lens esculenta*), vetch (*Vicia ervila*), wine, olives and other fruit species like pears, pomegranates, apples and figs (Halstead, 1992; Isager & Skydsgaard, 1992). In order to cultivate the soil the plough, how, spade and sickle or curved knife were used. Based on the accurate description of Hesiod's Works and Days II. 427 ff., in combination with the enormous depictions of ploughs and ploughing on statuettes in terracotta or bronze, on vase paintings and coins, it is known that the plough could not turn the soil as this is the case today. It partly destroyed the weed and scratched the surface, the cracks lead to better aeriation and make the surface porous and therefore more absorbent (Isager & Skydsgaard, 1992). In addition to terraces used for agricultural purposes, threshing floors are particularly noteworthy, shaping the environment. In analogy to modern threshing floors, they are circular and typical having a hole for the pole in the centre.

3.2.3 The agricultural terraces

Terraced agriculture is a formative element in the landscape of the Mediterranean. Farmers construct agricultural terraces to reshape slopes into stepped linear units with more or less flat surfaces to make them suitable for the cultivation of plants (Bevan & Conolly, 2011). Moreover, the construction of terraces is the most widespread form of soil conservation and plays an important role in the southern mainland and islands of Greece to cultivate new land. They can be classified by their geomorphic occurrence, function, morphology, and construction method (Frederick & Krahtopoulou, 2000). The agricultural terraces in the Stymphalia area are step-like, slope or contour parallel platforms, consisting of a vertical or near vertical wall or blank also called raiser. The terraces are characterized by the tread, a flat or nearly flat surface, which lies up-slope, behind the riser.

Investigating the stratigraphy of these terraces gives a direct view of their construction method, usage and which soil was predominant on the slope before the construction of the terraces. The following aspects should be taken into account: the pre-existing surface (usually a palaeosoil), the raiser, the raiser fill, the tread fill, the cultivation surface and the post-abandonment fill (Frederick & Krahtopoulou, 2000).

Frederick and Krahtopoulou (2000) provide an overview of the reasons, why people were constructing terraces. They mention for example the soil management, to modify slopes, to limit erosion with low inputs and less soil movement on steep slopes, and to increase soil depth. In addition, the water is managed catch, control, reduce the velocity and absorb run-off. At last, they describe the crop management to ease harvesting, provide drainage for crops and modify microclimate to facilitate plan growth.

The temporal classification, when agricultural terraces were erected is largely unknown, which is not least due to the recurring use of the terraces over centuries if not millennia. Price and Nixon (2005) define nine criteria for dating terraces:

- the datable material in the filling,
- the age of trees on terraces,
- the construction style,
- coincident construction style to neighbouring ancient structures,

- terraces built against ancient structures,
- lichenization,
- the degree of degradation,
- systems of terraces with ancient sites and
- antiquity, to be the period of greatest pressure on agricultural remains (Price & Nixon, 2005).

4 Methodology

4.1 Fieldwork

4.1.1 Tiryns

In connection with the ongoing archaeological excavations lead by J. Maran (Heidelberg University) in the north-western lower city of Tiryns, two geoarchaeological field campaigns of a team from the Institute for Ecosystem Research (Kiel University) were conducted in Tiryns in August/September 2017 and in September 2018.

In 2017, the campaign included the documentation and sampling of the Manessi River sediments in the excavation site (figure 9). Additional samples from fluvial deposits and cultural layers were collected during September 2018.

Sampling strategy: Since the fluvial gravel of the river within the lower city appeared in the middle of surrounding wall foundations, a rectangular trench was cut in the section TL 17 LII 25 with the dimensions 2.0 m x 1.5 m x 1.5 m. After the allocation of individual deposition packages due to different grain size composition and the fluvial-architectural appearance, four profiles were drawn and photographically recorded (appendix 7). Furthermore, all layers were sampled and the sediment colour was determined by using the Munsell soil colour chart.

For micromorphological analysis, three undisturbed samples from layers Y1a, 10, and Y3 in small aluminium containers were taken. In addition, three undisturbed sampling cylinders were taken from each of the fluvial deposits (layer 17) and culture layer Y3. The sampling cylinders have a volume of 100 cm^3. Moreover, six sampling cylinders with a volume of 250 cm^3 carried out for an undisturbed sample extraction (figure 9). Three sampling rings were taken from the Y3 (Tl 17 LII 25, grid square 86), the other three samples were taken from the fluvial deposits layer 8 (Tl 17 LII 24, grid square 74).

Figure 9: left: Undisturbed sampling from layer Y3 (Foundation); right: Undisturbed sampling from layer 8 (fluvial deposits) (photo: H. R. Bork).

4.1.2 Stymphalia

In the Styphalia polje five filed campaigns were undertaken during the years 2017 to 2019.

The first field campaign in April 2017 should provide information about the different existing soils as well as suitable sampling sites for the analysis of substrate genesis. In the subsequent campaigns in May and August 2018, samples were taken from the topsoil at different locations. In the last filed campaign in June 2019 further soil profiles were recorded and sampled.

Sampling and survey strategy: In order to capture the high variance of soil types in the Stymphalia basin, a dense sampling grid was laid over the entire catchment area (figure 10). Within this grid, 13 transects with up to seven sampling points were selected. A total of 64 locations were recorded, which are less than 1.1 km apart from each other. At each location, two samples were taken both directly at the surface and at a depth of approximately 20 cm below the surface. In modification of the sampling grid, the selection of the locations was based on a detailed examination of the surface conditions. In order to record soil conditions as undisturbed as possible, samples were taken at a sufficient distance from paths, roads, buildings and streams or drainage ditches. If the sampling location was on a terrace site, the samples were extracted in the middle of the terrace. In addition to the area surface sampling, seven soil profiles were recorded at selected sites in

the field. All sampling sites were recorded photographically and logged via GPS. In order to record the soil and substrate genesis adequately, information on the relief, modifications in the soil (application, erosion, and anthropogenic changes), land use, vegetation and weathering were recorded. A more detailed description of all sites can be found in Appendix 3.

To describe the surface topography the following parameters were taken into account:

- position in the relief
- the slope inclination, which was divided into six stages and measured by an inclinometer
- exposition
- curvature
- relief shape type, which can be divided into a culmination area, a depth range and a slope
- micro-relief was described by labelling its roughness

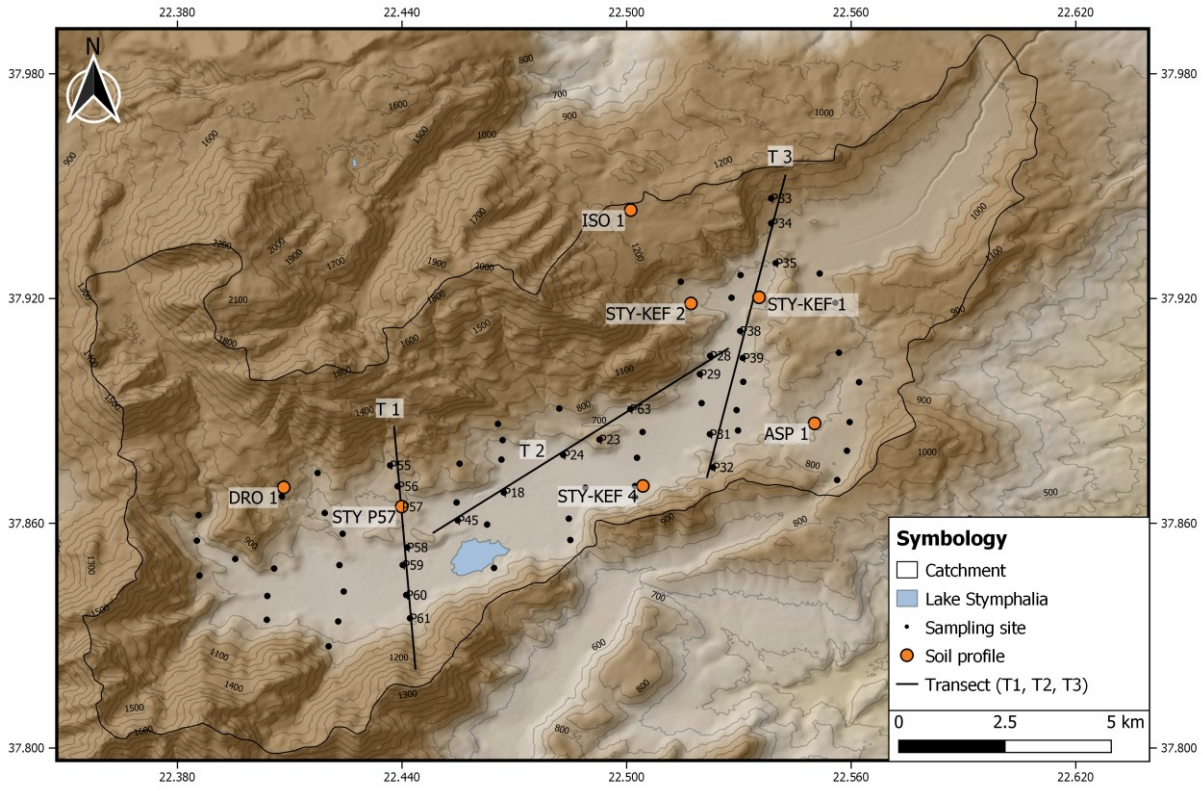

Figure 10: Map of the research area at Stymphalia with sampling sites and transects.

4.2 Laboratory methods

Following the protocol of Hartge & Horn (1992) all soil samples were air-dried and the resulting clods were crushed. To separate and remove the skeleton- from the fine soil, the samples were sieved with a mesh width of 2 mm.

Grain size distribution

All samples were measured by laser diffraction to get detailed information about the grain size distribution. The fine soil is weighed into centrifuge tubes according to its composition. For sandy soils, 0.8 to 1.0 g was used, while for clayey soils a maximum of 0.6 g of soil material. The organic matter was destroyed by adding 35 % hydrogen peroxide (H_2O_2). Before further treatment, the samples were flushed with distilled water and centrifuged.

To destroy the carbonates, a sodium-acetate acetic acid buffer was added to the samples in 10 ml steps. Due to the high carbonate content of the samples, the process was repeated up to three times until the pH dropped to approximately 5. As a final preparation step, the samples were filled up with distilled water, mixed with sodium pyrophosphate ($Na_4P_2O_7$) and shaken for about 16 h, to avoid agglomeration of soil particles.

After this step, the samples were measured by a Mastersizer 2000 Particle Size Analyzer in a combination with Hydro 2000 for fluids at the Institute of Geography (Kiel University). Each sample was measured for 45 sec, repeated 10 times by a measurement range from 0.02 µm to 2000 µm. Obscuration did not exceed or fall below the range of 10 to 30 %. According to the ad-hoc Arbeitsgruppe Boden (2005), the 70 classes of particle sizes were grouped to the seven grain size fractions to mention the soil type.

Loss on ignition (LOI)

To determine the organic matter content, approximately 3 g of the samples were weighed in porcelain crucibles. The samples were dried at 105 °C overnight. After weighing, the samples were combusted in a muffle furnace at 550 °C for 2 hours (LOI_{550}). After a one-day cooling phase in the desiccator, the samples were weighted again. The difference in weight between oven-dried and annealed

material gives the amount of organic matter in each sample. However, this results in methodical sources of error that must be considered: carbonate compounds may decompose, which causes carbon dioxide to form and escape. And the loss of water of crystallization can occur in soils rich in clay, which can be released at 105 °C by the clay minerals (Barsch et al., 1984). For the samples of the soil profiles, the inorganic carbon content was additionally determined by combustion at 950 °C for another 2 hours (LOI_{950})

pH-value

For the measurement, 10 g of air dried samples were put in 1:5 suspension (soil: 1 M KCl) and after 2 hours shacked for 5 minutes. The pH value was determined by a pH meter WTW pH 330i, SenTix 41.

C/N ratio

The soil samples were removed from plant remains and ground to powder for 30 seconds in an agate vibratory disk mill. The concentration of total organic carbon (TOC), total nitrogen (TN), and total inorganic carbon (TIC) was measured at the Institute for Ecosystem Research (Kiel University) using a Euro EA, Elemental Analyser.

Portable XRF scanning

To capture the geochemical compositions of the soils a portable or handheld X-ray fluorescence scanner (XL3t 900-series GOLDD+) was used. Therefore, the samples had to be grounded to less than < 60 µm in a vibratory disk mill. The grounded material was refilled in plastic tubes and covered by 4 µm a thin film (Fluxana TF-240-255). The water content can affect the pXRF measurement, hence only dry samples were used. The measurement was preformed for 300 seconds in the mining mode. For quantitative measurement of light elements, helium was added in the detector.

OSL dating

Optical stimulated luminescence dating (OSL) was only tested at two locations, STY-KEF 1 and ISO-1. Two samples from each soil profile were taken at night

under red light. The samples were analysed and dated at the Sedimentary Geology and Quaternary Research center at the Albert-Ludwigs-University in Freiburg, Germany. The samples were wet sieved with a mesh size of 100-200 µm. Further small aliquots (2 mm) of quartz were used, treated by preheating at 230°C for 10 s to all measurements. All ages calculated using the Minimum Age Model of Galbraith et al. (1999) assuming a sigma b of 0.15.

4.3 Soil quality index (SQI)

To estimate the environmental quality, agronomic sustainability, and the socio-economic capability, the soil quality index (SQI) often is used (Mukherjee & Lal, 2014). The index integrates the measured soil physical and chemical properties into a single parameter, which could be used as an indicator of overall soil quality in the polje. The procedure for creating an SQI is mainly based on the work of Amacher et. al (2007). The SQI presented in this work integrates 8 soil physical and chemical properties: the soil texture (vol. %), the coarse fragments (%), the Organic matter content (%), the C/N ratio, the soil pH, and the contents of potassium, magnesium and calcium (ppm). As the element concentrations may have changed due to recent fertilization, the elements (Ca, K and Mg) were included less weighted in the calculation. For all soil properties, the individual index values were summed to give the total SQI:

$SQI = \sum$ index values of individual soil properties

If the data is complete, the maximum value of the SQI is set to 24 (table 6). The total SQI is then expressed as a percentage of the maximum possible value of the total SQI for the soil properties that are measured:

SQI_{per} = (total SQI/maximum possible total SQI)*100

From the obtained percentages of the soil quality index 9 classes (table 5) were created, whose characteristics are explained in the following.

Table 5: Classification of the percentage of the SQI

Class	**1**	**2**	**3**	**4**	**5**	**6**	**7**	**8**	**9**
SQI_{per}	0-25	25-30	30-41	41-50	50-54	54-62	62-66	66-75	75-92

Table 6: Soil quality index values (with associated soil property threshold values and interpretations)(after Amacher et al., 2007)

Parameter	**Level**	**Interpretation**	**Index**
Soil texture (vol %)	> 17 % clay, < 15 % silt	High water storage capacity	4
	> 25 % clay, > 50% silt	High water storage capacity, but waterlogging effects and poor tillage ability	2
	< 50% silt, <17% clay	Low water storage capacity and high permeability coefficient	0
Coarse fragments (%)	< 50	possible adverse effects	2
	>=50	Adverse effects	0
Organic Matter (%)	> 6	High	4
	3 to 6	Moderate - adequate levels	2
	< 3	Low - loss from erosion or other processes	0
C/N ratio	< 10	Narrow C/N ratio, nutrient rich	4
	10 to 15	Moderate C/N ratio	2
	> 15	Wide C/N ratio, low biological activity	0
Soil pH	7.51 to 8.5	Moderately alkaline - preferred by plant adapted to this pH range	2
	7.21 to 7.5	Slightly alkaline - optimum for many plant species	4
	6.81 to 7.2	Near neutral optimum for many plant species except that prefer acid soils	4
	5.51 to 6.8	Slightly acid - optimum for many plant species, particularly more acid tolerant species	2
	4 to 5.5	Moderately acid - growth of acid intolerant plants	0
K (ppm)	> 13800	High - good reserve	2
	7001 to 13799	Moderate - adequate levels	1
	< 7000	Low - possible nutritional deficiencies	0
Ca (ppm)	> 93000	High - good reserve	2
	47000 to 9299	Moderate - adequate levels	1
	> 46999	Low - possible nutritional deficiencies	0
Mg (ppm)	> 6000	High - good reserve	2
	5999 to 4001	Moderate - adequate levels	1
	< 4000	Low - possible nutritional deficiencies	0

One of the most important soil parameters is the particle size distribution, which, depending on its composition, mainly influences the water storage capacity of the soil. The classification was therefore based on the usable field capacity and the water content depending on the soil type. The particle size distribution was considered, as it is changing relatively slow over time. The classification of the soils and their water storage capacity is based on the classification of the mean pF-curves in AG Boden (2005) and in particular on the available field capacity of the plant available soil water depending on the soil type.

The coarse fragment content has a great influence on adverse effects from infiltration rates. A content above 50 % of stones reduces the water storage capacity, aggravate the rooting and causes a greater difficulty in seed germination (Rodrigue & Burger, 2004).

The biodiversity strongly depends on the soil pH. Therefore, the diversity decreases with increasing acidification (pH <4) and on strongly alkaline pH levels (pH > 8.5). The potential availability of nutrients and pollutants is also controlled by the soil pH value. In addition, plant growth and thus the yield of crop plants depends on it (Amacher et al., 2007; Blume et al., 2010).

The content of organic matter in soil has a decisive influence on soil functions. In the topsoil, the influence of organic matter is particularly high. In addition, the humus in the soil has a high water storage capacity and, due to its aggregating effect, has an impact on the pore size distribution and the overall water balance (Blume et al., 2010).

The nutrient supply of the soil is of crucial importance for plant growth. In order to determine the nutrient supply of the soil, the element concentrations of calcium, potassium and magnesium were measured. Calcium promotes essential compounds in the plant, such as phytin, pectin and Ca-phosphate. Calcium is available to plants as Ca^{2+}-ion in the soil solution. Deficiency symptoms only occur in acidic soils. Potassium, which is absorbed by plants as a cation (K^{+}) from the soil solution, is decisive for the adjustment of the osmotic pressure and the regulation of the water balance. The promotion of metabolic processes is ensured by the availability of magnesium, which is available as Mg^{2+}-ion in the soil solution (Amacher et al., 2007; Blume et al., 2010; van Breemen & Buurman, 2002).

5 Results

The first part of this chapter describes the stratigraphy, which is present among the remains of the lower town of Tiryns. The different strata were examined with respect to the depositional conditions.
The second part of the chapter presents the results of the Stymphalia polje.

5.1 Local landscape changes at Tiryns

5.1.1 The stratigraphy of fluvial deposits below the urban area

The Late Helladic fluvial deposits of the Manessi River were exposed during the excavation in section LII 25 in the middle of the house structures (figure 11). In the lowest level, which was excavated by the archaeologists, some rounded river gravel could be documented. At this point, trench TS-1 was sunk which shows the following stratigraphic sequence (figure 19).

Figure 11: Aerial photograph of the excavated parts of the Lower Town of Tiryns Section LI-LII 24-26 and the location of the trench TS-1 (adapted after Maran & Papadimitriou, 2017).

In addition to the sedimentological profile description and the documentation of fluvial architectural forms, various chemical elements were measured by pXRF (chapter 4.2) in order to differentiate more precisely between the sedimentation phases and the individual strata. By performing a cluster analysis, using R version 3.6 and *hclust* form the stats package as well as Ward's method, the individual strata can be divided into 6 clusters (figure 12). Prior to analysis, the data were standardized by the vegan package. The analysis included the particle size distribution, the content of organic matter and the concentration of different elements. The first cluster is formed by the fine and medium gravel fraction of the river sediments, while coarse sand and fine gravel dominating. The clusters 2 and 3 comprise both sediment layers, which originate from different flooding periods. The layers which are assumed to be anthropogenic deposits form cluster 4. The cluster contains the application layer Y2 and the culture layers Y1a and Y1b. In these layers higher values of Rb, As, Zn, Fe, Ti, Ca and Al occur compared to the fluvial deposits (figure 13). Cluster 5 contains river deposits, which are characterized by slightly increased silt concentrations. Sediments of a former flood plain form cluster 6.

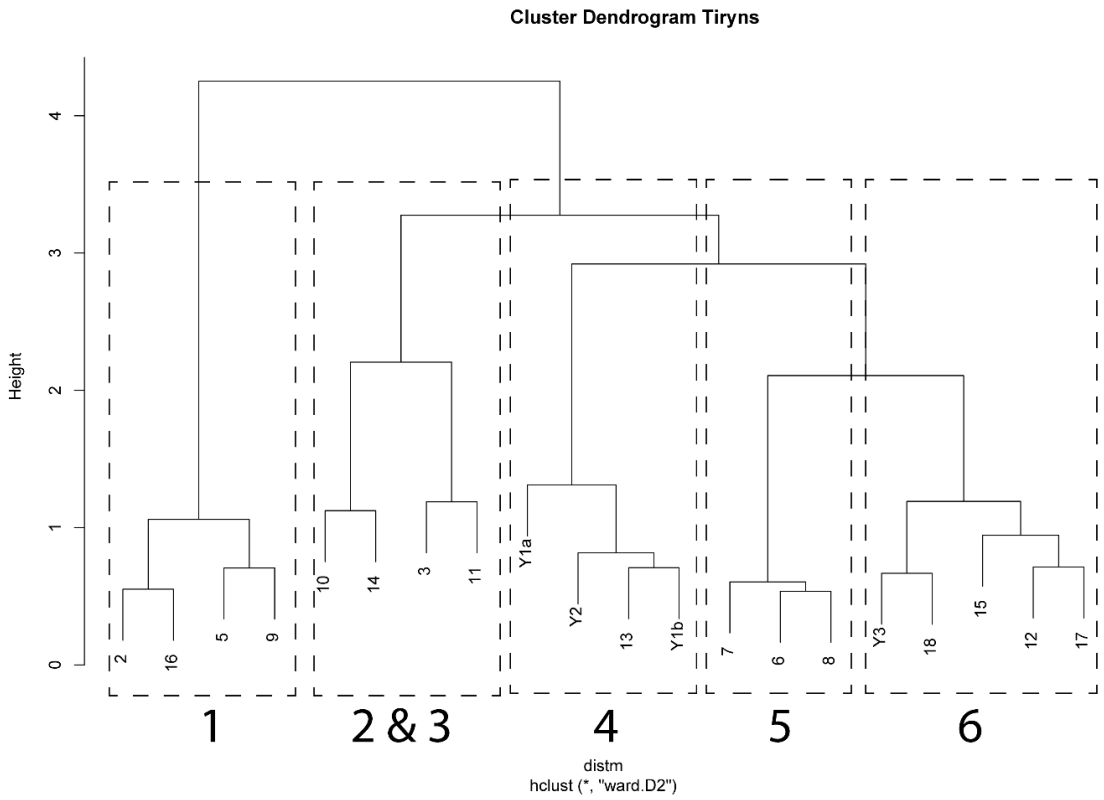

Figure 12: Cluster analysis of the different layers of trench TS-1.

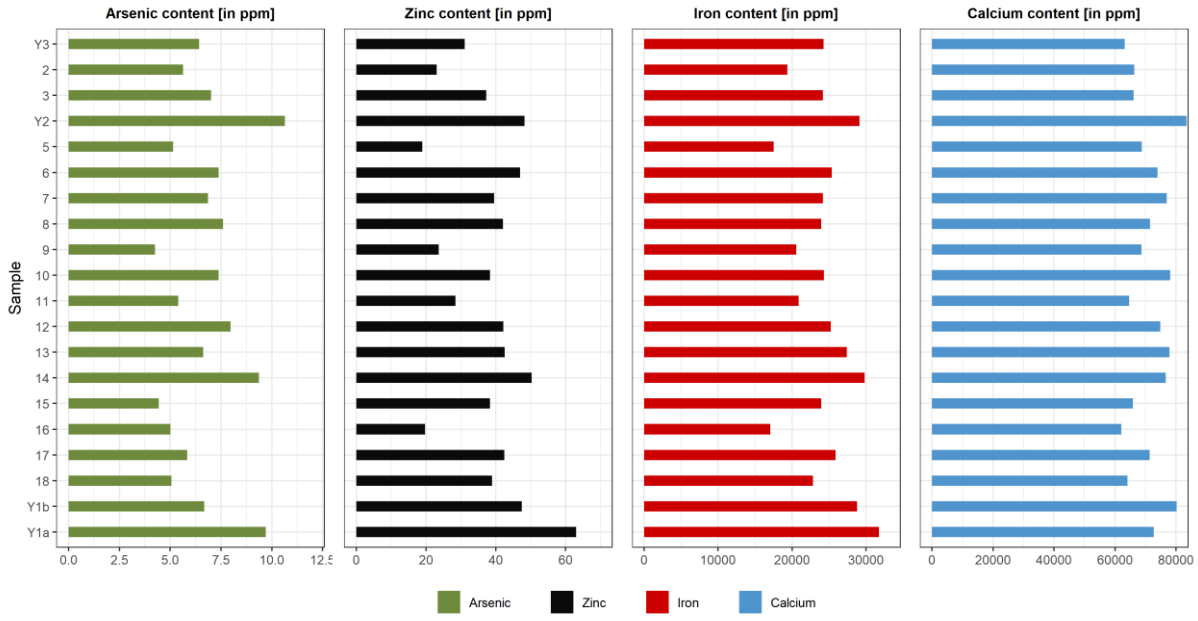

Figure 13: Element concentrations of the different layers across the profile.

Cultural layers (Y1a and Y1b)

At the base of trench TS-1, at a depth of more than 244 cm below surface, the dark brown humus-rich and loamy layer Y1a is exposed, the boundaries of which are not spatially oriented and wavy. Y1a is a cultural layer, which contains ceramic fragments in addition to charcoal and burnt clay. Based on the pottery, the layer is dated to the second half of the 14th century BC (Late Helladic IIIA2). Above the cultural layer lies the second anthropogenic deposit Y1b. It's boundary to the layer above is straight and consists of clayey-silty material. Both cultural layers have a comparatively high content of organic matter (2.33 %, figure 18). According to the current state of investigations, there is no evidence for a development of the area of the later north-western lower town during the time of deposition of these cultural layers. The wavy horizon boundaries, the increased content of organic matter and the pedogenetic features visible in the thin section TIR-MM3 (figure 14) confirm this assumption. A further identification feature as a cultural layer is given by the relatively high content of phosphorus (371.9 ppm) (figure 18).

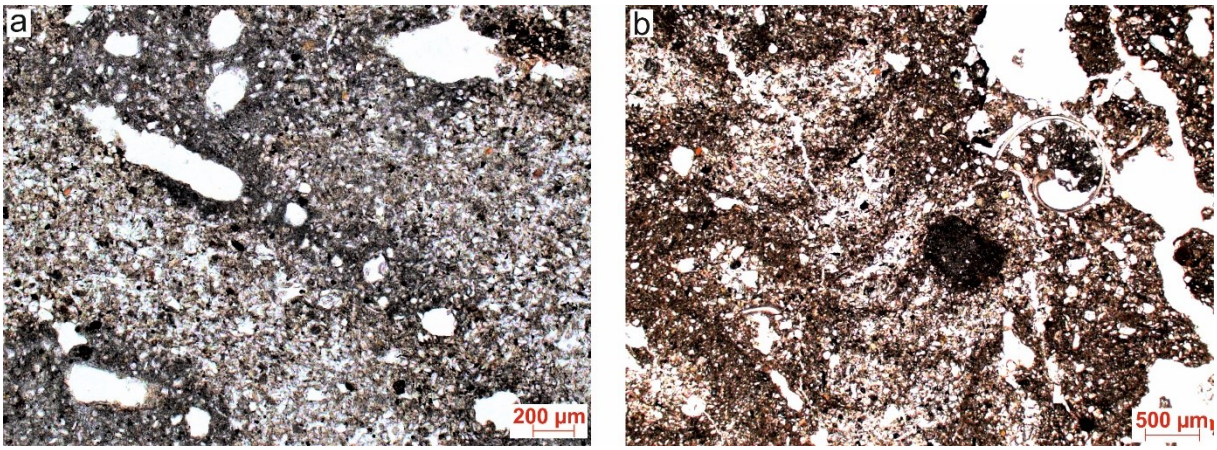

Figure 14: Microphotos of the thin section TIR-MM3, A: Pedogenetic hypo deposits along root and animal passages in cultural layer Y1b. B: Vermicular microstructure in culture layer Y1b, indicating intense biological activity. (Photo: S. Khamnueva-Wendt)

Flood sediments (A-LS)

Above layer Y1b, fluvial sediments (layers 17, 18) appear, which were deposited by flooding. This fine sandy and slightly clayey alluvial sediment has a thickness of 40 cm.

Due to low flow velocities, mainly fine sands were deposited (layer 18 has a fine sand content of 57 % and layer 17 of 46 %). The sediments are characterised by horizontally laminated fine sands (Sh) and fine laminated flood sediments (Fl). The fluvial architectural element shows a laminated sand (LS).

First occupation layer (B-B1)

Above the horizontally stratified flood sediments the profile shows a mixed layer consisting of brown silt sands (layer 15) and light grey sands (layer 16 with a middle sand content of 63 %). Due to the partly massive or weak laminar structures, both layers are assigned to the facies code Sm. However, these layers show considerably disturbed fluvial architectural elements, i.e. no planar flow or sedimentation patterns are recognizable and therefore can't be declared by natural processes. It is possible that shepherds with their herds passed this area of the floodplain more often, which probably caused particularly moist substrate to be moved and thus partly slightly mixed. This assumption is supported by the increasing phosphorus values in layer 15 up to 668 ppm.

Floodplain (C-FFp)

Fine stratifications consisting of very silty sands (layers 13 and 14) indicate numerous weak floods. Layer 14 comprises a total of 28 detectable small flood events. The laminar fine stratification (Fl), the slightly increased content of organic matter (2.1 %) and the higher silt and clay contents (silt: 49.5 %, clay: up to 5.8 %) in the sediments indicate a proximal flood plain (FFp).

Second occupation layer (D-B2)

Small channel systems, which have cut into the deposits of the flood plain (layer 13), prove a change in the discharge environment. Stronger flood event deposited first layer 9 with light greyish gravel (Gmm) followed by layer 10 with silt sands (with a high fine sand content of 41.1 %). However, the assignment of the facies code is uncertain, as also here, a later strong mixing has taken place. Several differently twisted blocks consisting of a laminar fine layer of fine sand and loamy alternating layers (Fl) are embedded in a loose coarse sand matrix. Natural deposition processes cannot explain this structure. Micromorphological investigations on the thin section TIR-MM2 (figure 15) support the assumption that these intermixing processes were caused by humans and/or animals. The both primary (e.g. coarse mineral grains) and secondary components (features produced by soil formation) visible in the thin section do not show any spatial orientation. Although the sand matrix in the lower part of the layer is relatively loose with a porosity of 30 to 40 %, thin vertical cracks are present in the finely layered blocks, especially in the upper part of the layer. Indicators of inspections such as compression, cracking, etc. only occur in the upper part of an affected layer (Nicosia & Stoops, 2017). It can also be assumed that the mixing took place under special conditions: the fine-grained fluvial stratification must have been drier than the underlying sand layer at the time of the disturbance. This would explain the good preservation of the blocks. Although it cannot be completely excluded that the mixing could have been caused by other processes, such as the throwing of substrate by humans, the absence of a tendency to sort coarser particles and the pore structure (no sponge-like microstructure) speak against this (Karkanas & Goldberg, 2018).

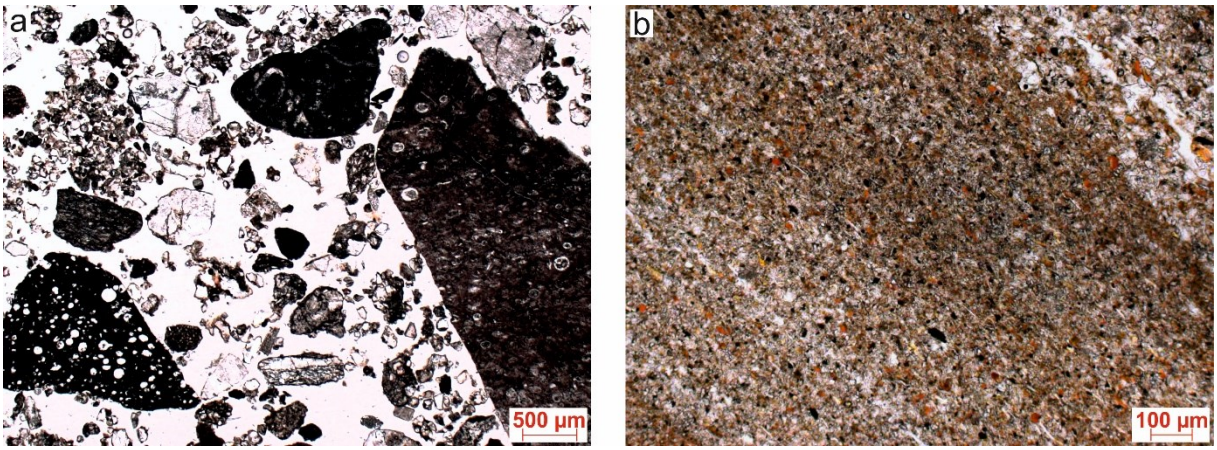

Figure 15: Microphotographs of the thin section TIR-MM2, A: Irregular orientation of coarse-grained particles in the sandy matrix. B: Layering and distinct orientation of silty particles within a clayey block. (Photos: S. Khamnueva-Wendt)

River deposits (E-SB/F-LS/G-GB)

Above the mixed layer, largely undisturbed flood sediments (layer 8), which consist of horizontally laminated silt sands (Sh), were deposited. An increase in the flow velocity then leads to the deposition of layer 7 with coarse sand and fine gravel-rich sediments (Sh). In layer 7 clear flow strips are visible (figure 16). Last flood events as well as high flow velocities are documented in layer 5 by higher coarse sand and gravel contents. The conspicuously high phosphorus content in these layers is due to subsequent contamination by animal or human excretions.

Figure 16: Photo of layer 7 with laminar fine layers and clearly recognizable flow stripes. (Photo: H.-R. Bork)

First foundation (Y2)

The river sediments are covered by an anthropogenic accumulation. The backfill consists of small clayey blocks in a fine sandy matrix. Both the grain size distribution (silt content: 53.5 %) and the organic content (2.2 %) of the backfill show a clear difference to the natural river sediments (figure 18). In addition, this layer is characterized by a slight increase of the phosphorus content to 244.9 ppm.

River gravel (H-CH)

The stratigraphy shows that the anthropogenic application and the associated levelling of the relief changed the flow regime of the river and as a result, it cut into the application layer by lateral and subsequent depth erosion. Several alternations of coarse sand (SB) and fine gravel bars (GB) in the former channel indicate high flow velocities and up to 8 stronger discharge events (layers 2 and 3).

Second foundation (Y3)

Above the fluvial gravel lies another anthropogenic fill Y3, consisting of fine sand with loamy fine sand blocks. The loamy fine sand blocks formed partly flat and horizontally stretched. This indicates with high probability that Y3 was deliberately compacted by humans. In the thin section TIR-MM1, which was sampled from this layer on the north-western profile wall, a weak sorting of the sand matrix can be seen, which, however, does not occur in layers, but in delimited areas (figure 17 A). Together with the embedded clayey blocks, which are mostly sharp-edged (figure 17 B), this can be interpreted as an indication of an anthropogenic fill. The compaction of clayey blocks cannot be clearly identified in the thin section due to subsequent strong bioturbation.

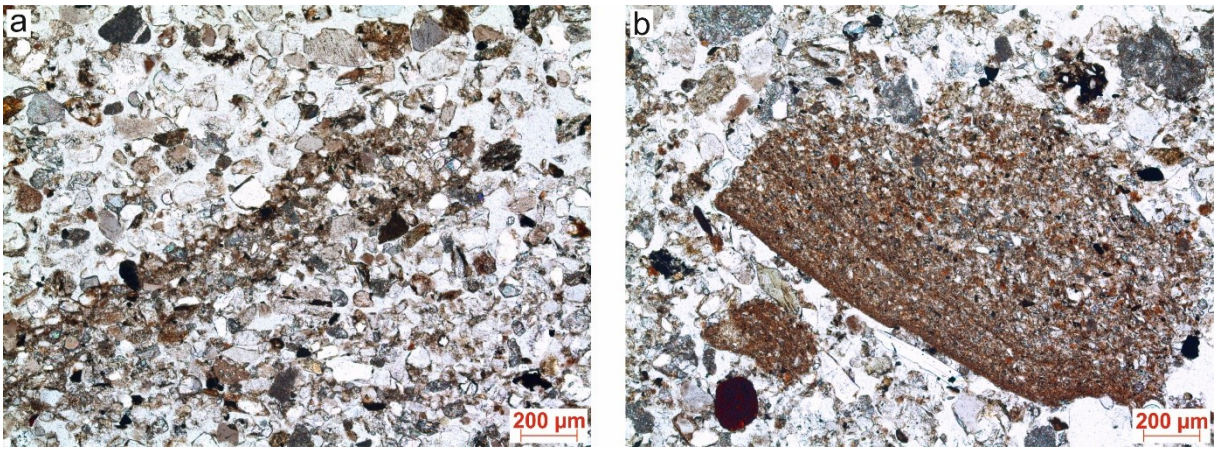

Figure 17: Microphotographs of the thin section TIR-MM 1, A: Weak sorting within the sandy matrix, which occurs fragmentary. B: Sharp-edged loamy block embedded vertically rotated within the sandy matrix. (Photos: S. Khamnueva-Wendt)

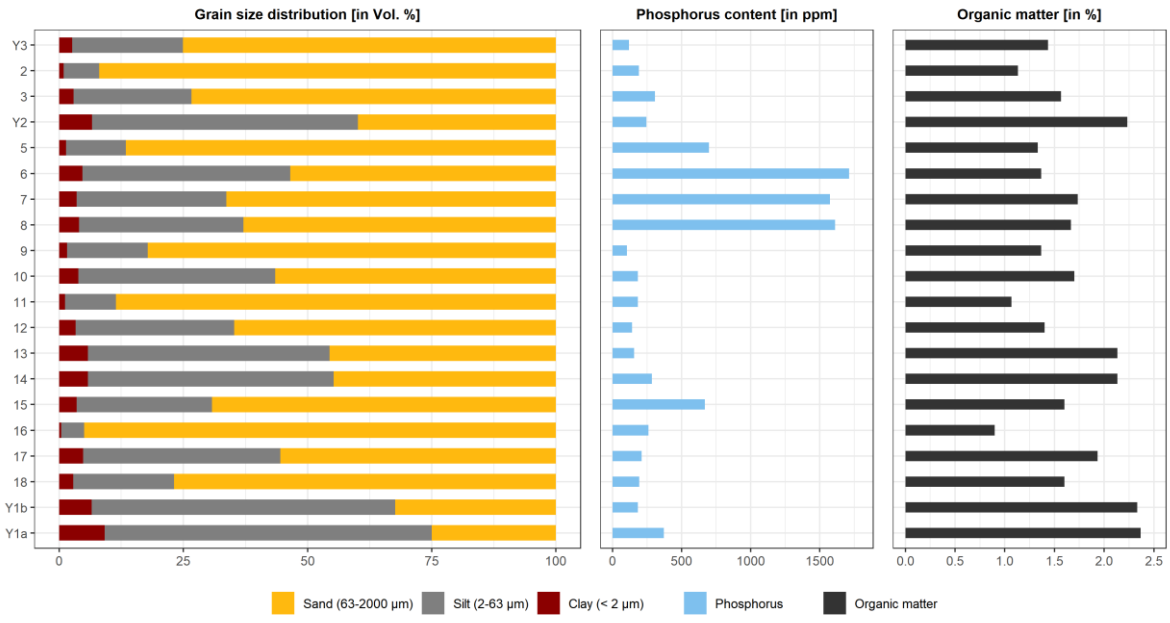

Figure 18: Sediment and cultural layer properties of trench TS-1 at Tiryns. Grain size distribution, Phosphorus content and organic matter.

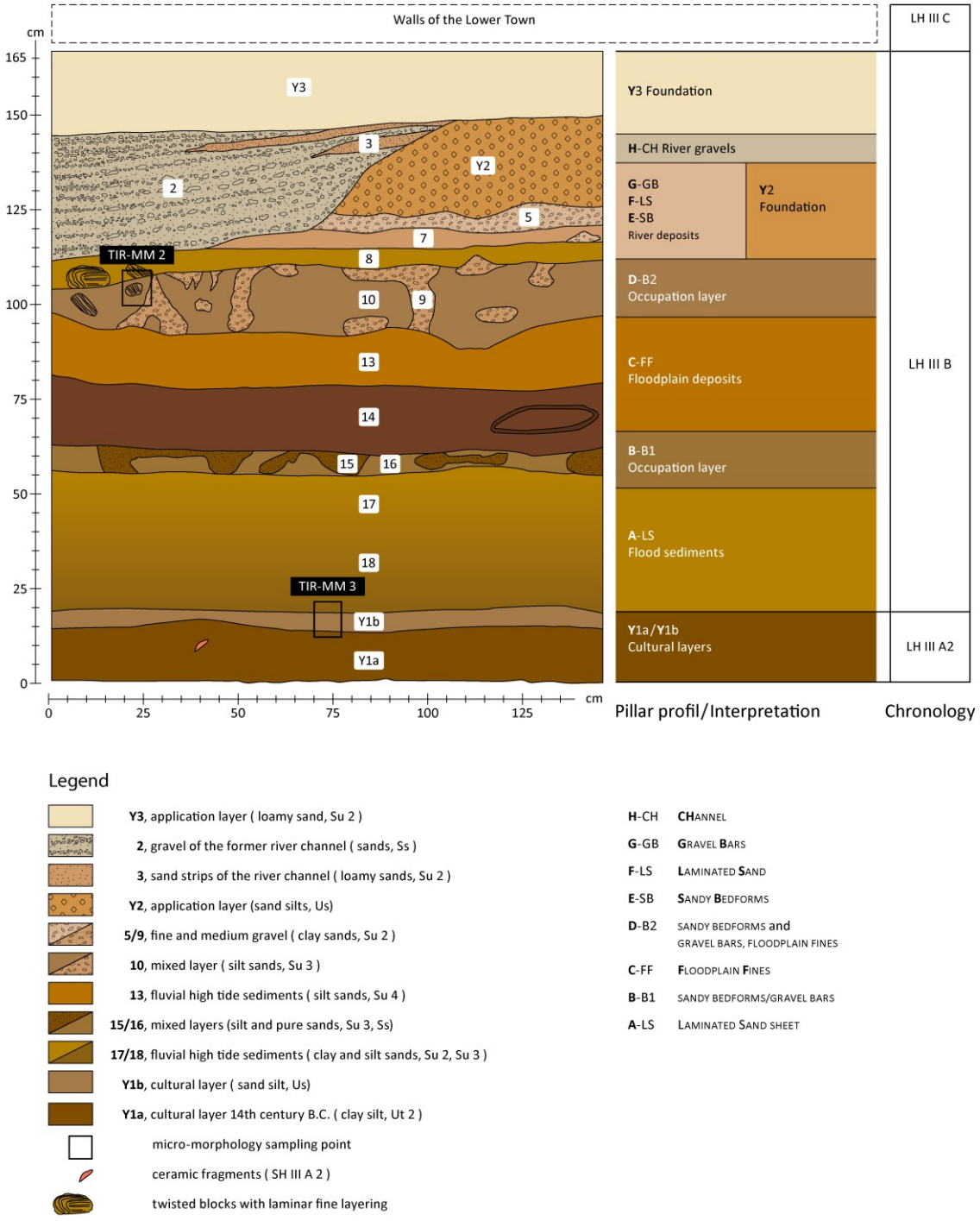

Figure 19: Profile stratigraphy of the trench TS-1 at Tiryns.

5.1.2 The foundation layer

This layer with a very flat surface probably served to create an extensive foundation on which the buildings of the lower town of Tiryns (dated to LH IIIC) could be erected and the floodplain area could be used. The accurate levelling of the area is also shown by the measurements taken during the excavation. For the investigation of the soil-physical properties of the Late Bronze Age building ground, undisturbed soil samples were taken with standardized sampling cylinders (figure 9, see chapter 4.1 for details). The sampling should provide information about the water holding capacity (field capacity), the storage density and the water permeability. For comparison, further undisturbed samples were taken from the layers that had been deposited by flooding (layer 17) and flood events (layer 8). The storage density of the two fills is only slightly different, but the different soil type, i.e. higher contents of silt and clay grain fractions in the fill Y2, leads to a reduction in water permeability (table 7).

Table 7: Saturated water conductivity (kf-value) as a function of soil type and effective storage density (Ld) based on RENGER et. al (2014)

Layer	**Dry density** (in g/cm³)	**Bulk density** (in g/cm³)	**Soil type**	**Kf-value** (class)	**kf** (in mm/h)
Y3	1.45	1.51	Su2	Very high (kf5)	42-<125
Y2	1.45	1.54	Us	Middle to high (kf3-4)	4-<42
8	1.45	1.50	Su3	High (kf4)	17-<42
17	1.53	1.56	Su3	High (kf4)	17-<42

Likewise, the foundation Y3 (TIR S7, S8, and S9) and the fluvial layer 8 (S10, S11 and S12) differed in their ability to retain soil water (figure 20). After complete saturation, the backfill shows a shorter decrease in suction stress than the fluvial sediments. This is due to the different grain size (figure 18), the associated pore space, the humus content and the structure, i.e. the aggregate stability. Based on these characteristics, the backfill can be regarded as an ideal foundation for the lower town.

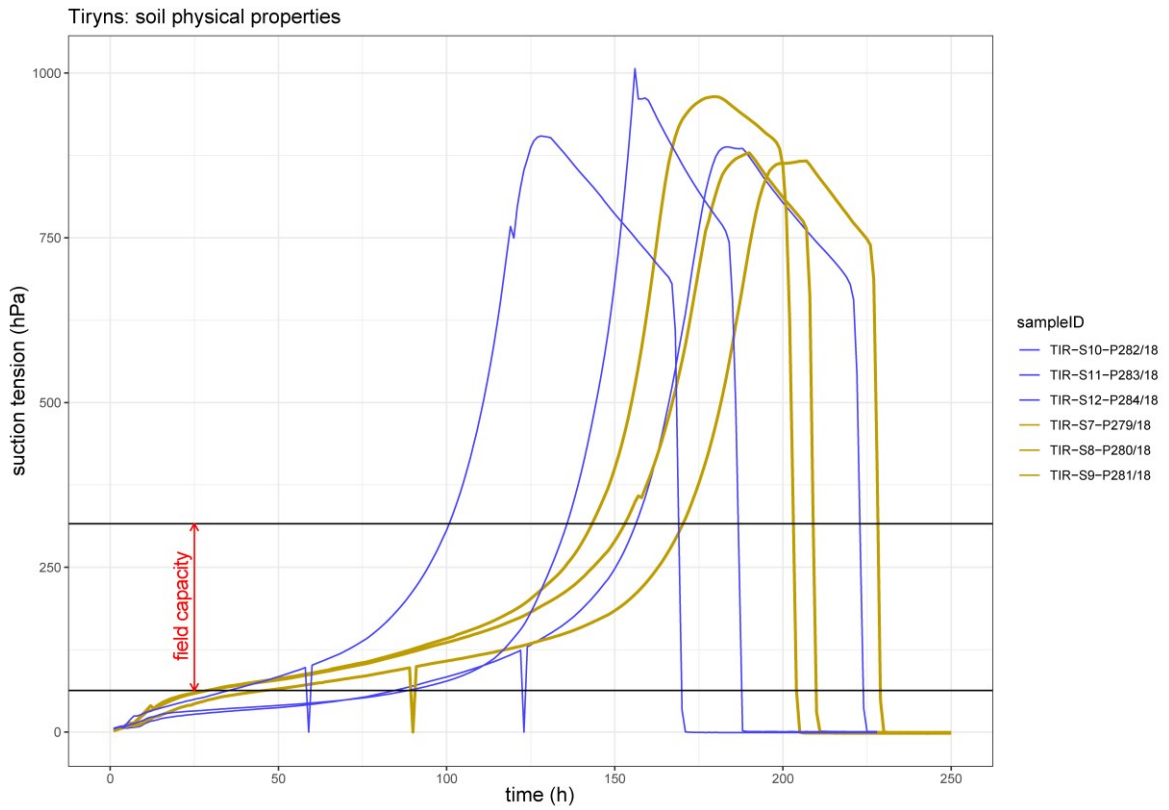

Figure 20: Suction tension as a function of time. From the fluvial layer 8: TIR S10, S11 and S12. From the anthropogenic fill Y3: TIR-S7, S8 and S9. (Graphic: I. Unkel)

5.2 Assessing the soil quality in the Stymphalia polje

The map in chapter 4.1.2 shows the sampling sites from the topsoils and the locations of the documented soil profiles (figure 10). Three transects, T1-T3, were investigated in more detail, which will be presented in this chapter. In order to reconstruct the origin of the soil sediments a cluster analysis was performed.

5.2.1 Statistics

The correlation of the soil parameters measured at Stymphalia was analysed using the R-package corrplot. As the parameters show no Gaussian normal distribution the Spearman correlation was applied and the data was prior standardized (figure 21). The strongest correlation is found in the elements zirconium and titanium (r_{sp} = 0.8). A similar high correlation of titanium exists with potassium (r_{sp} = 0.62),

rubidium (r_{sp} = 0.71), and iron (r_{sp} = 0.65). A further strong correlation exists between the pH value and the elements strontium and calcium and to a lesser extent also with magnesium. The C/N ratio correlates strongly with calcium concentrations and to a lesser extent with magnesium and the pH value of the soil samples. A strong negative correlation can be found between calcium and iron and titanium.

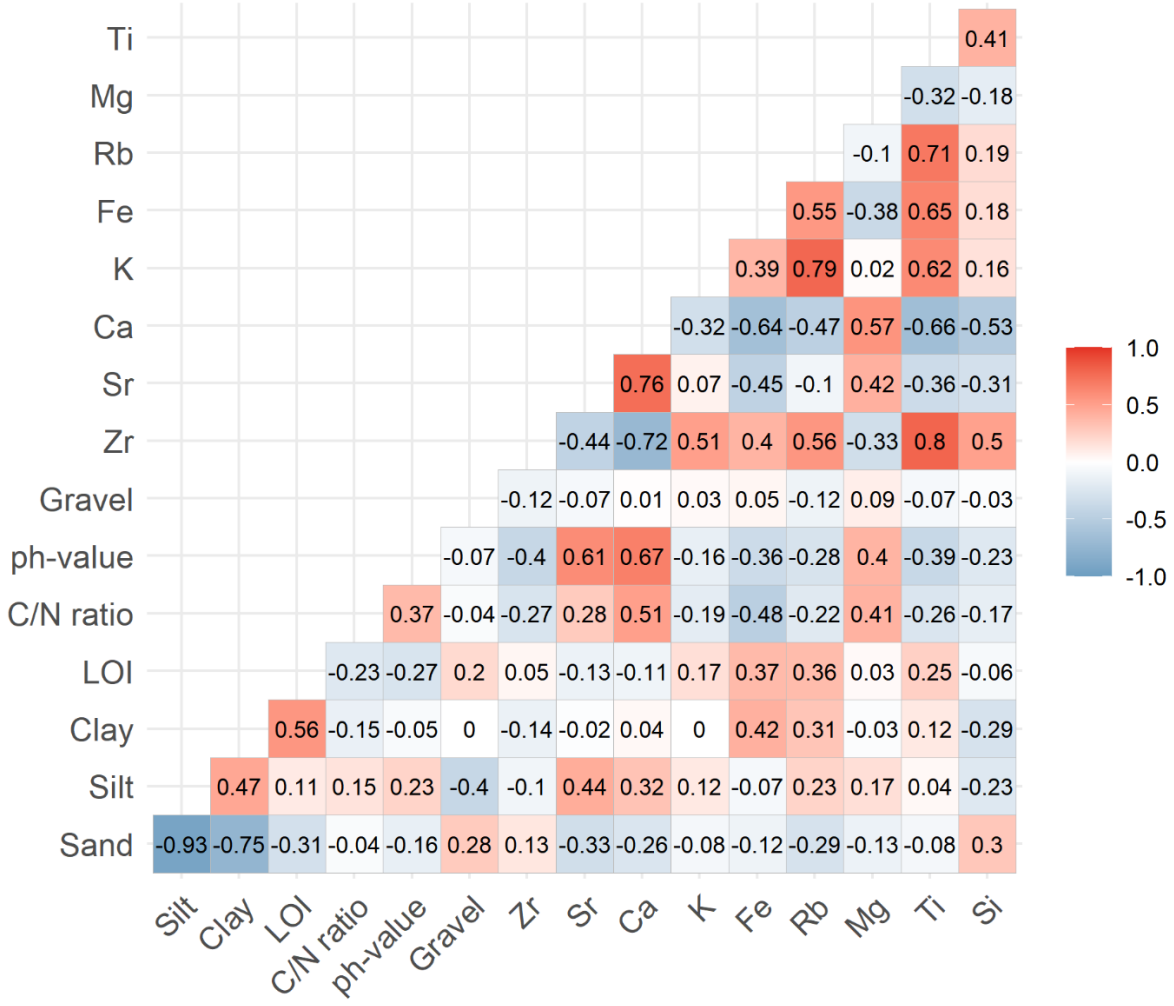

Figure 21: Correlation based on nonparametric Spearman rank correlation coefficient for soil properties measured. Strong correlations (>0.60) marked with a dark blue (strong negative) and a dark red (strong positive) colour filling. Moderate correlations (0.30<r<0.60) are marked with a light blue (negative) and a light red (positive) colour filling.

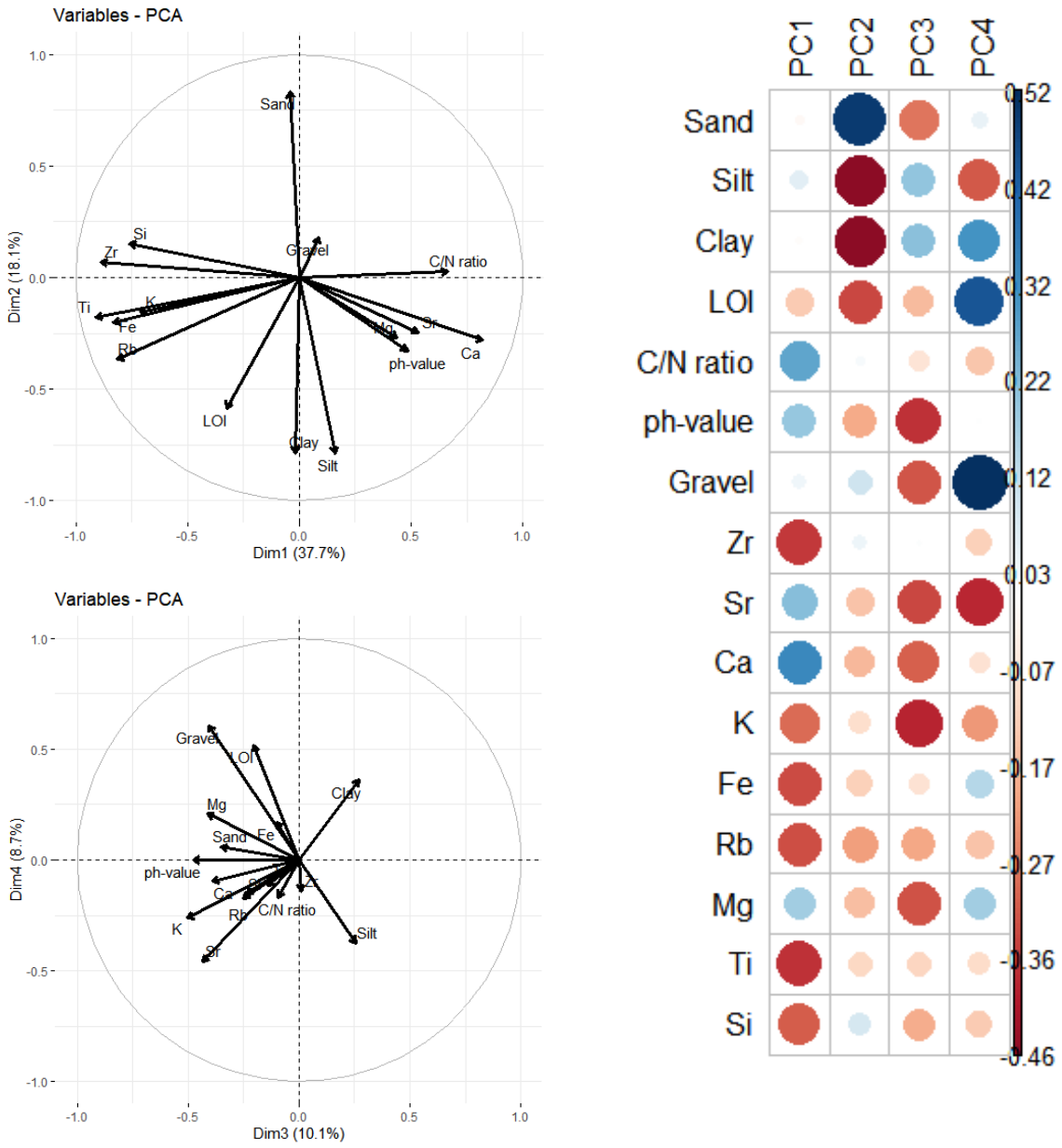

Figure 22: Principal component analyses (PCA) for all soil samples. (upper left) Variable correlation of PCA of soil properties shows correlation between PC1 (Dim1) on the x-axis and PC2 (Dim2) on the y-axis. (lower left) Soil properties correlation between PC3 (Dim3) on the x-axis and PC4 (Dim4) on the y-axis. (left) correlation matrix between soil properties and principal components PC1 – PC4.

Since the choice of the soil parameters is a subjective selection based on the current state of research in published literature (Amacher et al., 2007; Mukherjee & Lal, 2014; Nguemezi et al., 2020), a principal component analysis (PCA) was performed, using R-package prcomp, on all soil samples in addition to get a more objective view of the data. The principal components with high eigenvalues representing the maximum variation of the measured properties. Based on the Kaiser-Guttman

criterion in this study only components of Eigenvalues larger than 1 were examined. The first four components (PC1 – PC4) explain 74.52 % of total variance. The results of the PCA is given in Table 8 and Figure 22. The first principal component is associated with Ti, Fe, Ca, Zr and C/N ratio. PC-2 shows high Eigenvalues on Sand, Silt and Clay. The PC-3 is associated with K, Sr, Mg and the pH value, while the PC-4 shows high Eigenvalues in LOI and Gravel.

Table 8: Results of the principal component analyses (PCA)

	PC1	*PC2*	*PC3*	*PC4*
Eigenvalues	6.02	2.89	1.61	1.38
Variance (%)	37.67	18.06	10.11	8.66
Cumulative variance	37.67	55.73	65.85	74.52
Variables				
Sand	-0.02	**0.49**	-0.28	0.05
Silt	0.07	**-0.46**	0.20	-0.32
Clay	-0.01	**-0.46**	0.21	0.31
LOI	-0.13	-0.34	-0.16	**0.44**
C/N ratio	**0.27**	0.02	-0.07	-0.14
ph-value	0.20	-0.19	**-0.37**	0.00
Gravel	0.04	0.11	-0.32	**0.52**
Zr	**-0.36**	0.04	0.01	-0.12
Sr	0.22	-0.14	**-0.34**	-0.39
Ca	**0.33**	-0.16	-0.31	-0.08
K	-0.29	-0.09	**-0.40**	-0.22
Fe	**-0.34**	-0.12	-0.08	0.15
Rb	-0.33	-0.22	-0.20	-0.15
Mg	0.18	-0.16	**-0.32**	0.18
Ti	**-0.37**	-0.10	-0.11	-0.10
Si	-0.31	0.09	-0.19	-0.13

PC = principal component, underlined values are selected and bold values are highly weighted

5.2.2 Stymphalia Profiles

5.2.2.1 STY-KEF 1 (Kefalari)

Site information				
Profile	Latitude	Longitude	Altitude m a. s. l.	SiteID
STY-KEF 1	22.535380	37.920340	667 m	STYKEF

Figure 23: Northeast view of the site (left), Profile STY-KEF 1 (right).

Site description

The soil profile STY-KEF 1 is located about 1.9 km west of Kefalari, directly on the road to Asprokampos in the eastern area of the polje. The outcrop is located on the middle part of a southwest seceding alluvial fan. The slope is moderately steep (15-30%) and the shaping of the slope is convex in both, horizontal and vertical direction. The human influence is only visible through partially preserved remains of a field terrace. Nowadays these terraces are not in use and lie fallow.

The geological subsurface is developed as an alluvial cone, which is limited by conglomerates in the north, limestones in the south and older alluvial deposits of the polje aligned westward.

Soil description

Near the profile, a rock outcrop emerges downhill, about 200 m in western direction. It shows the conglomerates above described. Many coarse surface fragments, consisting of stones and boulders of limestones, covering the entire site. Furthermore, the area is affected by water erosion. Although the construction of the terrace counteracted erosion processes, clear traces of erosion can be seen due to the destruction of the terrace by the road construction.

The soil profile of the Chromic Luvisol has a thickness of 130 cm and was divided into three horizons (Ap-IBt1-IIBt2, figure 24 and table 9). In general, the soil profile shows a decrease in organic matter with increasing depth. The topsoil horizon shows the highest content of organic matter from 9.42 to 8.04 %, while the lowest Bt2 horizon shows the lowest content with 4.40 %. In addition, the stone content decreases with increasing depth, the range of variation is from 90 % in the topsoil to 40 % in the lowest Bt2 horizon. The dark brown top soil horizon has a thickness of about 15 cm. Due to the high stone content and the subsequent strengthening of the Bt-horizon the rooting depth is very low. While the sand contents in the upper 5 cm with 37.70 % clearly dominate, a strong increase of the silt with 70.80 % and clays with 28.29 % can be found in the parts below. This horizon is further characterized by a moderate C/N ratio ranging from 12.42 to 14.19 and a pH value of 7.2. The Ah-horizon also shows moderate Fe concentrations of about 47000 ppm (pXRF) and very high calcium concentrations up to 32474 ppm (pXRF).

The differentiation of the Ah- to the Bt-horizon below is shown by the increasing red coloration and changing grain size composition. The grain size spectrum shows a significant increase of the clay fraction in the IBt1 horizon, which rises from 20.85 % in the overlying Ah horizon to 27.58 % in the Bt1 horizon. At a depth of 55 cm, there is another abrupt change in the grain size composition. The sand fractions now dominating with 45.27 %. This horizon is further characterized by a low C/N ratio falling to 7.58 and a significant decrease in calcium concentration to 4281 ppm at 100 cm depth. Furthermore, the highest Fe concentrations of 57611 ppm are measured in the IBt1 horizon.

The transition to the lowest documented horizon (Bt2) is shown by sharp boundaries and a distinct brown coloration as well as again changing grain size

composition. The clay fractions falling to 9.07 % and the sand fractions dominating with 59.23 %. The C/N ratio slightly rises to 9.40 as well as the pH-value to 7.28. The Ca concentration reaches a value of 6495 ppm, while the Fe concentration is associated with a decrease down to 35766 ppm.

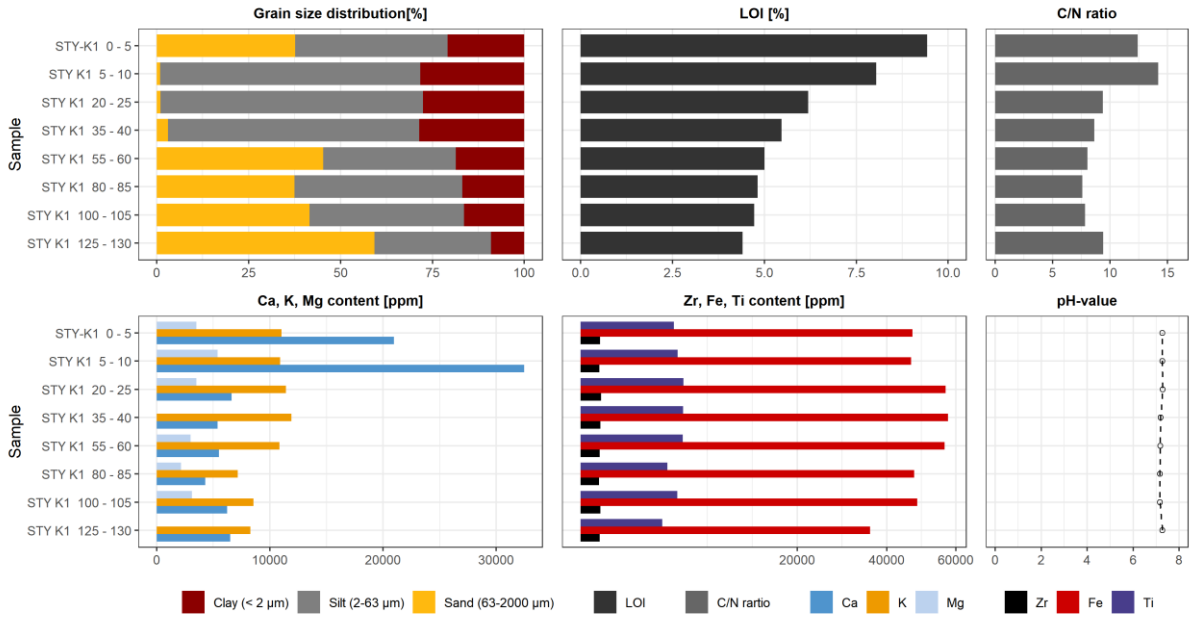

Figure 24: Soil properties of Profile STY-KEF 1.

Table 9: Soil description and classification of Profile STY-KEF 1 grouped by diagnostic horizons

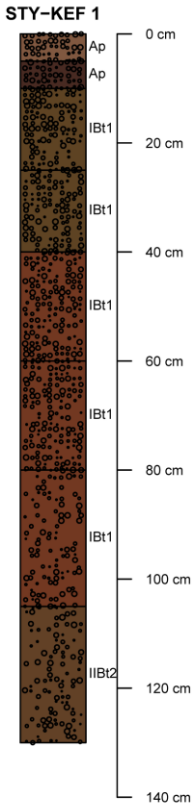

Horizon	Depth [cm]	Munsell Color	Soil type	Description	SQI [%]	Class
Ap	0-5	5YR4/4	Ls2	light brown with a lot of fine sediment interspersed with stones, increasingly loamy and dry	62.5	7
Ap	5-10	2.5YR2.5/3	Tu4		58.33	6
IBt1	20-25	10YR3/4	Tu4	Red soil, strongly weathered, loamy, solid no clay displacement	62.5	7
IBt1	35-40	10YR3/4	Tu4		59.09	6
IBt1	55-60	2.5YR3/6	Ls4		62.5	7
IBt1	80-85	2.5YR3/6	Slu		45.83	4
IBt1	100-105	2.5YR3/6	Slu		54.16	6
IIBt2	105-125	7.5YR3/4	Su3	Brown, slightly humic sediment with sharp horizon boundaries and low stone content	59.09	6

Two OSL dates were made on this profile (table 10). The first date is from the IBt1 horizon at a depth of 76 cm and has an age of 20.0±2.6 ka. The second date is from the IIBt2 horizon below at a depth of 115 cm and an age of 46.7±6.1 ka. These dates prove that the sediments in which the soil formed was deposited in the Late Pleistocene.

Table 10: Results of the OSL analysis from the soil profile STY-KEF 1

Sample	Depth (cm)	K (Bq/kg)	Th (Bq/kg)	U (Bq/kg)	D (Gy ka^{-1})	n	od.	D_e (Gy)	Age (ka)
STY-KEF 1 IBt1	76	253±26	30.3±1.8	36.3±2.1	2.07±0.27	30/28	0.38	41.3±5.1	20.0±2.6
STY-KEF 1 IIBt2	115	214±14	26.4±1.7	38.8±2.3	1.93±0.25	30/24	0.42	90.0± 11.4	46.7±6.1

5.2.2.2 STY-KEF 2 (Kefalari)

Site information				
Profile	Latitude	Longitude	Altitude m a. s. l.	SiteID
STY-KEF 2	22.5172	37.91871	726 m	STYKEF

Figure 25: North view of the site (left), Profile STY-KEF 2 (right).

Site description

The second soil profile is located 1.6 km from STY-KEF 1 to the west directly on the road to Kefalari on an east-facing flattened slope. The surface, of the alluvial fan running out from the west, is slightly inclined and the curvature is stretched in both horizontal and vertical directions. While the terrain flats out southeast towards the Polje, several large alluvial fans are formed in the western part. The outcrop lies in the middle of a former gully, which cuts into the alluvial fan. Further, up the hill some terraces connected to the village of Kefalari.

The geology of this location is dominated by quaternary deposits as well as in the south upcoming limestones. In addition, on the west side carbonate sediments from the Upper Cretaceous and Conglomerates on the northern area surrounding the soil profile.

Soil description

There is a low vegetation cover and many coarse surface fragments, consisting of stones and boulders of limestones, covering the entire site. The outcrop reaches a depth of 245 cm. The soil profile of the Cambisol was divided into five horizons (IAh-ICv+Bv-IIBv-IIIBv-IIIBv-Cv; table 11 and figure 26). The dark brown topsoil horizon has a thickness of 6 cm and shows an organic matter content of 6.74 %, which is strong humus. The stone content decreases with depth, but shows 95 % in the Ah-horizon. The horizon shows a wide C/N ratio of 43.46 and the pH-value of 7.3 is in the weakly alkaline range. The following ICv+Bv horizon below is characterized by the presence of alternating layers containing a very high stone content and raw soil Bv-material, which indicates different phases of surface runoff. These alternating deposits reaching a thickness of 80 cm. They have a low content of organic matter (2.45 %), a wide C/N ratio and a weakly alkaline pH value of 7.52. The stone content reaches a maximum of 85 %, while the grain size composition shows an increase in the sand fractions to 58.87 %. Below a depth of 80 cm, the soil profile shows an intermediary dark brown, IIBv-horizon with a thickness of 100 cm. It differs from the horizons above and below in its particle size composition, the percentage of organic matter, the C/N ratio and the measured elements. The soil has a high clay content of 33.18 and a very prominent silt content of 52.87 %. Further characteristics are an increase of the Zr concentration to 139.72 ppm, the high content of Rb with 94.66 ppm and the high Fe content with 41784 ppm. The horizon also shows an increase in Ca concentration to 67227 ppm and an increased K content to 15686 ppm. The IIIBv horizon follows by a depth of 180 cm. The sand concentration increases significantly to 53.24 %, while the content of organic matter decreases. The previously increased values of the elements Zr, Ca, Fe, Rb and K are also associated with a decrease in this horizon. The pH value of 7.54 is still in the slightly alkaline range. The lowest documented horizon IIIBv-Cv, represents a transitional horizon with a lower stone content of 70 %. The silt fraction with 47.80 % represents the dominant grain fraction, while the clay content with 7.59 % shows the lowest value of the whole soil profile. The organic matter is slightly humus at 2.86 and the pH value rises slightly to 7.63. The Zr, Fe, Rb as well as the K concentration reaching the minimum values in this horizon.

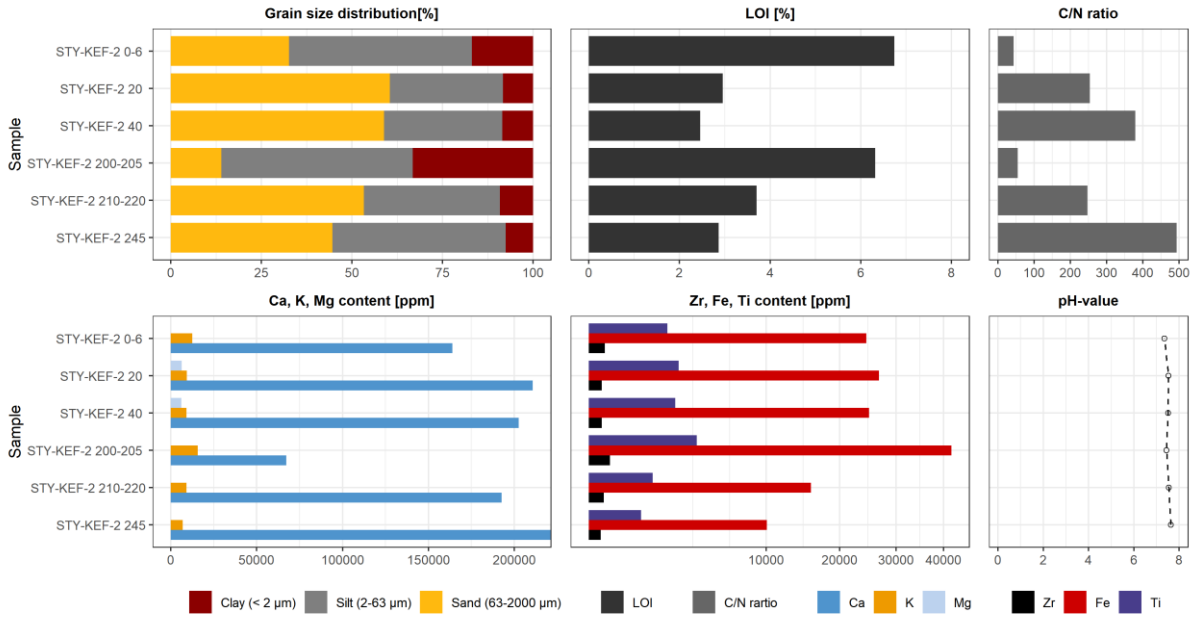

Figure 26: Soil properties of Profile STY-KEF 2.

Table 11: Soil description and classification of Profile STY-KEF 2 grouped by diagnostic horizons

STY-KEF 2	Horizon	Depth [cm]	Munsell Color	Soil type	Description	SQI [%]	Class
	IAh	0-6	10YR3/3	Uls	dark brown, strongly humic A-horizon	68.18	8
	ICv	20	5YR3/3	Sl3	Alternating layers of stony raw soil and brown topsoil sediment	29.16	2
	IIBv1	40	5YR3/3	Sl3	slightly humic and loamy subsoil	29.16	2
	IIBv2	205	7.5YR2.5/3	Tu3	Alluvial fan with interlayered Bv- material	59.09	6
	IIIBv3	220	7.5YR3/3	Sl3	Debris with strongly weathered stones and sparse fine soil	22.72	1
	IIIBv-Cv	245	10YR3/4	Su4	Transitional horizon with similar characteristics as Bv	18.18	1

5.2.2.3 STY-KEF 4 (Kaliani)

Site information				
Profile	Latitude	Longitude	Altitude m a. s. l.	SiteID
STY-KEF 4	22.50435	37.86999	621 m	STYKAL

Figure 27: Northeast view of the site (left), Profile STY-KEF 4 (right).

Site description

The next soil profile was documented about 3.2 km east of the village of Stymphalia in a gravel pit. It is located next to a road to Asprokampos, leading south along the lake, in the southern area of the polje. In the north direction of the outcrop there are adjoining agricultural areas, which are spreading from the lower slope far into the polje. South of it, many field terraces stretch up the slope, whose size and extension appearing very heterogeneous. The field terraces were abounded and felt shallow. The site itself is characterized by several meters thick alluvial deposits. The relief has a slightly concave shape in both directions.

Conglomerates characterize the geological structure in the southern part of the study area. Downhill, to the north quaternary deposits dragging in the direction to the polje filling.

Soil description

While the fields of the polje still use for agriculture, the field terraces lie fallow and were unused. The surrounding area at the outcrop is dominated by shrub vegetation and on the surface, a large number of loose stones, mostly limestones, can be found. The ideal conditions of the Outcrop shows different phases of erosion, which occurred at least since the Pleistocene. Furthermore, there are alternating layers consisting of layers of gravel and red soil sediments that were deposited at this site. The boarders of most of these layers are very sharp in shape and the gravels often rounded, which underlines the assumption of previous occurred erosion processes.

The soil profile of the Cambisol STY-KEF 4 shows three different soil horizons (IC-IIAh-IIBv, figure 28 and table 12). The first horizon shows a 25 cm thick light grey debris layer, consisting of mainly rounded limestones with pivoting diameter from 2 to 10 cm. At a depth of 25 cm the dark brown IIAh horizon connects below. The stone content decreases to 70 % and the dominating grain size fraction is silt with 43.63 % proportion of the fine soil. The slightly humic topsoil contains 4.43 % organic matter and has a wide C/N ratio of 50.40. The pH-value, of the 17 cm preserved horizon, lies at 7.36 in the slightly alkaline range.

The following grey-brown IIBv horizon reaches a thickness of 33 cm and is documented to a depth of 75 cm. It shows a decrease of the sand fractions and increasing clay and silt contents. Thus the clay fractions rising to 21.74 %, while the silt fractions increasing slightly to 53.64 %. The organic matter content remains slightly humic, as in the horizon above. In addition the IIBv horizon shows a wider C/N ratio and with 7.50 a slightly more acidic pH-value. Clear differences of both horizons can be seen in the pXRF measurements. Therefore, the element concentrations of Rb, Fe Mn, Ti, K, P and Mg significantly increasing with increasing depth.

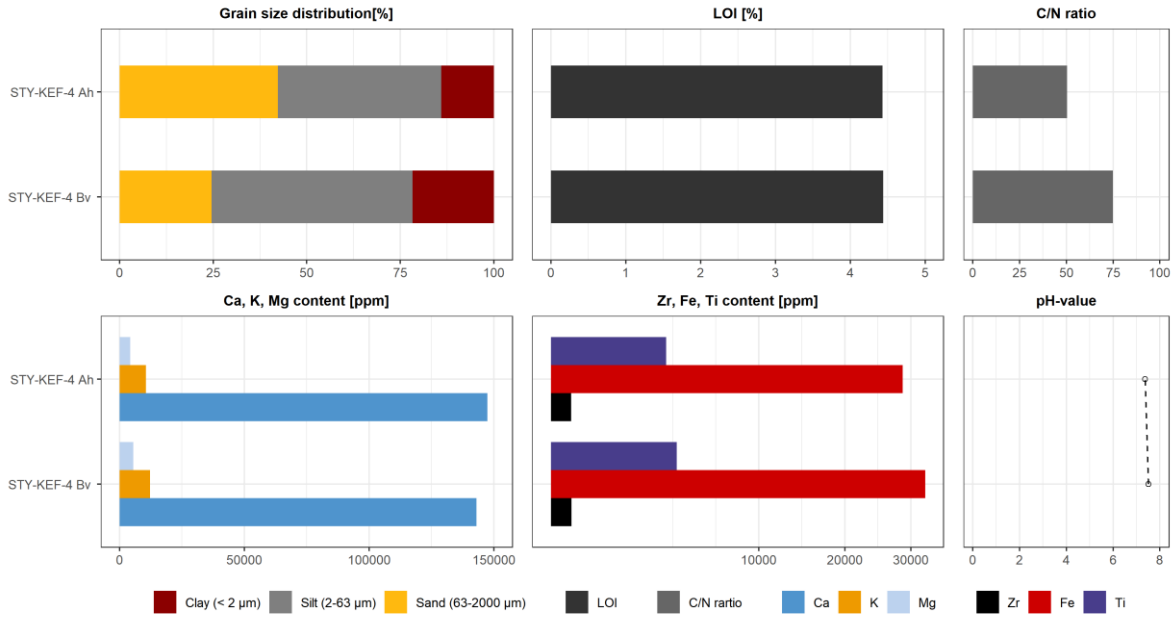

Figure 28: Soil properties of Profile STY-KEF 4.

Table 12: Soil description and classification of Profile STY-KEF 4 grouped by diagnostic horizons

STY-KEF 4	Horizon	Depth [cm]	Munsell Color	Soil type	Description	SQI [%]	Class
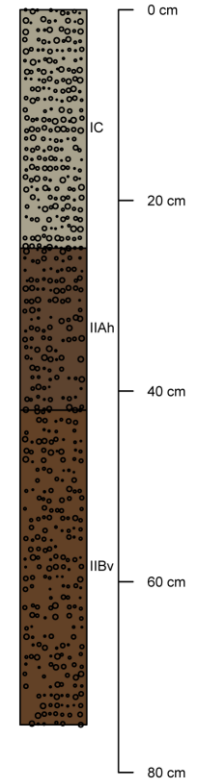	IC	0-25	-	fO	Debris cover of rounded limestones	-	-
	IIAh	25-42	7.5YR3/3	Slu	slightly humic, dark brown topsoil	41.66	3
	IIBv	42-75	7.5YR3/4	Lu	slightly humous, much more cohesive than Ah	50	5

5.2.2.4 ISO-1 (Isomata)

Site information				
Profile	Latitude	Longitude	Altitude m a. s. l.	SiteID
ISO-1	22.50109	37.94362	1.155 m	ISO

Figure 29: Southwest view of the site (left), Profile ISO-1 (right).

Site description

The soil profile ISO-1 is located 2.5 km in west-north direction from the village of Kefalari, directly on the connecting road from Kefalari to Manna. The high plateau connects directly on the east side to the foothills of Mount Kilini at 1.155 m above sea level. Unlike the previous sites, the area is partially covered by coniferous trees (*Abies sp.*). Nevertheless this location is characterized by forest clearing for formerly cultivated field terraces. In contrast to the terraces on the middle slopes of the expiring alluvial fans on the edges of the polje, narrow, stepped terraces on slightly inclined slopes dominate the area. In addition, pasture areas are increasingly appearing. The plateau, which is not that difficult, but rather/distant from the nearest villages, is not marked by arable land and terraced farming has ceased, but the old terraces are still clearly visible.

Pliocene Conglomerates form the parent rock soil material at the Isomata plateau. Further to the west, limestones and dolomites of the Lower Cretaceous and Upper Triassic are present.

Soil description

The surface is formed by a small open space which was probably used for grazing and is surrounded by individual trees. Single larger stones with a diameter of up to 40 cm are lying on the surface. Four different horizons were identified in this soil profile of the Luvisol (M(Ap)-IBt-IBt-Cv-ICv, figure 30 and table 13). The 15 cm thick, dark brown topsoil horizon is very rich in humus and contains 6.48 % organic matter. In the grain size spectrum, the sand fractions dominate with 51.70 %, followed by silt with 36.77 % and clays with 11.51 %. The C/N ratio is moderately narrow by 12.91, while the pH-value with 6.09 lies in the weakly acidic range. The M-Ap-horizon shows wavy borders and a low stone content of 15 %. Below follows a 45 cm thick dark red IBt horizon. The clay content reaches 20.49 %, which indicates clay enrichment and the silt content increases to 49.90 %. The content of organic matter is associated with a slight decrease to 6.05% and the C/N ratio with 8.10 is very close. The pH value of 5.55 is classified as moderately acidic. At a depth of 60 cm, a transitional horizon follows, which has the characteristics of a Bt-horizon with high clay contents at 21%, but appears much brighter than the Bt above it, which is caused by the increase in sand. The soil organic matter drops to 5.64 % and the C/N ratio also becomes narrower. In addition, the pH value (5.43) is increasingly drifting into a more acidic range.

The lowest documented horizon shows clear differences to the previous ones and begins at a depth of 81 cm. The ICv-horizon shows a further increase in the sand fractions to 43.19% and the clay fractions to 15.33%. In addition, the organic matter content reaches the lowest value of 5.07%. In contrast to the transitional horizon above, the ICv has a slightly wider CN ratio and the pH value at 4.85 now lies in the strongly acidic range.

The pXRF measurements show the highest values of Zr with 234 ppm in the MAp horizon.

Although the concentration of Zr in the IBt-Cv-horizon seems to increase slightly, it is generally associated with a decrease to 134 ppm in the ICv-horizon. The Fe concentration of the soil profile shows very high values. They reaching in the top soil 49405 ppm, increasing in the IBt to almost double at 84905 ppm and flatten in the ICv at a value of 69404 ppm. The potassium concentration shows an increase in the IBt horizons up to a value of 14847 ppm. The concentration of Rb also

increases in the IBt horizons, they reaching values of 86 to 95 ppm, while the IMAp and ICv-horizons showing values from 60 to 67 ppm. A decrease with increasing depth shows the concentration of Ti, the highest values are measured in the MAp-horizon with 6022 ppm.

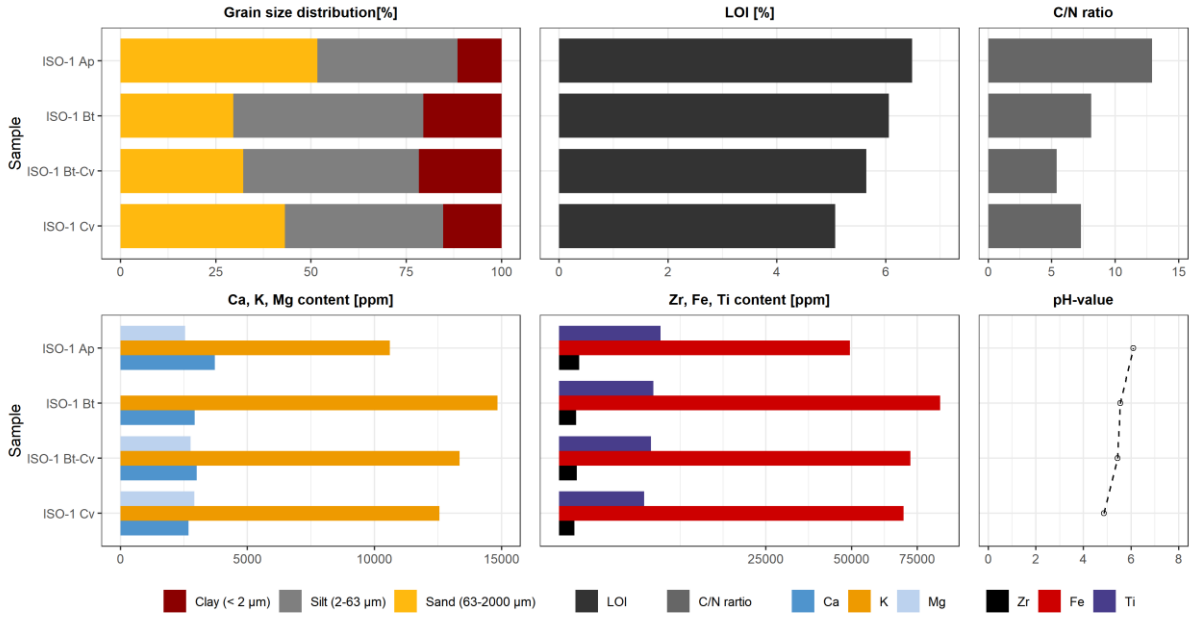

Figure 30: Soil properties of Profile ISO-1.

Table 13: Soil description and classification of Profile ISO-1 grouped by diagnostic horizons

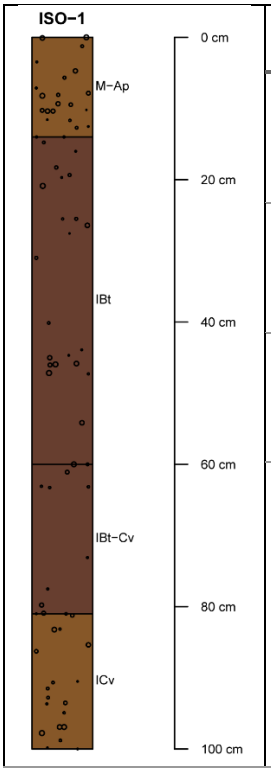

Horizon	Depth [cm]	Munsell Color	Soil type	Description	SQI [%]	Class
MAp	0-15	7.5YR4/6	Sl3	light brown strongly humic topsoil, clearly flat and unsorted	62.5	7
IBt	15-60	2.5YR3/4	Ls2	Red-brown subsoil horizon enriched with clay	72.72	8
IBt-Cv	60-80	2.5YR3/4	Ls2	slightly humic, transition horizon with weathered stones	54.16	6
ICv	80-<100	7.5YR4/6	Slu	overall brighter, many weathered stones, carbonate bonded	37.5	3

This profile is also dated on two different horizons. The M-Ap horizon has an age of 0.19+0.04 ka at a depth of 14 cm. The sediment, in which the Luvisol with the IBt horizon has formed later, has an age of 12.5+1.3 ka at a depth of 33 cm. According to this, the profile reaches a soil development of the Bt horizon of about 45 cm (table 14).

Table 14: Results of the OSL analysis from soil profile ISO-1

Sample	Depth (cm)	K (Bq/kg)	Th (Bq/kg)	U (Bq/kg)	D (Gy ka^{-1})	n	od.	D_e (Gy)	Age (ka)
ISO1-M-Ap	14	392±25	48.0±3.0	57.0±3.0	3.03±0.58	30/30	1.00	0.58±0.11	0.19±0.04
ISO1-IBt	33	390±30	44.7±2.8	49.3±2.9	2.95±0.30	20/13	0.42	37.0±3.5	12.5±1.3

5.2.2.5 STY-P 57 (Stymphalia)

Site information				
Profile	Latitude	Longitude	Altitude m a. s. l.	SiteID
STY-P 57	22.43991	37.86447	686 m	STY

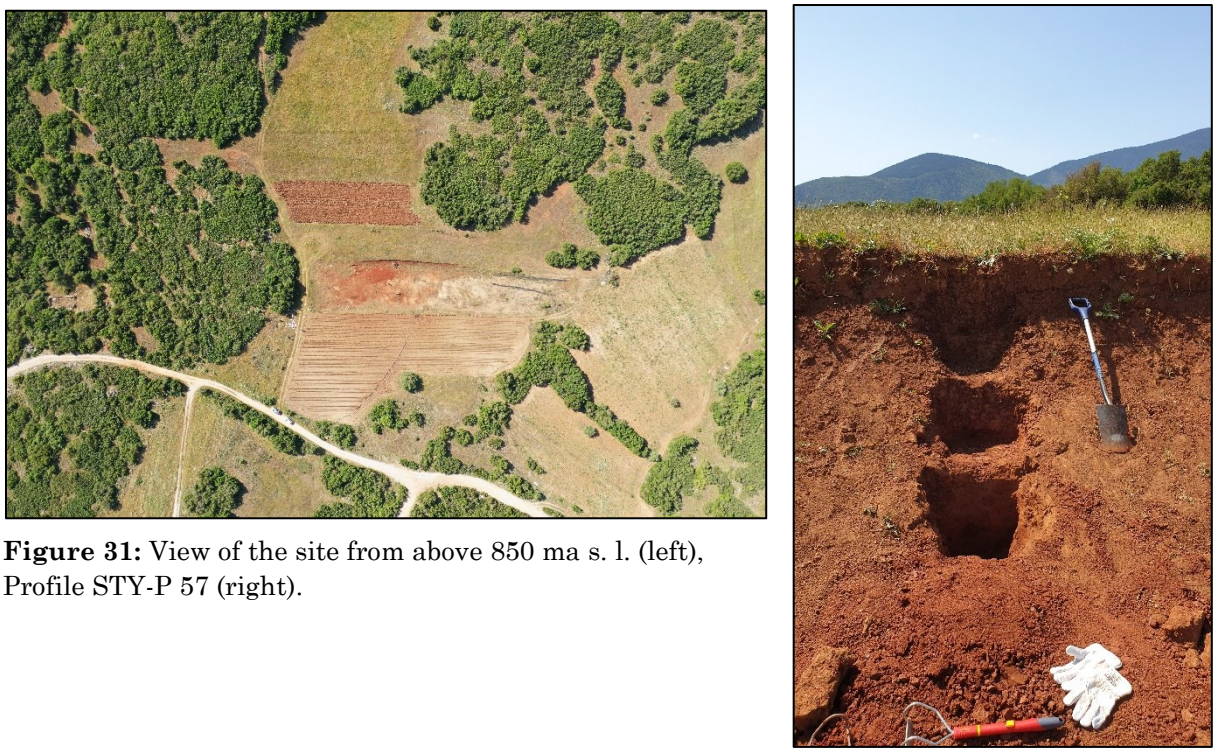

Figure 31: View of the site from above 850 ma s. l. (left), Profile STY-P 57 (right).

Site description

The following location is about 2.2 km west of Stymphalia and can be reached via a small side road that leads from the small village of Kionia to Drosopigi. The small high valley, in the north-western part of the polje, rises north of Lake Stymphalia. The site shows a low gradient and is exposed to the north. The curvature of the relief is elongated downhill and horizontally convex. The management measures include fallow and cultivated fields as well as isolated but abandoned terraces further down the slope. Besides Phrygana, grassland and fallow arable land dominating the area.

The geology of the site is characterised by conglomerates and alluvial deposits in the north. Further northeast, limestones of the Upper Cretaceous occurring. The site itself shows both alluvial and breccias and in the southern part undifferentiated limestones are joining.

Soil description

The surface relief shows a slight waviness with occasional smaller loose stones. The soil profile of the Vertic Luvisol can be divided into four horizons (M(Ap)-M(Bt)-IBt-IBht, figure 32 and table 15). The upper most light brown M-Ap horizon reaches a thickness of 22 cm and containing 15 % coarse soil material. The strong humid top soil, with 6.52 % organic matter content, shows a wide C/N ratio of 35.10 and a slightly alkaline pH value of 7.44. Remarkable are the high silt fractions (58.41 %) and clay fractions reaching 23.84 %. In the following M-Bt-horizon an increase of the clay fractions can be observed. The organic matter content slightly declining to the medium humus range and the C/N ratio with 12.97 is ranked in the middle segment. The pH decreases with increasing depth and reaches a value of 7.48 in the M-Bt-horizon. At a depth of 72 cm a further change of soil horizon occurs. The IBt has a thickness of 45 cm and shows 5.86 % organic matter content. The sand fractions decline, while the silt fractions reaching their maximum at 63.01 %. In addition, the clay fractions increasing slightly to 30.70 %.

The deepest IBht-horizon shows the highest clay content of the whole profile related with a very high organic matter content of 6.42 %. Both, the narrower C/N ratio of 6.75 and the slightly lower pH value of 7.10 distinguish this horizon from the one above.

The measurement of the element concentrations of the horizons showed the following result:

The concentration of Zr increases with increasing depth. In the uppermost horizon 186 ppm were measured while the lowest Bht-horizon shows 236 ppm. This increasing trend is also present due to the Fe, Rb, K and Ti concentrations. The Fe concentrations in the MAp show values of 33799 ppm and rising to 64168 ppm in the IBht-horizon. The potassium distribution shows low values of 11260 ppm in the map horizon, rising to 16992 ppm in the IBt horizon and falling to 15965 ppm in the lowest Bht horizon. However, the Ca and Mg concentrations show a decrease with increasing depth. The topsoil has a Ca content of 66370 ppm and the subsoil a significant decrease to 4063 ppm. The magnesium content in the topsoil is also many times higher than in the subsoil.

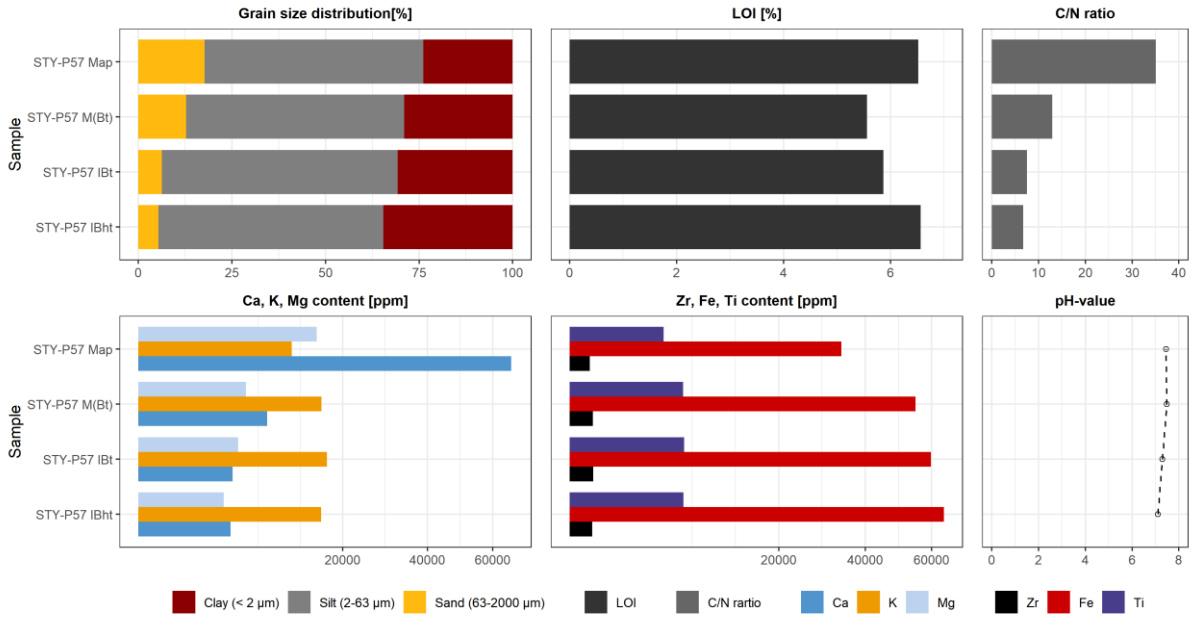

Figure 32: Soil properties of Profile STY-P57.

Table 15: Soil description and classification of Profile STY-P 57 grouped by diagnostic horizons

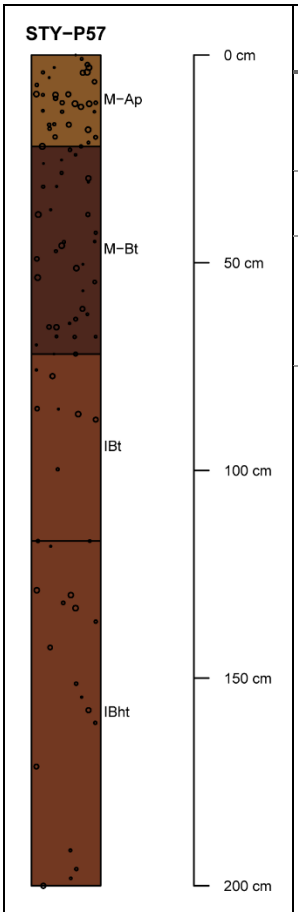

Horizon	Depth [cm]	Munsell Color	Soil type	Description	SQI [%]	Class
M-Ap	0-22	7.5YR4/6	Sl3	light brown strongly humic topsoil	75	9
M-Bt	22-72	2.5YR2.5/4	Ls2	dark-brown colluvium	70.83	8
IBt	72-117	2.5YR3/6	Ls2	Red-brown, clay rich subsoil horizon	75	9
IBht	117 -	2.5YR3/6	Slu	Red-brown, clay rich subsoil horizon, humic rich	70.83	8

5.2.2.6 DRO-1 (Drosopigi)

Site information				
Profile	Latitude	Longitude	Altitude m a. s. l.	SiteID
DRO-1	22.50109	37.94362	858 m	DRO

Figure 33: Northeast view of the site (left), Profile DRO-1 (right).

Site description

The soil profile DRO-1 is located about 970 m southwest of the village Drosopigi in the north-western part of the polje. The site can be reached via a narrow unpaved road that leads from Drosopigi in a westerly direction to the small mountain village Kastania. The outcrop is located on the Middle slope with a steep gradient towards the south-east. The macro-relief appears wavy and the outgoing slope in the south was intersected by a large erosion gully. Field terraces, which are no longer in use, are dominating the site. Here the terraces were arranged by following the convex relief vaults. Although there is a dense vegetation cover, mainly Phrygana, there are also areas of denudation, with only very stony raw soils.

The parent material is mainly formed by phyllite-schists of the Phyllite-Quartzite Unit (figure 3). The phyllites extend over large parts of the site and are only occasionally interrupted by limestones and quaternary deposits are also prominent at this site.

Soil description

The surface is dominated by dense Phrygana growth and an enormous amount of loose small angular limestones and phyllites. The micro relief appears wavy and the surface is further characterised by linear erosion. The soil profile of the Luvisol DRO-1 was divided into 4 characteristic horizons (M(Ap)-M(Bt)-IBht-ICv, figure 34 and table 16). The uppermost, light grey M-Ap horizon shows high sand and silt contents and rather low clay contents with 5.63 %. The 15 cm thick topsoil contains 30 % stones and is weakly humus with 4.47% organic matter. Furthermore, the pH-value of 5.45 is in the moderately acidic range and the medium wide C/N ratio lies at 17.

The underlying M-Bt-horizon shows a significant increase in clay fractions up to 15.77 % and also the silts increase slightly to 53.69 %. With approximately the same C/N ratio, stone content and a slightly more acidic pH value, the content of organic matter increases slightly to 4.76 %. The colluvium reaches a thickness of 15 cm.

From a depth of 30 cm, a red-brown 40 cm thick, IBht-horizon is developed. It shows a slightly higher stone content but the sand fractions are in the lower range with 17.95 %. Furthermore, the clay fractions increase significantly and reach a value of 23.16 %. Furthermore, the horizon shows a narrow C/N ratio of 8.34 and an increase of the humus content to 5.58 %. With a pH value of 4.32, the IBht has to be classified as strongly acidic.

The lowest ICv horizontal has a very high stone content of 95%. The sand fractions now come to the fore with 53.09 % and the organic matter content is also associated with a considerable decrease to 2.83 %. The C/N ratio rises to 12.93, while the pH value continues to tend towards the strongly acidic range.

The Zr concentration shows the highest value in the topsoil with 420 ppm and decreases with increasing depth to 275 ppm in the IBht horizontal. In contrast, Rb concentrations show an increase in the M and IBht horizons. Values of 144 and 129 ppm were measured there. The Fe concentrations show an increase up to the IBht horizon where they reaching the highest values of 58282 ppm. The Ti and Mg concentrations show a heterogeneous distribution, on this occasion the values of the MAp increasing slightly compared to the M-horizon, decline in the IBht and then reaching the lowest values in the ICv-horizon. The potassium distribution in

the soil profile remains more or less constant around 20000 ppm, whereas the Ca concentrations decrease with increasing depth, reaching the lowest value in ICv at 979 ppm.

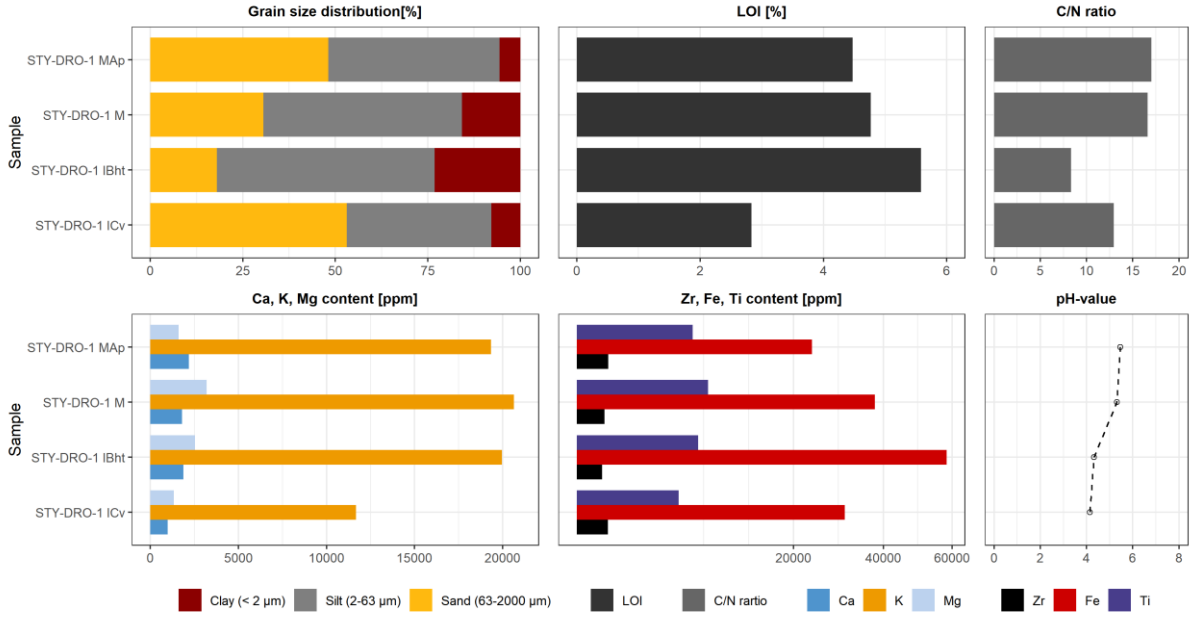

Figure 34: Soil properties of Profile DRO-1.

Table 16: Soil description and classification of Profile DRO-1 grouped by diagnostic horizons

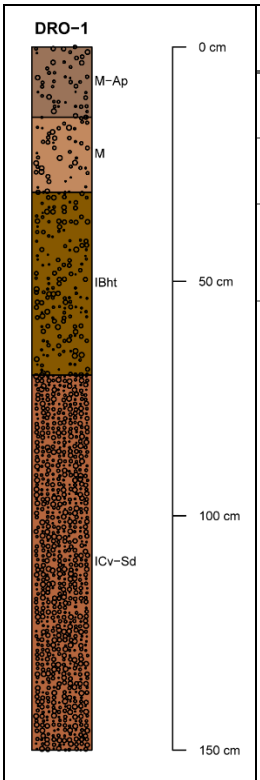

Horizon	Depth [cm]	Munsell Color	Soil type	Description	SQI [%]	Class
M-Ap	0-15	5YR5/4	Su4	light brown and humic topsoil	25	1
M-Bt	15-30	5YR6/6	Uls	dark-brown colluvium	41.66	3
IBht	30-70	10YR4/8	Lu	Red-brown, clay rich subsoil horizon	58.33	6
ICv	70 - <150	2.5YR5/8	Su3	Red-brown horizon, very stony	12.5	1

5.2.2.7 ASP-1 (Asprokampos)

Site information				
Profile	Latitude	Longitude	Altitude m a. s. l.	SiteID
ASP-1	22.55021	37.88668	668 m	ASP

Figure 35: Southwest view of the site (left), Profile ASP-1 (right).

Site description

The next site ASP-1 is located in the east side of the polje, which is situated about 970 m west of the centre of the small village Asprokampos. The outcrop was documented directly on the road coming from Stymphalia to Asprokampos, on the top of a slope, before the small valley basin connects into the east direction. The strongly inclined slope, which is exposed to the northwest, shows a convex shape in horizontal and vertical direction. Mainly Phrygana shaping the landscape, but also some Aleppo pines are present. In the near surroundings, there are mainly vineyards cultivated. The geology mainly consists of Marls, which includes sandy marls, sandstones, sands, pebbly- and marly conglomerates from the Upper Pliocene Diluvium. The basin itself, is dominated by old and new cones of debris and slope debris as well as alluvial deposits on the valley floor.

Soil description

At this site, young stocks of cypress and thuja trees (*Cupressaceaeas*) well as heavy landslides occur partial caused by erosion. Four different horizons are developed in the soil profile ASP-1 (Ah-Bt-Cv-cC, figure 36 and table 17). The topsoil of the Luvisol reaches a thickness of 6 cm and is very humus with 10.84% organic matter. The grain size distribution in the Ah horizon shows 50.68 % silt, 18.19 % clay and 31.12 % sand proportion. The stone content of the dark brown soil horizon lies at 3% and the C/N ratio lies in the medium range with 14.23.

Underneath follows the 34 cm thick brown Bt horizon, which shows a considerable increase of the skeleton soil. This horizon is further characterised by a lower proportion of organic matter and a significant increase in clay fractions to 23.99 % as well as a significant decrease of the sand contents.

The pH value moves increasingly into the slightly alkaline range with 7.47.

From a depth of 40 cm a light grey Cv horizon with a high C/N ratio is formed. In the grain size spectrum the silt fractions now dominate with 71.03 %, while the sand fractions reaching the minimum of 12.31 %. The organic matter content shows a clear decrease to 3.16 % and the pH value of 7.71 moves further into the alkaline range.

The light grey subsoil cC-horizon lies at a depth of 70 cm and has a thickness of 40 cm. The silt fractions continue to dominate the grain size composition with 73.99 %, while the sand contents continue to decrease. Minor changes to the overlying horizon can be seen in the content of organic matter and the pH value.

The measured elements showing clear differences in the individual soil horizons. Both, the Ah and Bt horizon reaching high values of Zr with up to 187 ppm, whereas in the subsoil horizons only 53 ppm were measured. The Fe concentrations staring in the Ah with 44507 ppm, rising in the Bt to 49262 and decreasing until the cC subsoil to 8932 ppm. These element fluctuations can also be seen in the Ti, K and Mg concentrations. Accordingly, the Bt horizon shows an enrichment of these elements. However, a different fact is given by the Ca concentrations, which increasing by increasing depth. The lowest values are prominent in the Ah horizon at 12769 ppm, increasing slightly to 18098 ppm in the Bt and rising many times higher in the Cv to 284770 ppm an reaching their peak in the Cc with 305807 ppm.

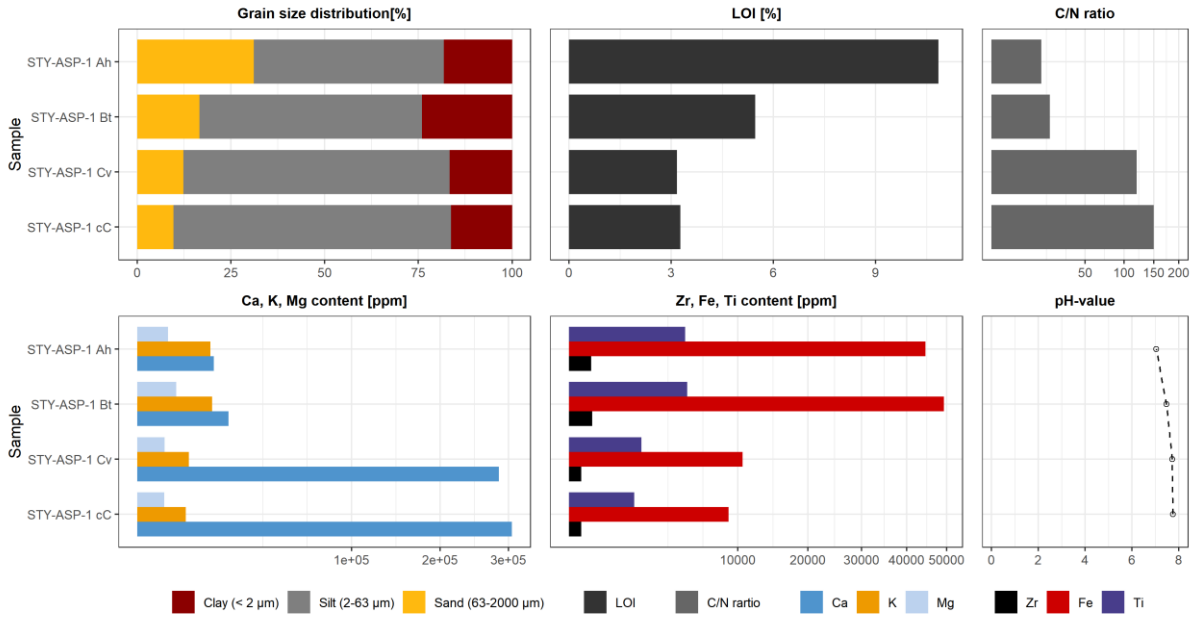

Figure 36: Soil properties of Profile ASP-1.

Table 17: Soil description and classification of Profile ASP-1 grouped by diagnostic horizons

ASP-1	Horizon	Depth [cm]	Munsell Color	Soil type	Description	SQI [%]	Class
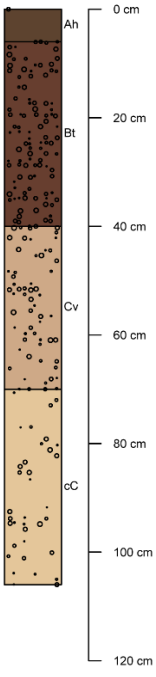	Ah	0-6	7.5YR3/3	Lu	dark brown and humic rich topsoil	75	9
	Bt	6-40	2.5YR3/4	Lu	dark-brown and loamy subsoil	70.83	8
	Cv	40-70	7.5YR7/4	Ut3	Light beige and silty C-horizon	75	9
	cC	70 - <106	10YR8/4	Ut3	Light beige and much fine slack material	70.83	8

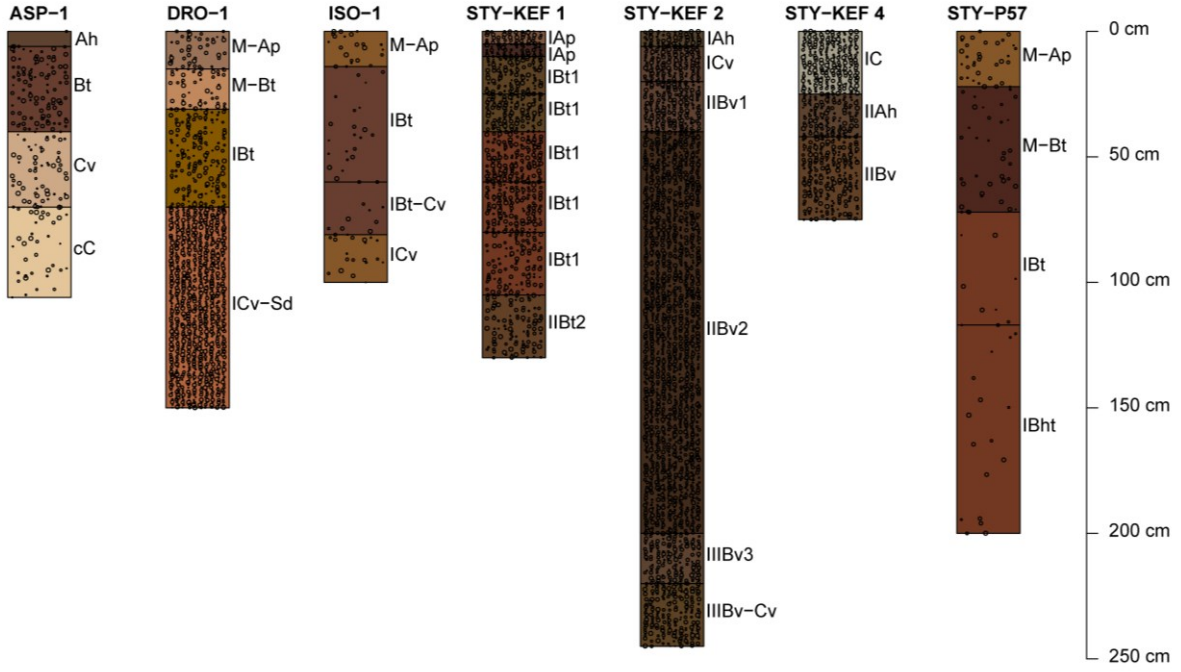

Figure 37: Overview of the documented soil profiles in the study area.

Figure 37 shows a summary of the predominant soils in the study area. Except for the site at Asprokampos, the profiles show the anthropogenically induced but also the geomorphological dynamics of this region. Colluvial deposits were found at three sites. The B-horizons documented below the colluvial horizons show sharp and flat horizon boundaries, indicating previous erosion processes. Calcium carbonate has often cemented the material, which leads to an extremely high soil stability. The colluvial deposits are characterized by humuic and fine-grained topsoil material. Two sites (STY-KEF 2 and STY-KEF 4) are characterized by strong hemp debris flow with high stone content and interconnected humous fine-grained topsoil sediment. Accordingly, Leptosols, Luvisols, Vertic Luvisols and Cambisols are predominant in the study area.

5.2.3 Spatial distribution of soil sediments

5.2.3.1 Transect 1

Transect 1 is located in the western part of the polje and comprises a total of 7 sites. The transect extends from north to south over a length of 4.6 km. The distances between the sampling points are between 600 m and 1.1 km (figure 38, figure 39 and table 18).

The northernmost site of the transect, **STY-P 55** is located on a central slope at 810 m above sea level, which is exposed to the southwest. The slightly inclined slope shows a wavy micro-relief and convex curvatures parallel to the slope as well as downhill. The terraced site shows extensive erosion and represents a fallow arable land, which appears as open area with less or no vegetation. The grain size distribution shows a slight increase in sand fractions with increasing depth. According to this, up to 34.02 % sand content is reached at a depth of 20 cm. The organic matter content on the surface reaches 6.80 % and decreases to 5.27 % at a depth of 20 cm. The C/N ratio at this site is moderate at 10.70 and ideal for the B sample at 8.55. The nutrient availability indicates high reserves of potassium with up to 15776 ppm and a moderate availability of magnesium with 4906 ppm. Possible deficiencies occur only at the calcium concentration, which is at a maximum value of 8421 ppm. The soil of this site shows a decrease of the SQI with increasing depth but still shows a high soil quality with 79.16 and 62.5%.

Site **STY-P 56** is located 660 m southeast of STY-P55, also exposed to the south on a slightly inclined slope 730 m a. s. l. The curvature of the slope is concave in both directions and the micro relief appears smooth. This site was also terraced, is affected by extensive erosion and was used as arable land, which now lies fallow. In contrast to STY-P 55, this site has an enormously high skeletal content in the soil of 75 %. There are also significantly lower amounts of organic matter with 4.51 and 4.90 %. Furthermore, a low C/N ratio occurs at this site. The grain size composition shows a clear decrease of the sand fractions with increasing depth. The pXRF measurements of potentially available nutrients show significantly higher Ca concentrations in both sampling points. The values reached 53666 ppm in STY-P56A (0 cm) and 66085 ppm in STY-P56B (20 cm).

Site **STY-P 57** is located 600 m south of STY-P 56 on the same slope/in the same side valley of the polje at 727 m a. s. l. The risk of erosion at this open area is rather low. The relief is vertically elongated and horizontally convex while the roughness appears wavy. Both horizons A and B are only slightly different at this location. The content of organic matter with 7.24 and 6.27 % is significantly higher than STY-P 56 and the stone content with 15 and 10 % is also clearly lower. While the Ca and K concentrations in the soil are not very different, the Mg concentrations show significantly higher values compared to the last sampling point. These are many times higher with 15372 and 11155 ppm.

Following the Transect in a south-easterly direction about 1.1 km from the last site, **STY-P 58** is located in the transition area of alluvial fans and the sedimentary deposits of the polje. Samples were collected at the steep southeast inclined central slope. The relief appears stretched in vertical and convex in horizontal direction. The relief, characterized by erosion, appears stretched in vertical and convex in horizontal direction. In the grain size composition the clay fraction now dominates with values of up to 34.88 % with only low sand content of up to 3.76 %. The topsoil has an enormously high content of organic matter, the values of the A-horizon show 18.11 % and those of the B-horizon 15.00 %. While the potassium values did not differ much from the previous site, the magnesium content is significantly lower in both horizons. They are only reaching values of 3966 to 3115 ppm.

Site **STY-P-59** is located about 500 m to the south and 1.1 km west of the lake. The terrain declines slightly to the south and has a convex shape in both directions. Like most parts of the polje, the site is used for agriculture. The grain size composition is dominated by the sandfraction with 47.17 % in the A-horizon, while the B-horizon shows high values of silt fraction with 50.82 %. In addition, the soil offers a medium humus content and a moderate C/N ratio. The potassium concentration of the A and B horizons increases slightly to 19133 and 18892 ppm respectively. Significant differences to the site STY-P58 can be seen in the much lower Ca concentrations in the soil.

Further 880 m to the south the next site **STY-P 60** follows, which is located on the southern edge of the flat polje area. The slightly northward sloping terrain shows a stretched curvature with wavy roughness. The site is at 640 m a. s. l. and also used for agriculture. The difference to STY-P 59 is mainly reflected in the

concentration of Ca at 55190 ppm. The slightly higher values of magnesium are also noticeable, with the concentration rising to 6042 ppm in the A-horizon and to 7309 ppm in the lower horizon. In addition, the soil is characterized by a low C/N ratio, a decrease in organic matter and very high silt contents up to 67.13 %.

Site **STY-P 61** is the last location of this transect. It is located another 700 m uphill in the southern part of the study area. The strongly inclined slope is north-exposed and shows in vertical direction a concave, in horizontal direction a stretched curvature. Furthermore, the site is located on the central slope on a former agricultural terrace at 710 m above sea level. The grain size analysis shows a significant high clay content, which rise to 22.90 %. The proportion of organic matter in the soil is also considerably higher than in the polje with 14.33 and 7.49 %. The Ca and Mg concentrations also show a significant difference to STY-P 59. The Ca concentrations increase to 101821 ppm and the Mg contents reaching 18833 ppm.

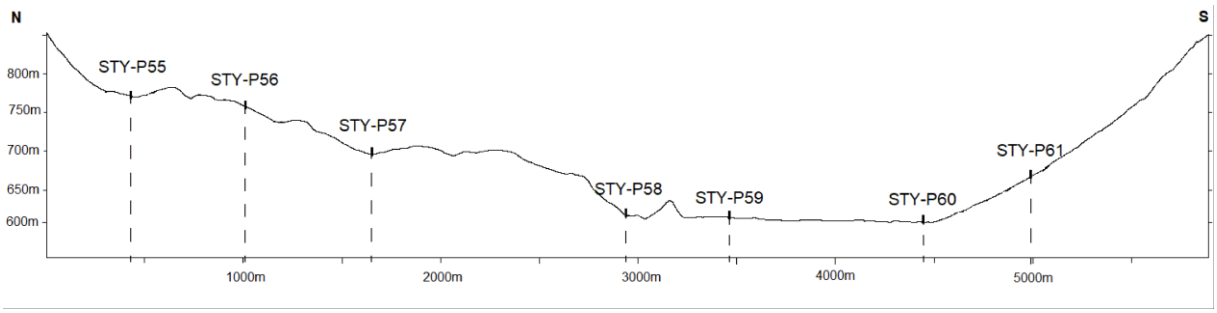

Figure 38: Cross section of Transect 1.

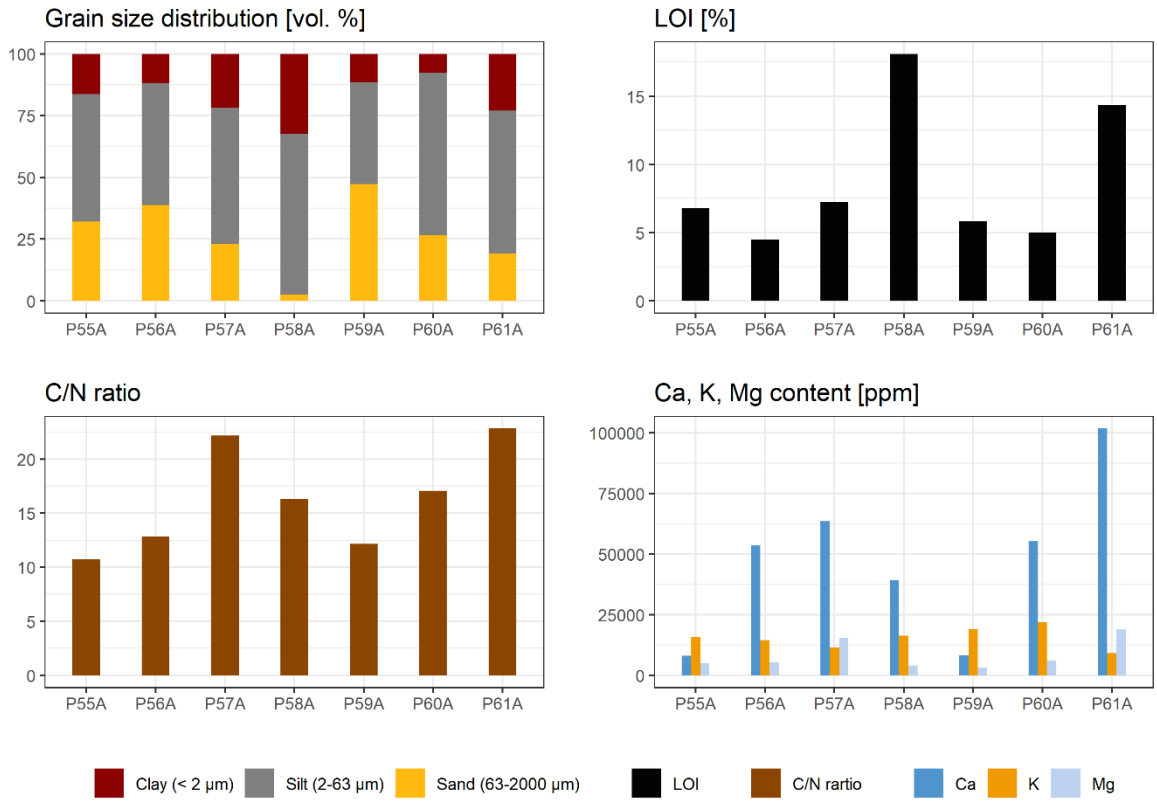

Figure 39: Soil properties of Transect 1.

Table 18: Site specific and relief referring characteristics of Transect 1

Site	STY-P55	STY-P56	STY-P57	STY-P58	STY-P59	STY-P60	STY-P61
Altitude	810	730	727	654	648	640	710
Inclination	N2	N2	N1	N4	N2	N1	N3
Exposition	SW	SS	NN	SO	SS	NN	NN
Position	M	M	T	M	T	T	M
Appearance	T	T	P	FE	FE	P	FE
Curvature	V, V	V, V	G, X	G, X	X, X	G, G	V, G
Type of use	BA	BA	A	G	A	A	BA
SQI A	79	50	75	50	41	70	79
SQI B	62	54	66	70	58	70	79

5.2.3.2 Transect 2

Transect 2 cuts through the middle of the polje over a distance of 7.8 km along its longitudinal axis in northeast to southwest direction. It includes a total of 7 sites, which are located about 1 to 2 km apart (figure 40, figure 41 and table 19).

STY-P28 the northernmost site of the transect is at 625 m a. s. l., on a slope that inclines strongly to the east. The relief of the alluvial fan is developed convex in both horizontal and vertical direction. The grain size spectrum is dominated by silts, but the clay fractions show high values in the A-horizon and the highest values of the transect in the B-horizon with 30.23 %. In addition, a narrow C/N ratio and a high humus content are predominant. Potassium concentrations also provide the highest values of the whole transect with up to 19403 ppm in the B-horizon. Comparatively medium concentrations are reached for calcium and magnesium.

Site **STY-P 29** follows further to the southwest. The site, which also faces east, has only a slight incline and is also used for agriculture. At this location, a clear increase of the sand fractions to 35.12 % in the B-horizon can be recognized. The humus content is similar to site STY-P 28 with a decrease and the C/N ratio reaches higher values. Concerning the nutrient availability a relatively high Ca value of 87449 ppm (A-horizon) and 80569 ppm (B-horizon) is shown. The potassium availability decreases slightly but the magnesium concentration also shows slightly higher values than site STY-P 28.

Site **STY-P63** is located in a southwest exposed position of a south facing/dipping alluvial fan. The central slope is strongly inclined and has a concave shape in horizontal and vertical direction. The soil physical and chemical properties of the soil are very similar to those of the site STY-P28. A slight discrepancy can be observed in the content of organic matter, which is slightly higher in the A-horizon with 10.15%. In contrast, potassium concentrations are slightly lower at 17828 ppm.

STY-P23 is located about 1.1 km from STY-P 63 at 775 m above sea level. The site itself is located on an easterly exposed hillside on a formerly used field terrace. The soil treatment is shown by a concave slope shape in vertical direction. The dominant grain size fraction in the A- and the B-horizon are the silt fractions with

59.11 %. The humus content decreases slightly with increasing depth from 6.90 to 5.57 %. Furthermore, the site is characterized by an enormously high Ca concentration, which reaches 131374 ppm in the topsoil and slightly decreases to 120643 ppm in the lower horizon.

Site **STY-P 24** approximately 950 m southeast at 615 m a. s. l. is located on the northern margin of the plain. The agriculturally used site drops slightly to the south. Significant differences to the previous site can be seen in the Ca concentrations, which are clearly lower here, dropping to 64787 ppm. Also, the skeleton content is significantly reduced to 5 %, whereas the K concentrations show a slight decrease. The grain size spectrum shows a significant increase in sand fraction to 37.77 % in the A-horizon and 35.47 % in the B-horizon. The content of organic matter ranges from 5.64 % to 5.92 % in the medium humus range and the C/N ratio can be classified as moderate. Another deficit of this site is its availability of nutrients. The Ca concentrations show clearly lower values than the previous sites and also the potassium concentration is only moderate.

STY-P 18 is located about 1.4 km north-east of the Lake Stymphalia at 600 m above sea level. The relief is slightly inclined to the south in the direction of the lake and has an elongated shape. The site was formerly used for agriculture. Compared to site STY-P 24, this location has a higher sand content, which is now 37.77 % in the A-horizon and 35.47 % in the B-horizon. Both horizons are in the medium humus range and have a moderate C/N ratio. The slightly elevated magnesium content of 4123 ppm in the A horizon is remarkable.

STY-P 45, the last location of this transect is 600 m north of the lake at 600 m above sea level. The lowland plain shows a slightly northeasterly dropping terrain with an elongated curvature. Silts with 64.17 % dominate the grain size spectrum, while the clay fraction presents the second largest group with 24.03 %. Considerable differences in connection with the availability of nutrients occur with increasing depth. The Ca concentrations decreasing but the potassium values increasing to 15290 ppm in the lower horizon. The magnesium concentrations also rises from 3822 ppm in the A-horizon to 5418 ppm in the B-horizon.

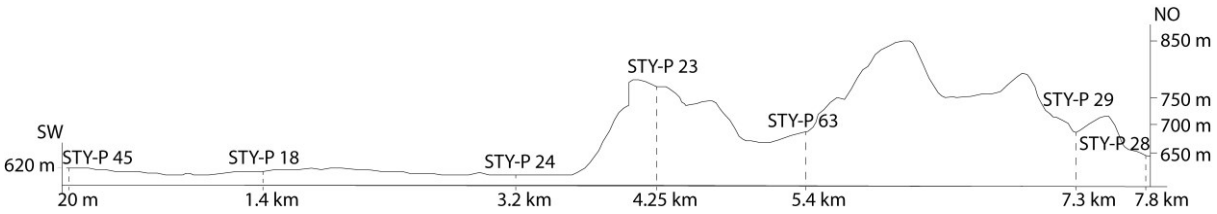

Figure 40: Cross section of Transect 2.

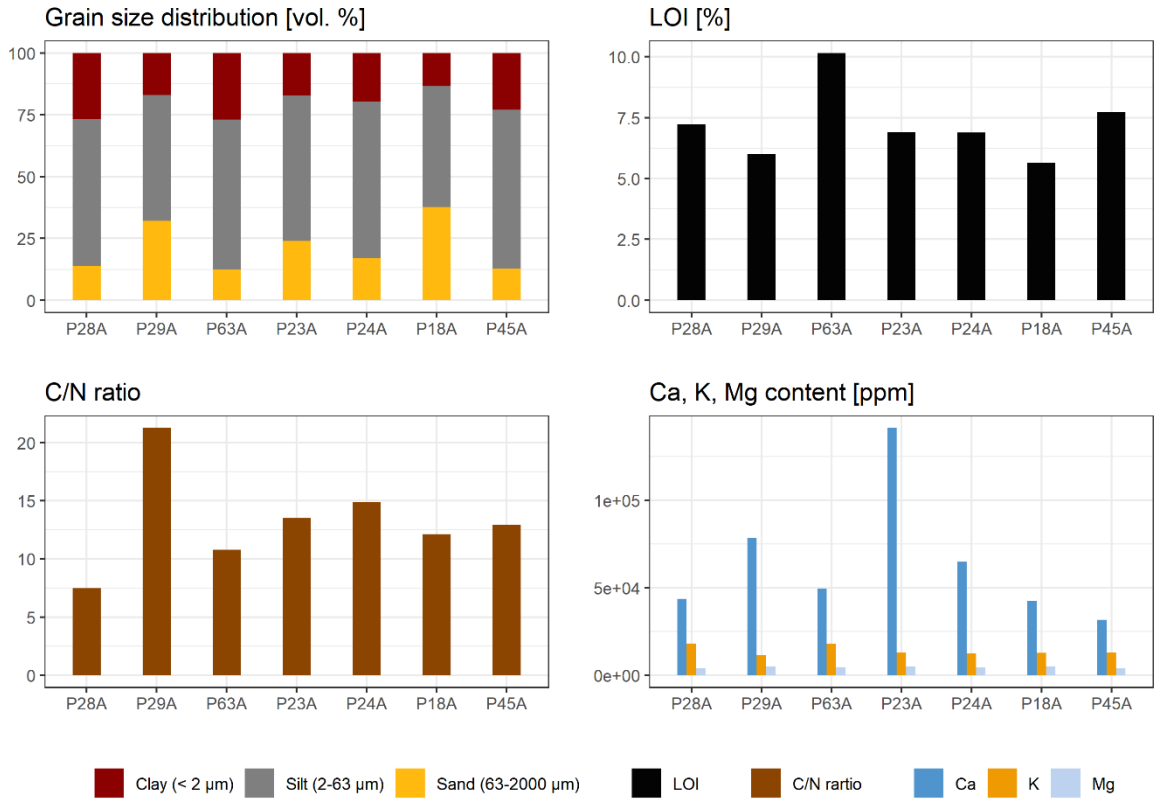

Figure 41: Soil properties of Transect 2.

Table 19: Site specific and relief referring characteristics of Transect 2

Site	STY-P28	STY-P29	STY-P63	STY-P23	STY-P24	STY-P18	STY-P45
Altitude	625	610	680	775	615	600	600
Inclination	N4	N2	N4	N4	N2	N2	N1
Exposition	EE	EE	SW	EE	SS	SS	NE
Position	U	T	M	O	T	T	T
Appearance	FE	P	P	T	P	T	P
Curvature	X, X	X, X	V, V	V, X	V, G	G, G	G, G
Type of use	A	A	BA	BA	A	BA	A
SQI A	70.83	70.83	66.67	75.00	79.17	41.67	70.83
SQI B	62.50	62.50	62.50	70.83	75.00	58.33	79.17

5.2.3.3 Transect 3

Transect 3 extends in the east of the polje from northeast to southwest over a distance of 8.1 km. Along the transect a total of 7 sites were investigated. The sampling points are between 600 m and 2.2 km apart from each other (figure 42, figure 43 and table 20).

STY-P 33 the northernmost site is located on a south-facing central slope. The site shows a field terrace, which is no longer in use. Like many other sites, this one has a concave slope shape downwards due to anthropogenic use. The sand fractions dominate in the A-horizon while they decrease slightly towards the bottom. A decrease can also be seen in the organic matter content to 5.32 % with increasing depth. On the other hand, an increase of the stone content is observed. The C/N ratio is moderate at both extraction depths. While the potassium and magnesium concentrations do not show any significant differences, the Ca concentrations demonstrate significantly higher values in the B-horizon, increasing from 7303 to 12605 ppm. Site **STY-P 34** is located 630 m to the south on a steep eastern slope at 810 m a. s. l. The curvature of the agriculturally used slope appears stretched in horizontal and vertical direction. Due to the location in the terrain and soil cultivation, clear signs of erosion are evident. The site shows a significant decrease in sand fractions from 47.11 % to 35.32 % at depth. The humus content also decreases in the B-horizon and the C/N ratio worsens significantly with increasing

depth from 13.42 to 27.68. Clear differences are also evident in the Ca concentrations, which doubles in the B-horizon.

Site **STY-P 35** is located on a field terrace at 750 m a. s. l. The strongly inclined central slope shows concave curvatures in both directions and is exposed to the west. Compared to site STY-P 34, STY-P 35 shows a higher organic content of 6.63 % and a closer C/N ratio of 9.98. Significant differences can be seen in the Ca concentrations, which have a maximum value of 4527 ppm.

Site **STY-P 38** is located about 2 km southwest of STY-P 35 on a slightly westerly inclined Lower slope. The surface of the formerly agriculturally used alluvial fan is shaped straight. The grain size spectrum is dominated by the sand fractions which increase slightly with increasing depth. The grain size spectrum is dominated by the sand fractions which increase slightly with increasing depth. The medium humus topsoil also has a moderate C/N ratio of 11.33. While a low Ca concentration was measured at site STY-P 35, the concentrations in the A- and B-horizons are several times higher at 31178 and 20345 ppm.

Site **STY-P 39** is following the Transect further to the southwest, also on an alluvial fan dropping to the west. The site is located at 640 m a. s. l. on a field terrace that is still in use. The grain sizes in the soil of both horizons show an approximately equal distribution. The fine soil consists of 13.46 % clay, 43.38 % silt and 43.15 % sand. The medium humus topsoil shows a C/N ratio of 7.97 in the upper part and 12.98 in the lower part. The potential nutrient availability compared to the previous site STY-P 38 shows much lower values in the Ca concentrations while the potassium and magnesium concentrations differ only slightly.

Site **STY-P 31** lies on an agricultural area of the plain at 615 m a. s. l. The soil shows a clear difference in the grain size composition. The silt fractions dominate with 58.70 and 59.40 % while the sand fractions recede. The middle humus A-horizon shows in the upper part a wide C/N ratio of 22.54 and in the lower part a rather moderate ratio of 10.71. The Ca concentrations are many times higher than at the previous site, they are reaching 98531 ppm for STY-P31 A and 45838 ppm for B.

Site **STY-P 32** in the southern part of the polje is located on a strongly inclined north-west slope at 740 m a. s. l. Due to its agricultural use, the slope has a concave

curvature in horizontal and vertical direction. The grain size spectrum shows slightly higher clay contents with 17.11 % in the A horizon and 18.92 % in the B-horizon. The stone content is slightly higher and the organic matter content is still in the middle range but the nutrient availability shows significant differences to the previous site. The Ca concentrations show values from 127588 to 132226 ppm and the Mg concentrations presenting higher values.

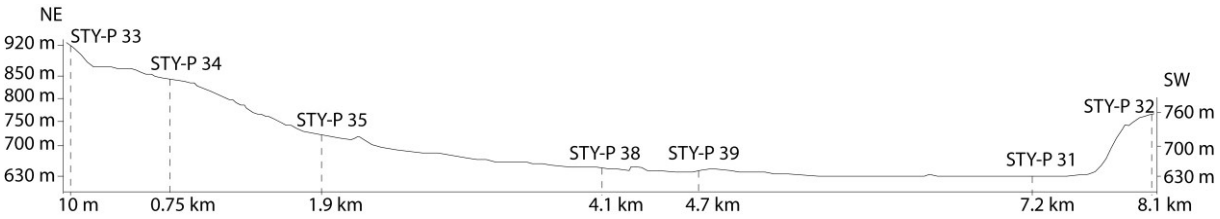

Figure 42: Cross section of Transect 3.

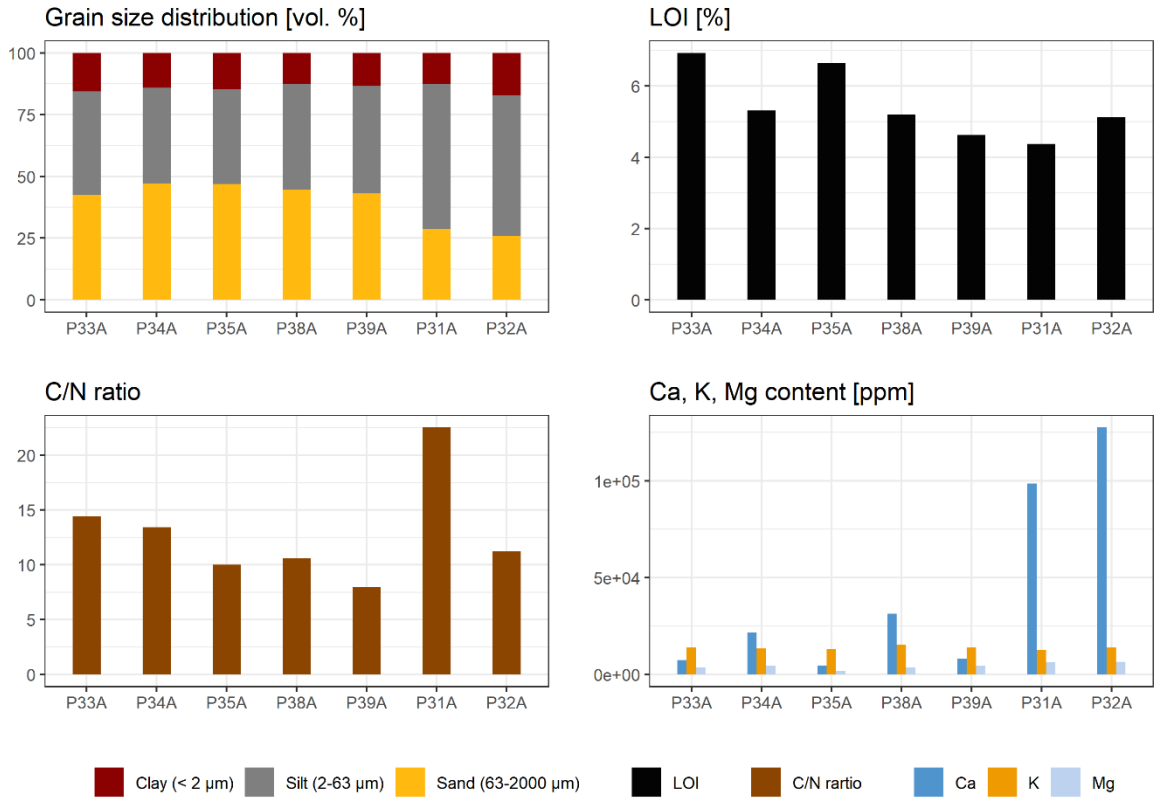

Figure 43: Soil properties of Transect 3.

Table 20: Site specific and relief referring characteristics of Transect 3

Site	STY-P33	STY-P34	STY-P35	STY-P38	STY-P39	STY-P31	STY-P32
Altitude	920	810	720	640	640	615	740
Inclination	N0	N4	N5	N2	N2	N0	N4
Exposition	SS	EE	WW	WW	WW	WW	NW
Position	M	M	M	U	U	T	U
Appearance	T	P	T	FE	T	P	T
Curvature	V, G	G, G	V, V	G, G	V, G	G, G	V, V
Type of use	BA	A	GW	BA	A	A	A
SQI A	54.17	50.00	54.17	50.00	62.50	62.50	79.17
SQI B	37.50	54.17	37.50	50.00	70.83	66.67	70.83

5.2.3.4 Key profiles and the origin of the sediments

Cluster analysis was used to further differentiate the soil types and sites and to identify common features of the sediment distribution in the polje (figure 44 and figure 45). The analysis included the grain size fractions, the content of organic matter, the C/N ratio, the pH value and the elements Zr, Ti, Sr, Rb, Zn, Fe, Ca and K. A total of 8 clusters were distinguished, which will be briefly introduced in detail here:

The first cluster comprises the profile of the Isomata plateau, the sites STY-P35, STY-P54 and the IBt horizon of the soil profile at Drosopigi (DRO 1). The cluster is characterized by high iron contents and low Ca concentrations. The organic matter content is moderate and the C/N ratio varies between 5.4 and 14.40. Another characteristic of this cluster is the slightly acidic pH level.

The second cluster includes the M-horizons of the site at Drosopigi and the sites STY-P 1 and STY-P4.2. The sites are all located in the west of the polje on central slopes with a high relief gradient. Also in this group the pH value is slightly acidic. Moreover, the humus supply is low and the C/N ratios are very variable. Compared to cluster 1, the iron content is significantly lower.

The third and largest cluster is formed by some horizons of the soil profile STY-KEF 1, the topsoil horizon STY-ASP-1 and many sites of the polje, which occur in the eastern as well as in the western part of the study area.

Cluster 4 is formed by the diagnostic horizons of the STY-P57 soil profile. These are both the colluvial deposits of the M(Bt) horizon and the IBht horizons. Furthermore, the locations in the western part of the Polje can be identified in this cluster. STY-P 2, 3, 4.1, 5 and 8 are the most important sites. High concentrations of iron and calcium are found at these sites. A unique feature of this cluster are the high clay contents in the sediment samples. STY-P 20 forms an independent cluster, as it is a sample material from the lake.

The large cluster 6 shows the group of topsoil horizons of the soil profiles STY-P57, STY-KEF 4 and STY-KEF 1. For a few exceptions, the sites with the same soil characteristics of this cluster are located on the slopes on the margins of the polje.

Cluster 7 is concentrated on the eastern side of the lake in the plain. However, no diagnostic horizon from the soil profiles could be assigned to these sediments.

Cluster 8 shows the horizons of the STY-KEF 2 alluvial fan and the subsoil horizons of the site at Asprokampos.

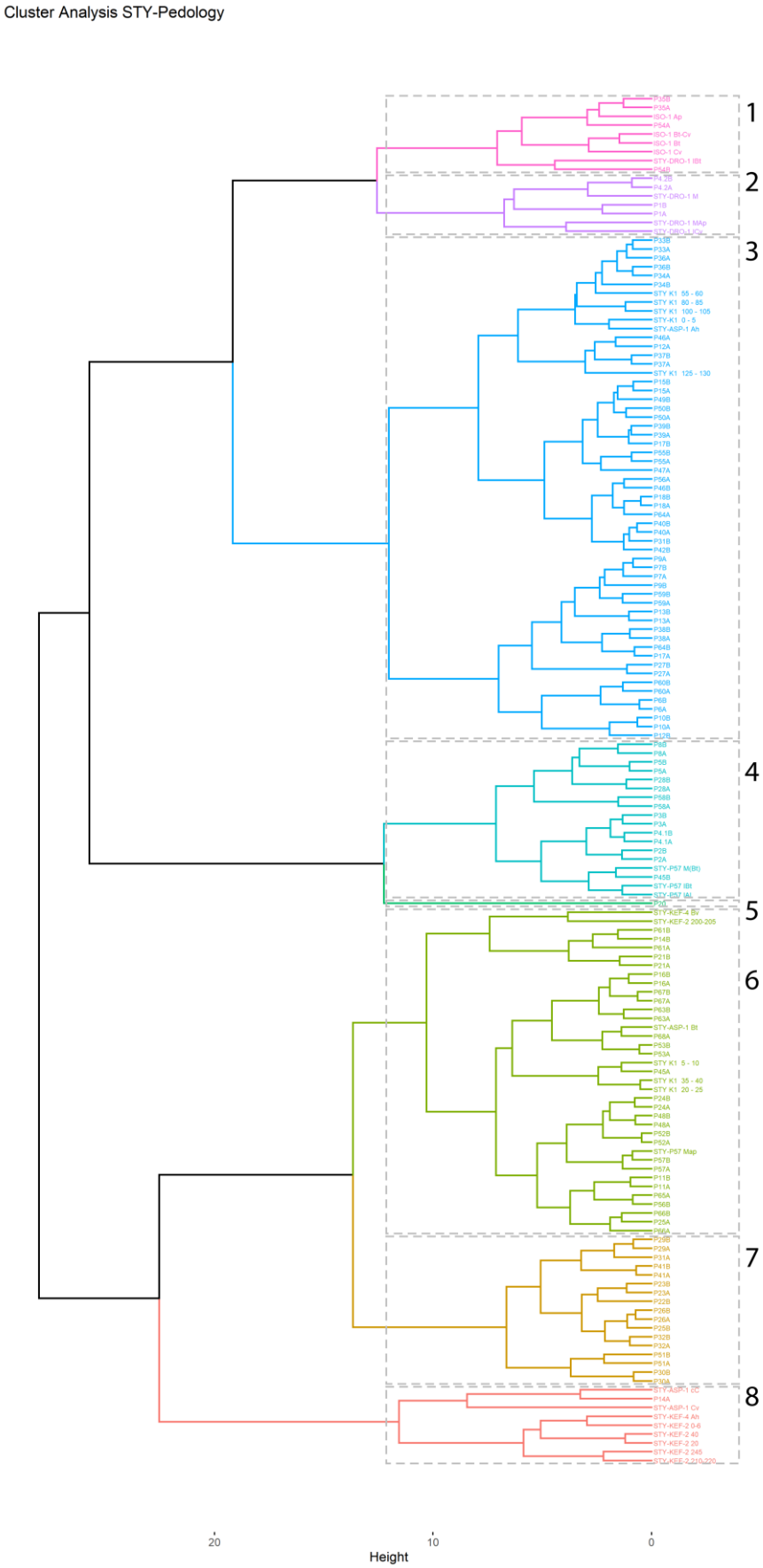

Figure 44: Cluster Analysis of soil diagnostic horizons and sediment samples from A- and B-horizons.

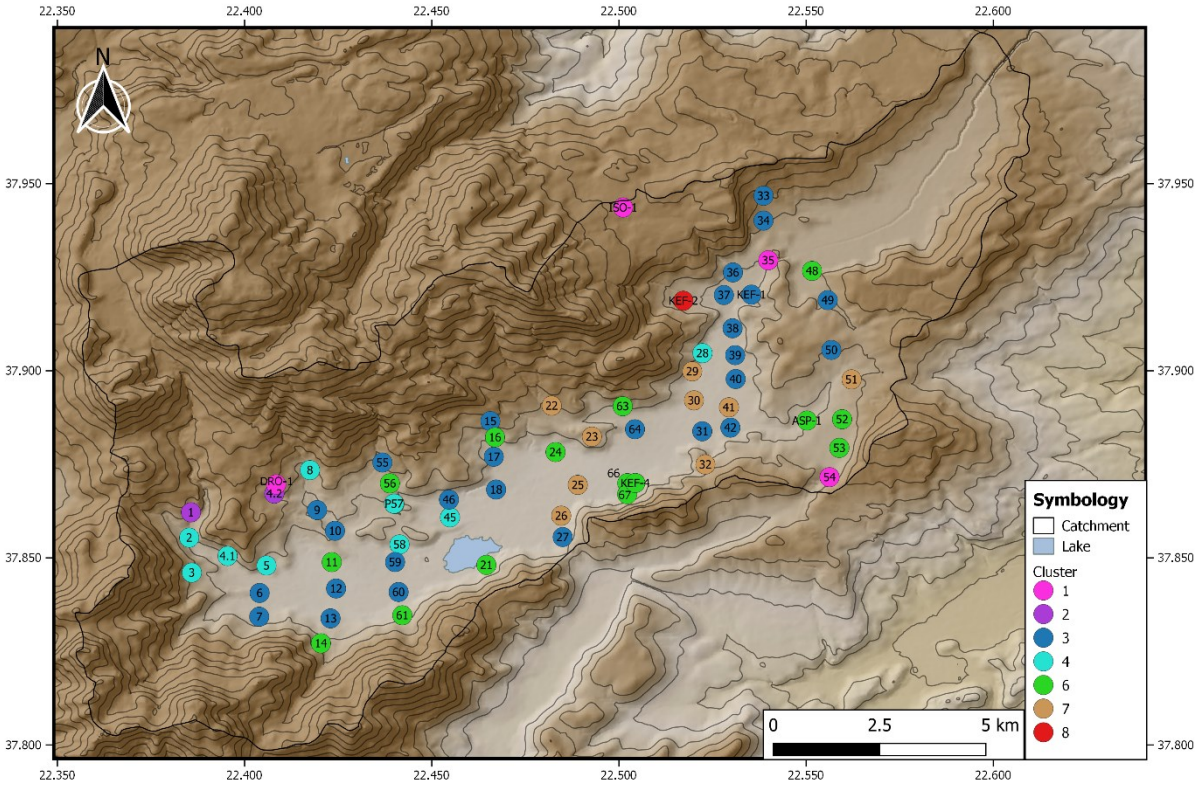

Figure 45: Map with the respective clusters, corresponding key profiles and sediment origin.

5.2.4 The Classification of the soil fertility and degradation status

The classification of the soil fertility and degradation status is based on the calculated soil quality index (chapter 4.3): Classes 1 and 2 are characterized by very high sand contents, moderate silt components and very low clay fraction contents (figure 46). The soil types are dominated by weak to medium loamy sands, weak to medium clayey sands and silt sands. A low percentage of organic matter and a high proportion of skeletal soil further characterize the two classes. Class 1 shows very low concentrations of calcium and magnesium. The potassium and C/N ratio can be classified as moderate. In addition, class 1 has an average acidic pH value of 4.79. Class 2 shows a better potential nutrient availability, but has a wider average C/N ratio of 27.64. The difference of class 3 to 4 is clearly shown by the supply of the soils with organic matter. Class 3 shows a significantly lower amount of organic substance and a higher C/N ratio than class 4. The pH value of class 3 is also in the slightly acidic range. Classes 5 and 6 now show significantly higher silt and clay fractions than the previous ones. A moderate supply of potassium, calcium and magnesium also characterizes both classes. Class 5 shows with 24.24 a rather wide C/N ratio and the pH value moves towards the slightly alkaline range. The situation is different in class 6, where the C/N ratio is 13.59 on average in the moderate range and the pH value is in the neutral range. The grain size spectrum of the two classes 7 and 8 shows high silt and clay concentrations. The clay content increases on average to 17.77 % in class 7 and to 19.61 % in class 8. The humus supply of the soils of both classes can also be classified as strong humus. The C/N ratio is in the moderate range. Differences can be seen in the nutrient supply of the soils, where class 8 shows higher concentrations of calcium and magnesium and also the stone content is very low in this class. In class 7, soils with a slightly acidic pH value also occur. The lowest value is in the slightly acidic range at 5.66.

Class 9 shows high contents of silt and clay fractions. The soils of this class are highly humus and have low stone contents with 15 %. The C/N ratio is often less than 10, and these soils have a high potential nutrient supply.

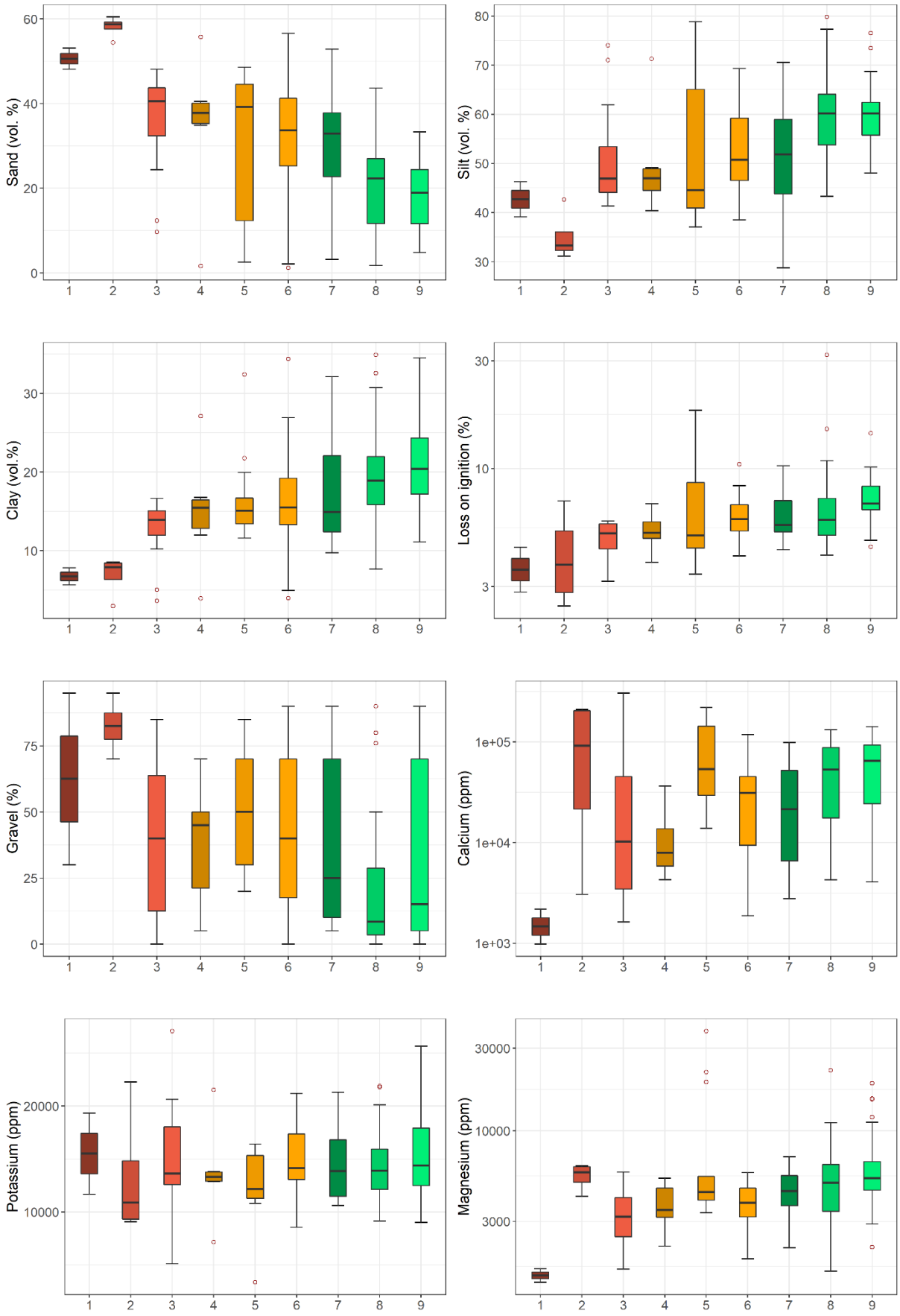

Figure 46: Soil properties and their proportions based on the classification.

Based on the recorded soil physical and chemical parameters and the soil quality index derived from them, the soils and sediments in the Stympahlia polje were divided into 9 classes. These classes can now be further divided into three soil fertility groups to evaluate the current soil fertility status (figure 47).

The first group represents poor fertile soils, including classes 1, 2 and 3. This group includes a total of 30 soil samples, being the smallest group. The soils of this group are characterized by high sand content and low clay fractions. The C/N ratio is in the average far apart and also the proportion of organic matter in the soil can only be classified as slightly humous. The nutrient supply is primarily ensured by calcium while the magnesium and potassium contents are reduced. The pH value of the samples is remarkably low, which is only 6.23 on average.

The second group contains soils with an average soil fertility (n =50). Silt is the most strongly represented grain size fraction. The organic matter content of these soils is classified as highly humous. As C/N ratio is on average still far apart but approaching the optimum. The fine substance of the soil also shows higher values on average than in the poor soils. The soils show an above-average high concentration of calcium and low values of potassium availability, while the magnesium concentrations are more than twice as high as in the previous group. The pH value is now close to neutral.

Group 3 (n = 78) represents very fertile soils, including classes 7, 8 and 9, which are characterized by a high percentage of silt and clay fractions. These soils also show high contents of soil fine material. The C/N ratio is now on average moderate, while the content of organic matter is very humous. The pH is slightly alkaline. The group describes a clear difference in the potential nutrient supply, which shows a balanced ratio of calcium, magnesium and potassium.

Figure 47: Soil fertility groups according to SQI classes. Group 1 (left) poor fertile soils represents SQI classes 1 -3 with mean values of the three classes. Group 2 (middle) moderate fertile soils represents SQI classes 4 – 6 with mean values of the three classes. Group 3 (right) very fertile soils represents SQI classes 7 – 9 with mean values of the three classes.

Comparing the soil quality index of the A- and B-horizons (figure 48), with the position on geomorphological striking sites shows clear differences. A comparison of the A-horizons of the respective sites shows a high soil quality in the plain followed by the terraces and with a lower quality, the alluvial fan sites can be identified. The median soil quality of the alluvial fans reaching 54.16 % in the A-horizons, while the soil quality in the B-horizons increasing slightly, with the lowest values in the A-horizons at 29.16 %. By comparing the soil quality with the two horizon depths, a decrease can be observed with increasing depth. The median of the A-horizons lies at 70.83 %, while it clearly decreases to 62.5 % in the B-horizons. The terrace sites vary in the opposite direction to the plains. The soil quality of the topsoils reaching 62.5 % and rises to 66.66 % in the below occurring B-horizons. A prominent feature is the narrow range of the soil quality index of the A-horizons.

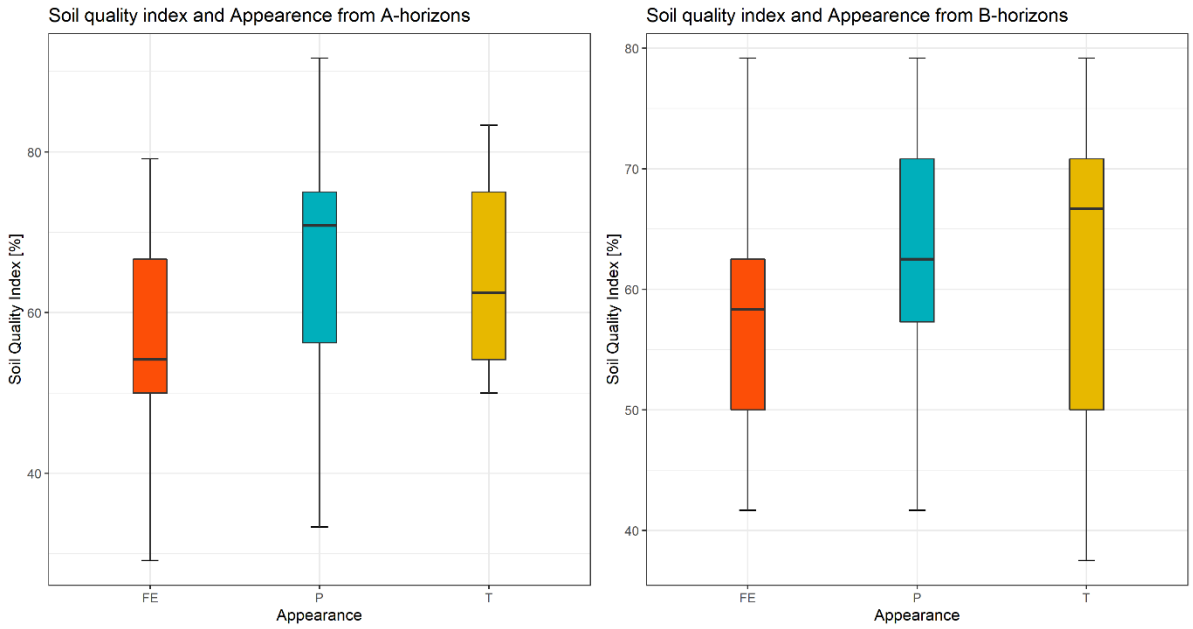

Figure 48: Comparison of the soil quality index and Appearance for A- and B-horizons. Fe = alluvial fan; P = plain; T = terrace.

The comparison between the various sites shows a clear difference in the stone content of the soils. Sites located on alluvial fans show the highest percentage (figure 49). The terraced sites show an average of 30 % stone content. The lowest stone contents were found in the polje on flat surfaces. Likewise, the organic matter content is at lowest in the plain, followed by the alluvial fans, and highest values were measured on the terrace sites. The C/N ratio shows the narrowest values on the terraces, while for the alluvial fans the ratio is slightly higher. The widest C/N ratio was determined at the plain locations.

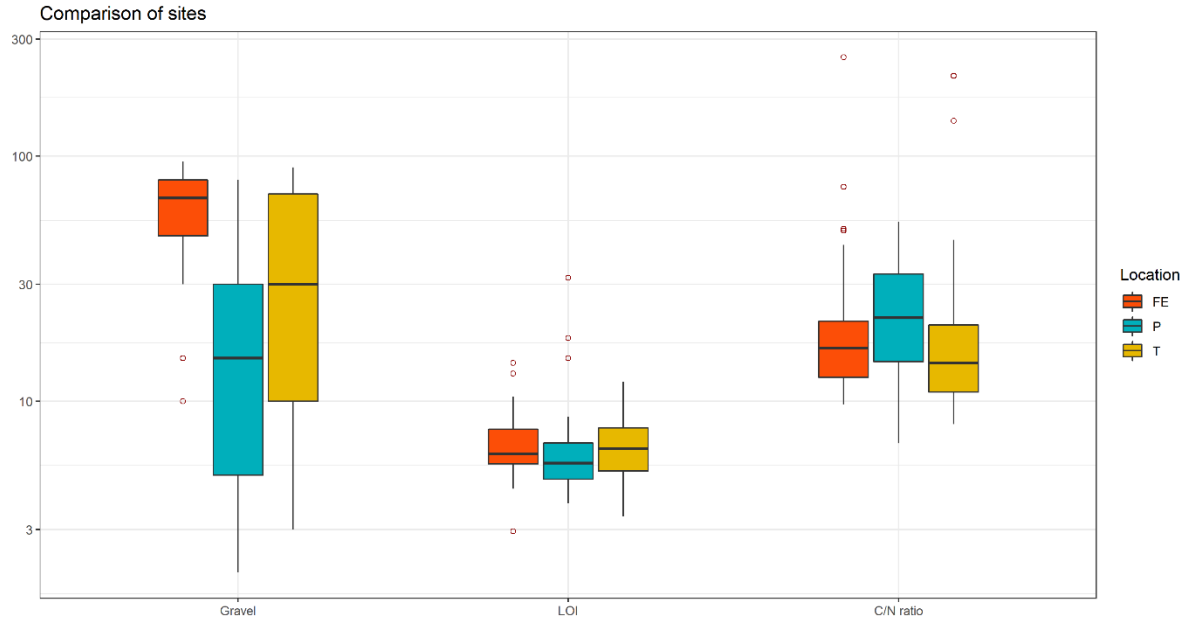

Figure 49: Comparison of different soil properties referring to different sites. Gravel = stone content in %. LOI = Organic matter content in %. C/N ratio = C_{org}/TN.

6 Discussion

6.1 The environmental conditions during the postpalatial period at Tiryns

6.1.1 Reconstructing the sedimentary environment

In order to reconstruct the depositional conditions within the sediment archive, fluvial architectural elements were determined. These elements are based on the grain size distribution, the organic material and the shape of the respective layers. In respect to shape, laminated sands and laminar fine-laminated sands of the proximal flood plain dominate in the fluvial deposits.

The differentiation of fluvial sediments deposited by rivers and the description of the sediments that form an alluvial plain is still a strongly discussed topic in research. The work of Blair and McPherson (1994) showed that alluvial deposits differ from river deposits in their morphology, hydrological and sedimentary processes and the resulting facies and facies assembles. The morphological appearance as the main distinguishing feature of alluvial fans is characterised by a semiconical shape, restricted radial length, plano-convex cross-profile, and comparatively high values of radial slope (Blair & McPherson, 1994). The restriction of alluvial deposits to steep slopes, debris flow and sheet flood dominated deposits was strongly debated and is no longer applicable according to the current state of research (Nichols & Fisher, 2007). The profile below the lower town of Tiryns shows clear signs of fluvial development: the recurrent alternation of laminating sands indicates slight flooding. Laminar fine stratification indicates nearby flood plains. Coarse-grained sediments and gravel indicate high flow rates of the river, which are still preserved in the channel. At Tiryns, we can see both proximal and distal sedimentary features, which points to multiple relocations of the river. Rivers in the proximal areas are often bedload-dominated and characterized by gravelly and sandy sediments. Braided river systems present cross-bedding and the preservation of bar forms. Sufficient flow velocity must be available to transport coarse gravel over a certain period of time to develop braided river bar forms. Due to the lateral displacement of the current line, no or limited overbank fines are found in the proximal areas (Nichols & Fisher, 2007). However,

these are occasionally visible in the profile in the form of laminated fine layers, which indicate distal areas. The results in Tiryns ideally show that the investigation of flood sediments can not only indicate long-term changes but also reflect short-term effects of the discharge regime. The profile in the trench TS-1 therefore shows a record of flood magnitudes through time.

The geoarchaeological results from the TS-1 profile allow to prove the settlement activity in the archaeological context by recording various element concentrations. Accordingly, the sedimentological stratigraphic interpretation of the layers Y1a, Y1b and Y2 as cultural horizons is supported by the measurement of the element concentrations. The exposed cultural horizons show high contents of rubidium, iron, arsenic, calcium and aluminium, which cannot be detected in this concentration in fluvial deposits. High concentrations of iron and arsenic are increasingly found at former workplaces (Alexandrovskaya & Panova, 2003). The alloying of bronzes and the ceramic production with arsenic also seems to be reflected in these layers. The differences in the storage density of the two anthropogenic layers indicate different phases of building activity.

6.1.2 The river history

The geoarchaeological investigations of this study in the lower town of Tiryns underline the great importance of geoarchives at archaeological excavation sites. The reconstruction of fluvial-morphological dynamics and related processes in the lower town allows the derivation of the following scenario: a first phase shows an undeveloped floodplain area during the Late Helladic IIIA2 Lower Phase, in which pottery indicates a first anthropogenic impact. This is followed in a second phase by recurring, weak flood events which indicate a river shift to the northern side of the palace. In the following third phase the use of the floodplain area by humans and animals after the floods takes place. In the 4th phase, recurring periodic flooding occurred. After the flood events, a renewed use of the area by humans and animals can be reconstructed (5th phase). Further floods mainly with sand accumulation and higher flow velocities in drainage channels in the coarse material accumulation are detectable in a 6th phase. An initial development of the

floodplain area allows the foundation in the floodplain area during phase 7. The stratigraphy shows in phase 8 that the river eroded this foundation locally due to the reorganisation or structural development of the floodplain area by humans. Further human interventions followed in the 9th and last phase. In the floodplain, the people of Tiryns piled up a level foundation for the lower town. Since the last fill in phase 9 was not altered or covered by fluvial deposits in the investigated areas, the construction phase of the Kofini dam and the construction of the canal most likely falls into the beginning of phase 9.

In total, up to 150 flood events in the respective flood sediments could be detected around an in the 13th century BC due to the laminated fluvial fine sands. The associated pottery allows an unusually precise chronological delimitation of the investigated section of the river history. It lasts for about one and a half centuries, beginning in Late Helladic IIIA2 and ending with the construction of the lower town at the beginning of Late Helladic IIIC. The finely layered alternating layers are the remains of regularly recurring, weaker flood events and not of one extreme events. The investigations do not provide any evidence that would confirm the thesis of Zangger (1993) that the lower town was buried by the river sediments.

The geoarchive investigated in Tiryns provides significant results for the interpretation of human-environment interactions of late Bronze Age societies and shows how people reacted to flood events by means of successful river basin management and how a permanent flood control was achieved. Due to the ideal outcrop conditions with the fluvial deposits and the temporally exact delineation, the profile under the lower town of Tiryns represents one of the most important geoarchives for the reconstruction of river history in semi-arid areas.

6.2 Assessment of soil fertility and degradation at Stymphalia

6.2.1 Stymphalia profiles

High Quality Soils: A very high soil quality (group 3, classes 7-9, figure 47) is found at the locations of the soil profiles STY-P57 and ASP-1. The site of STY-P 57 provides ideal conditions for agriculture in terms of soil physical and soil chemical properties. The grain size spectrum is dominated by silt concentrations and high clay contents, i.e. a high proportion of medium pores. Although the colluvium, which is overprinted by arable farming, still shows slightly increased sand contents, the proportion of organic substance is significantly increased in comparison, which in turn leads to an increase in the medium and fine pores in the horizon and thus increases the water storage capacity. The profile shows a close C/N ratio and high levels of organic matter. It also reveals a sufficient nutrient availability and an almost neutral pH value. The Vertic Luvisol also shows strong volume changes due to regularly occurring shrinkage and swelling periods, which is due to highly swellable clay minerals. As this site is characterized by soil accumulation rather than erosion, degradation tendencies can only be observed here due to the increase of iron in the subsoil horizons. The ASP-1 profile also shows high silt and clay contents, which are decisive for the water availability of plants. In the topsoil, the profile shows high levels of organic matter and a C/N ratio that is characterized by high biological activity by soil organisms. An existing degradation feature is the low preserved thickness of the topsoil, which can occur as a result of land use and erosion.

Medium Quality Soils (group 2, classes 4-6): The STY-KEF 1 and ISO 1 soil profiles indicate a medium soil quality. The profile STY-KEF 1 shows very high clay contents in the lower Ap-horizon and upper part of the Bt-horizon, which leads to a reduction of the plant available soil water, which is mainly present in the fine pores. Compared to the other profiles, the soil shows a low potential nutrient availability. A high potassium concentration is characteristic for these soils. The highest values are found in the B- and C-horizons, while calcium dominates in the topsoil. As this is the case of the study of Yassouglu (2017), the results of this work show that on conglomerates soils are developed with a moderate quality and thus soil fertility.

Low Quality Soils (group 1, classes 1-3): The soil profiles STY-KEF 2, STY-KEF 4 and DRO-1 show a low soil quality. The STY-KEF 2 and STY-KEF 4 profiles are formed on alluvial fans. Thus, the STY-KEF 2 profile in the topsoil indicates alternating layers of erosion events and horizontal stratification. Slope debris deposits caused by erosion events also overprint the STY-KEF 4 profile. Both profiles have high sand contents and a high C/N ratio. The soils are still classified as medium humus and also the nutrient availability is mainly determined by the Ca supply. Due to the high stone content, these sites are only suitable for plants with a high root depth. The profile of Drosopigi (DRO-1) has a high sand content, a low humus cover and an equally high C/N ratio. In addition, there is an over-represented supply of potassium for plant growth. Due to the high proportion of large pores and stone content, this location is also poorly suited for field cultivation. In addition, the low soil pH, which is only suitable for acidification tolerated plants.

6.2.2 The soil quality of the topsoil

The N-S stretching transect 1 in the western part of the Stymphalia polje (figure 38, chapter 5.2.3.1) shows that the soil quality can vary strongly from one the individual sites to the other. However, it also shows that the soil quality in the soils of the plain decreases with increasing depth. The locations STY-P 56, STY-P 58 and STY-P 59 show a low soil quality of the A-horizons (SQI class 3 and 5), which have a moderate nutrient supply and C/N ratio, a high stone content and a high proportion of coarse pores and thus a low water storage capacity. The soil quality in the B-horizons of these sites, however, shows significantly higher silt fractions and a slight increase in Ca, K and Mg concentrations. The improvement of the soil quality in the depth is limited to the sites in the plain, while no significant changes are visible on the slope sites. The terrace locations STY-P55 in the north and STY-P61 in the south of the transect indicate a very high soil quality (SQI class 9). The slopes of the alluvial fans show concave shapes due to the long agricultural use. The lower soil qualities prevail mainly on sites based on conglomerates parent material, while sites on dolomitic limestone show a higher quality.

Transect 2 shows a very high soil quality especially in the A horizons (figure 40, chapter 5.3.2.2). Occasional differences become apparent when comparing north-eastern and south-western locations. Accordingly, the soil quality deteriorates with increasing depth at STY-P 23, STY-P 28, STY-P 29 and STY-P63, while the quality of the south-eastern sites improves with increasing depth.

As for transect 1, the STY-P18 and STY-P63 sites, which are located on conglomerates, show moderate to poor soil quality (SQI class 3 and 7). As STY-P63 is a terraced site, the slightly higher soil quality compared to STY-P18 could be explained by the addition of organic fertilizer. This assumption is supported by the high content of soil organic matter.

The N-S oriented transect 3 in the eastern part of the study area (figure 20, chapter 5.2.3.3) shows clear differences in soil quality, which increases from north to south. In the northern locations, quality classes 3 to 6 are represented, while classes 7 to 9 occur in the southern locations. The sites STY-P 33, STY-P 34 and STY-P 38 show higher sand fractions and lower Mg concentrations. In contrast to previous transects, the northernmost sites of these transects show a degradation of soil quality with increasing depth. The comparatively high soil quality of the terraced site STY-P 32 (SQI class 9) on conglomerates can be attributed to the high proportion of medium-sized pores, a moderate C/N ratio and an adequate supply of nutrients.

Soil physical properties

The classification of the soils with regard to their soil physical properties is mainly based on the grain size distribution. Since the pore size distribution and thus the water storage capacity of the soils is strongly dependent on the grain size distribution, the grain size is of particular importance for soil fertility. Soil with high sand contents and coarse interstitial pores have a much higher saturated hydraulic conductivity than finer-textured soil, which have narrower interstitial pores. Furthermore, the soil type influences the speed at which nutrients are leached out. The higher the field capacity and thus the water storage capacity of the soil, the slower the nutrients are transported to deeper lying horizons. A high

field capacity means that a maximum of easily soluble nutrients is available in the root zone (Blume et al., 2010; van Breemen & Buurman, 2002).

Class 1 soils can provide a water content of about 30 to 40 % on average of the available field capacity and can therefore react better to stress periods than class 3 soils (figure 50 and figure 51). Class 1 contains a high sand content and therefore a high proportion of coarse pores. The water content in the area of the available field capacity is less than 30 % and can lead to considerable restrictions for agricultural use in dry phases. Class 2 contains mostly very clayey soils - the soil type group is the silt clays. This class is to be classified as moderate because the water in fine pores is only available to a small extent for plants and in addition clay rich soils are considerably more difficult to cultivate.

Soils with high silt content mainly appear in the south-eastern part of the polje. Occasionally they also occur in the west. In the southeast, the grain size distribution is due to the marl formations which are present around Asprokampos. The heterogeneous distribution in the west of the polje can be explained by the intensive cultivation in this area. Differences with increasing depth are hardly noticeable. Thus, isolated significant grain size changes occur in the north-western area on the south-exposed slopes. There, sand fractions dominate in the A-horizons while in the B-horizons a finer texture is given by silts. The following maps were created with QGIS version 3.4.4 Madeira. The interpolation method is based on inverse distance weighting.

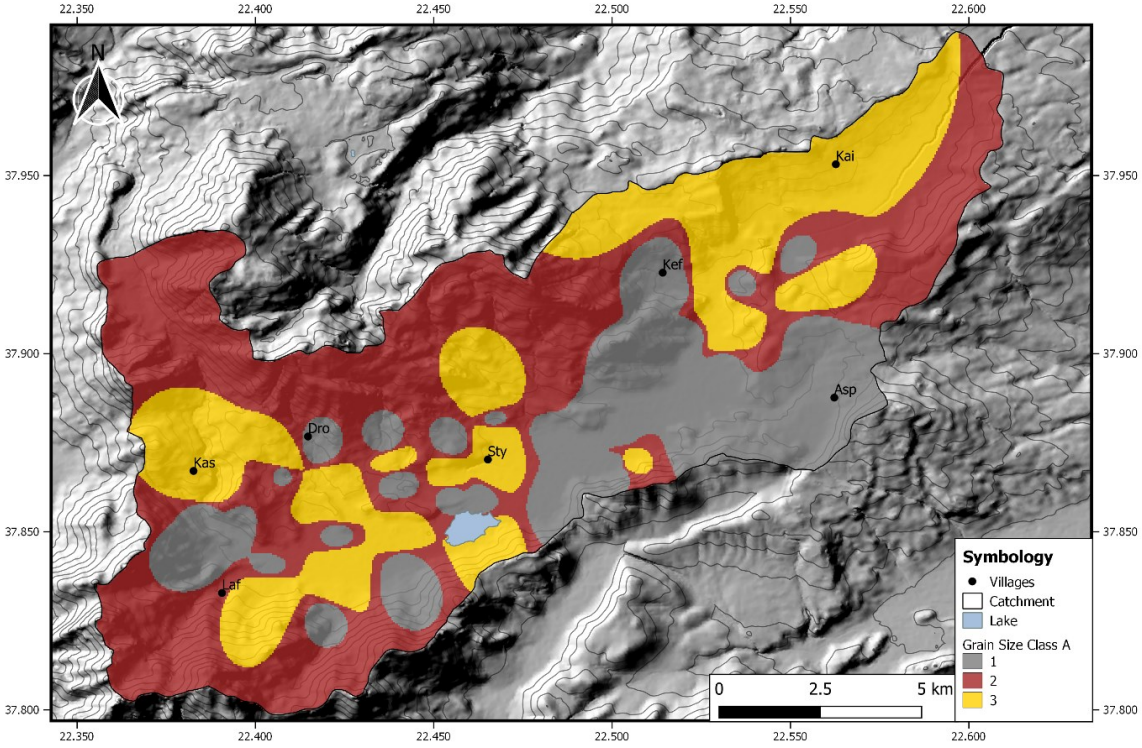

Figure 50: Map of the grain size distribution in the A-horizons of Stymphalia. Class 1: normal clays, clay loams, sand silts, loam silts, clay silts; class 2: silt clays; class 3: loam sands, silt sands and sand loams.

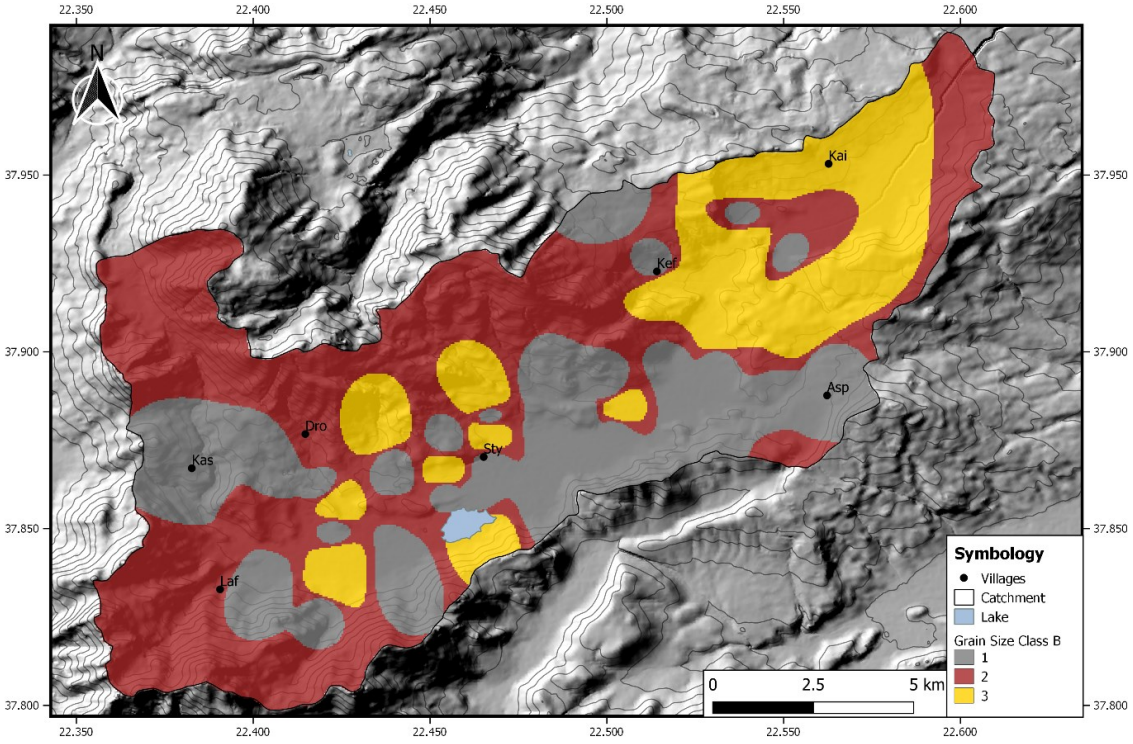

Figure 51: Map of the grain size distribution in the B-horizons of Stymphalia. Class 1: normal clays, clay loams, sand silts, loam silts, clay silts; class 2: silt clays; class 3: loam sands, silt sands and sand loams.

Organic matter content

Sites with a high organic matter content are also characterized by a stable aggregate structure. Due to the increased aggregate stability, soils tend to be less capping, which in turn counteracts erosion. Strikingly high values in the topsoil were found around the lake (for example sites STY-P20, STY-P21 and STY-P61). This may indicate a lateral expansion of the lake and thus oxygen-reducing conditions or it may indicate colluvial sediments due to deposition by previous erosion processes.

The results of the measurement of organic matter (figure 52 and figure 53) show a higher percentage of organic matter at the margins of the polje, i.e. on the slopes, in contrast to the flat polje surface (chapter 5.2.4). On the one hand, A-C-profiles such as Syrosem ((L)Ai-C) and/or Rendzina soils (L-Ah-Cv-C) have been preserved on the slopes, i.e. the topsoil has a higher content of organic matter due to its natural soil formation sequence. On the other hand, terraced agriculture plays a decisive role in this process. As the majority of the samples come from former arable terraces which counteract erosion and absorb slope material of the topsoils. The signal becomes even clearer with the artificial addition of humus material.

However, why do the soils in the flat area of the polje itself show a lower organic matter content? This could be caused by previous detachment of the B-horizons on the slopes. The profiles on the slopes show, on the one hand, the complete absence of B-horizons, on the other hand, clear erosion events can be identified, such as sharp horizon boundaries and alternating layers of humus, fine-grained and gravel layers on alluvial fans that reaching the polje from the slopes. The eroded soil sediment of the B-horizons was then ploughed into the soils in the plain, and in the course of thousands of years humus-rich topsoil material was mixed with subsoil material from the slopes.

A reduction of soil C-states is detectable since the onset of agriculture in the Neolithic. Blume et al. (2010) describes deforestation, cultivation, tillage, and drainage as the most important factors that can lead to a reduction in soil organic matter. By changing the forms of use, this can lead to a disturbance of the balance between supply and reduction. For example, the humus dynamics are altered by clearing and management of forests but also by the change of grassland and arable land (Blume et al., 2010; Von Lützow et al., 2008).

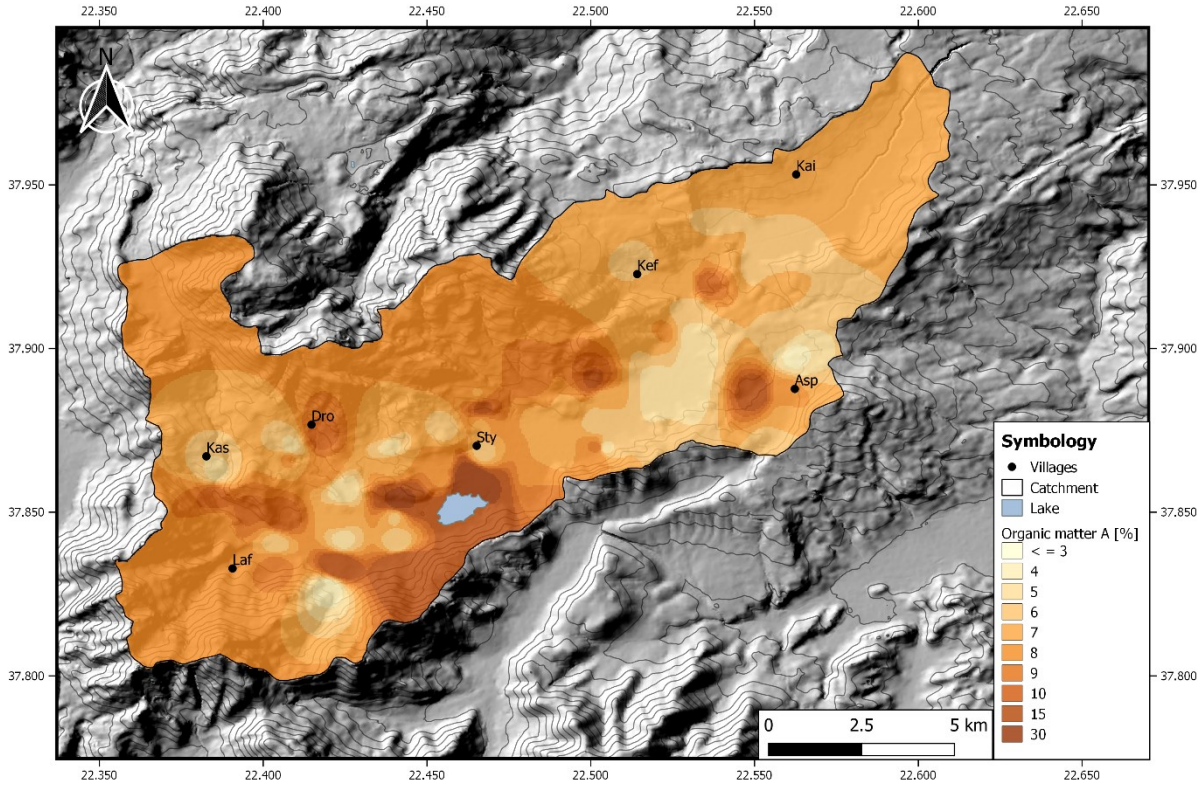

Figure 52: Map of the organic matter content of the A-horizons in Stymphalia.

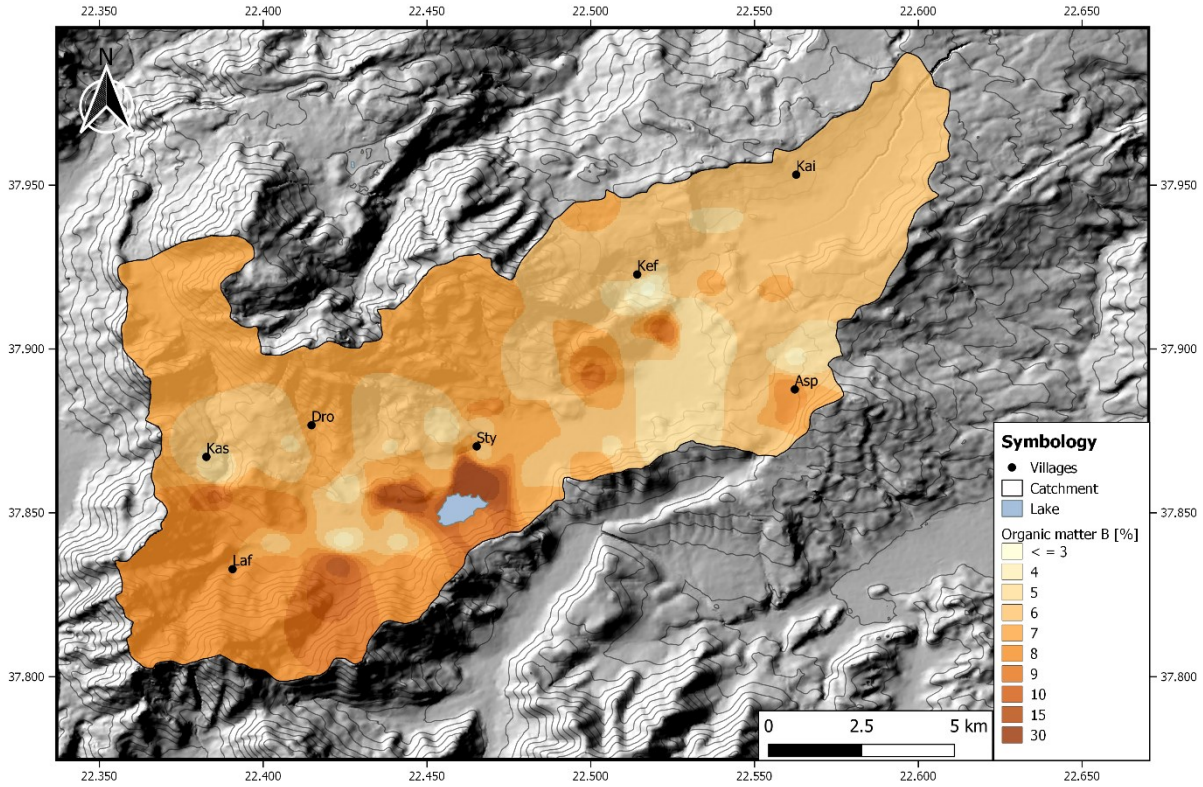

Figure 53: Map of the organic matter content of the B-horizons in Stymphalia.

C/N ratio

The amount of nitrogen in the soil is mainly determined by the organic N content in the form of dead, organic material. The parameters temperature, C/N ratio and soil water content, aeration and the pH value determine the transformation of nitrogen, mineralization and nitrification. The mineralization is the more intense the more N-rich and easily decomposable the organic substance of the soil is and the better the living conditions for soil organisms are (Andreae et al., 2016). On arable and grassland sites, the C/N ratio in the topsoil is usually at < 10 to 15 while in forest soils the ratio lies in the range of 25 to 38. The nitrogen compounds available to plants are nitrate (NO^{3-}) and ammonium (NH^{4+}). A high nitrogen leaching occurs in intensive vegetable cultivation, while it is lower in intensive- and extensive grazing and forestry (Blume et al., 2010). The C/N ratio of the individual locations is shown in figures 54 and 55, whereby a lower C/N ratio can be observed in the plain, which improves even more with increasing depth. This is due to recent fertilization, as the plain is still used for cultivation and there is currently no arable use on the slopes.

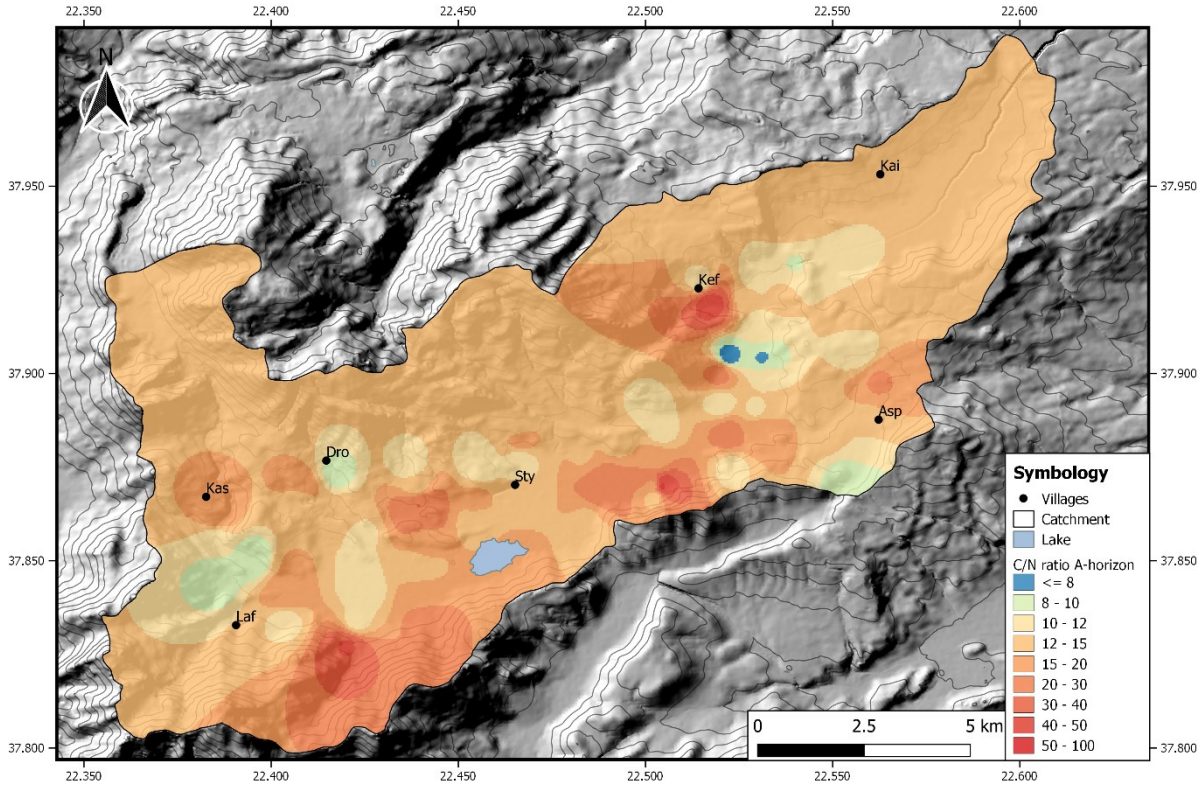

Figure 54: C/N ratio of the A-horizons in the research area.

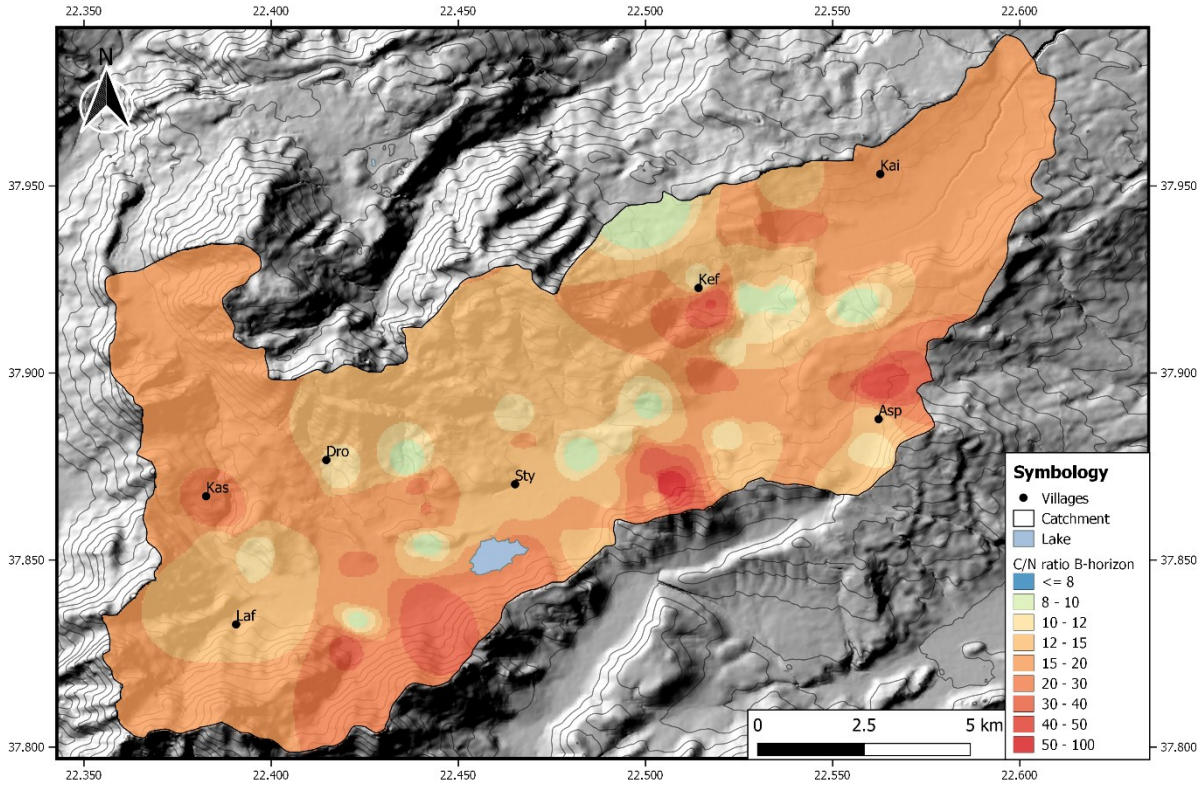

Figure 55: C/N ratio of the B-horizons in the research area.

6.2.3 Limitations of the soil fertility in terms of soil reaction

The soil pH indicates its suitability as a plant habitat, the habitat for soil organisms and filter capacity against pollutants. The pH value in the soil controls both directly and indirectly the species composition and function of soil organisms. Therefore, bacteria prefer a pH range of 5 to 7, whereas in acidic conditions fungi dominate. Some soils in the study area show moderate to strong acidification (figure 56 and figure 57). With increasing acidification, the proportion of Al^{3+} in the CAC increases, especially below pH 4.5 (Blume et al., 2010; van Breemen & Buurman, 2002). This is shown by the profile of the Isomata Plateau (ISO-1, chapter 5.2.2.4) as well as that of Drosopigi (DRO-1, chapter 5.2.2.6). Both profiles indicate increasing acidification with increasing depth, while the aluminium concentrations increase downward. In close proximity to these profiles, the STY-P4.2, STY-P54 and STY-P35 sites also show slight soil acidification. Since elements Ca, Mg and K are essential nutrients for plants, the supply of these nutrients to

plants decreases with increasing soil acidification. High Al concentrations lead to strongly inhibited root growth and increased susceptibility to drought stress. From a pH value of 4.5 below, Al^{3+} increasingly participates in the ion coating, which in turn has a negative effect on the alkali- and alkaline earth ions. In soils with a high carbonate content, the dissolution of carbonates with consumption of protons is the dominant buffer system. The HCO_3- dissolved in water is washed out together with Ca^{2+} (or other cations). Only when calcite is present in coarser limestone residues (as is the case in Stymphalia), the pH value of the soil solution can fall well below pH 7 before a horizon is carbonate free (Blume et al., 2010). For arable land, the pH value should be higher than 5, that no toxic and antagonistic concentrations of Al^{3+} and Mn^{2+} occur. A rising pH value, on the other hand, can lead to a lower plant availability of some macronutrients (Mn, Cu, Zn and B). A rising pH value, on the other hand, stimulates the activity of microorganisms and thereby increases the degradation of humic substances, which leads to the release of nitrogen and promotes the aggregation of clayey soils. The optimal pH values for arable land with regard to the clay and humus content are for soils with less than 4 % organic matter and less than 5 % clay between pH 5.0 and 5.5. For soils of 5 to 12 % clay the recommended pH value is between 5.4 and 6.0. In addition, soils with more than 13% clay should have a pH value between 6.0 and 6.5. If the organic matter content is above 4 %, a lower pH value of 5.0 to 6.0 is recommended (Amacher et al., 2007; Blume et al., 2010).

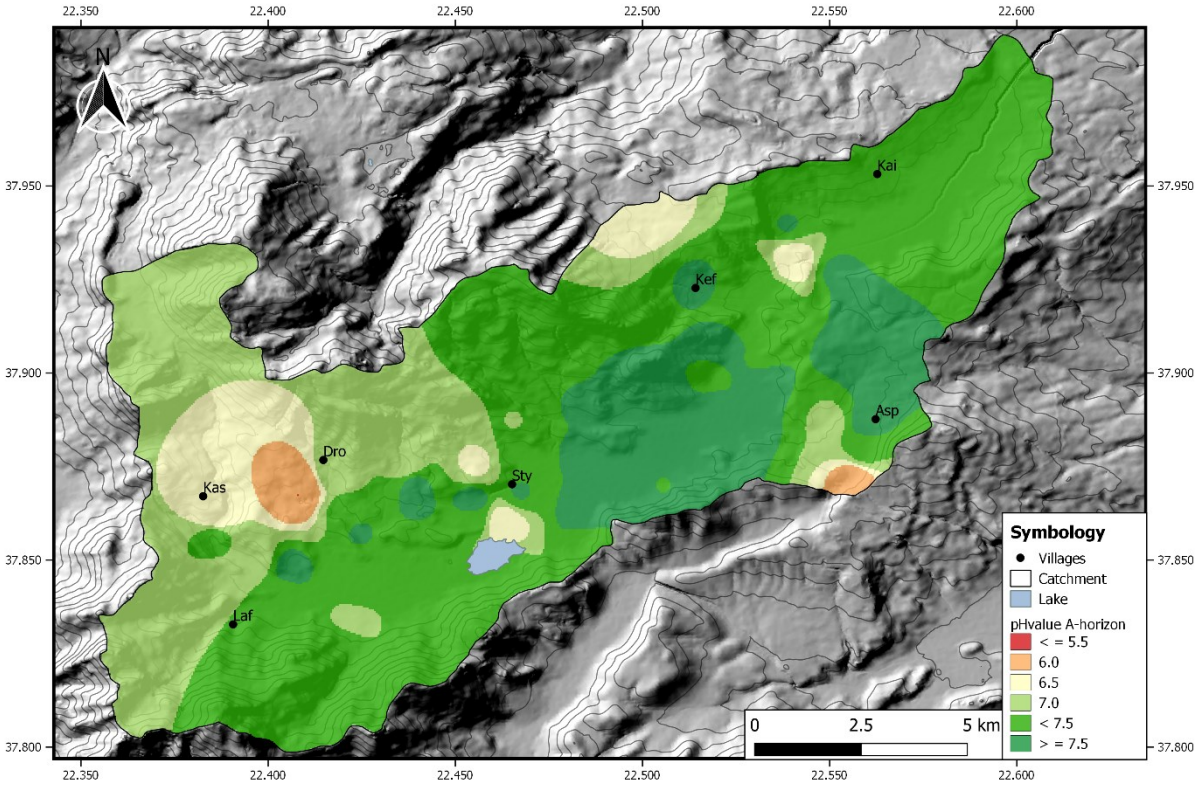

Figure 56: Soil pH of the A-horizons in Stymphalia.

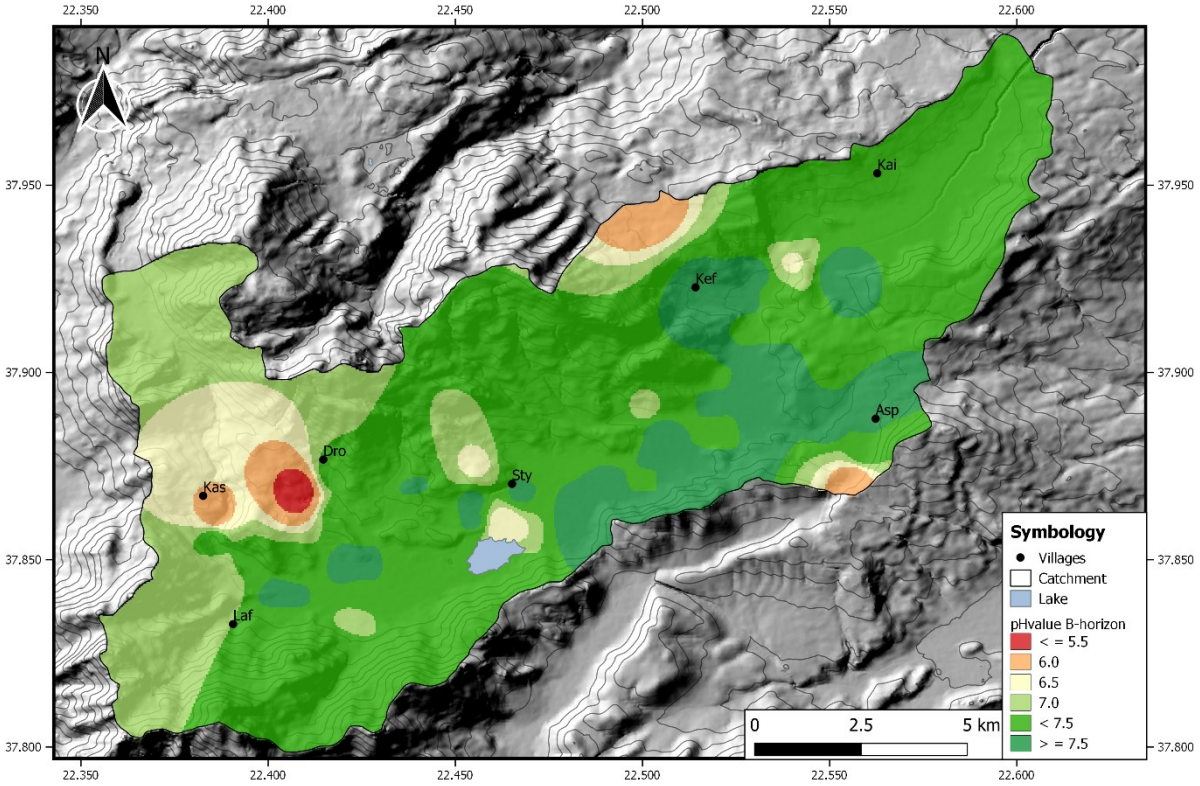

Figure 57: Soil pH of the B-horizons in Stymphalia.

6.2.4 Soil nutrients (Ca, K, Mg)

The spatial distribution of Ca, K, and Mg in the soil, reflecting both input and output processes, is displayed as maps in figures 59-65. Of the total amount, only a small part is usually directly available to plants in the soil solution. Influencing factors that control nutrient availability include the rate, i.e. soil moisture, temperature and the activity of microorganisms and the intensity, i.e. the concentration, speciation and relation between nutrients. Another major influence on the nutrient supply is the subsoil. Not only the leaching from the topsoil and thus the duration and intensity of precipitation is of importance, but also the rooting and weathering conditions play an essential role. (Blume et al., 2010).

The nutrient supply of soils is mainly determined by the parent rock. Figure 58 shows that the proportion of calcite and dolomite in the soils is bound to the parent rock. As in many other semi-arid areas, calcareous crusts (calcrete) occur in the soil profiles due to leaching of dissolved $Ca(HCO_3)_2$ in the deeper horizons. On the dolomite rocks, increased amounts of calcium and the highest concentrations of magnesium were detected.

Due to the high K fixation capacity of the clayey soils of the STY-KEF 1, ISO-1, STY-P57, DRO-1 and ASP-1 sites, K leaching is very low. These soils show a good nutrient availability with potassium. This is not the case for the sites STY-KEF-2 and STY-KEF 4 where significantly lower potassium concentrations can be detected.

The highest Ca concentrations occur in the southern part of the polje and west of Kefalari. When comparing the different site conditions, it becomes clear that the soils in the eastern part of the study area have a low nutrient supply. The lowest magnesium and potassium concentrations can be found there. A further supply limit of potassium occurs in the south-western part of the polje, where the soil is excessively rich in Ca and Mg. In the northwest, potassium concentrations dominate due to the presence of phyllites. At these nutrient-poor locations, only a cultivation of e.g. tubers is conceivable. In contrast to cereal crops, the requirements for the plant's nutrient supply are rather low and the soil fertility can be renewed by a long lasting fallow (Deutsches Institut für Fernstudienforschung an der Universität Tübingen, 1997).

The middle of the polje, east of the lake, offers an excellent, balanced supply of nutrients. Here potassium, magnesium and calcium are present in high concentrations, which also affects the overall quality of the soils. Considering the locations near Kastania, high potassium values are present and a K-fixation seems to be impossible, since the soils there are not cohesive or clayey - high values are due to the parent material there.

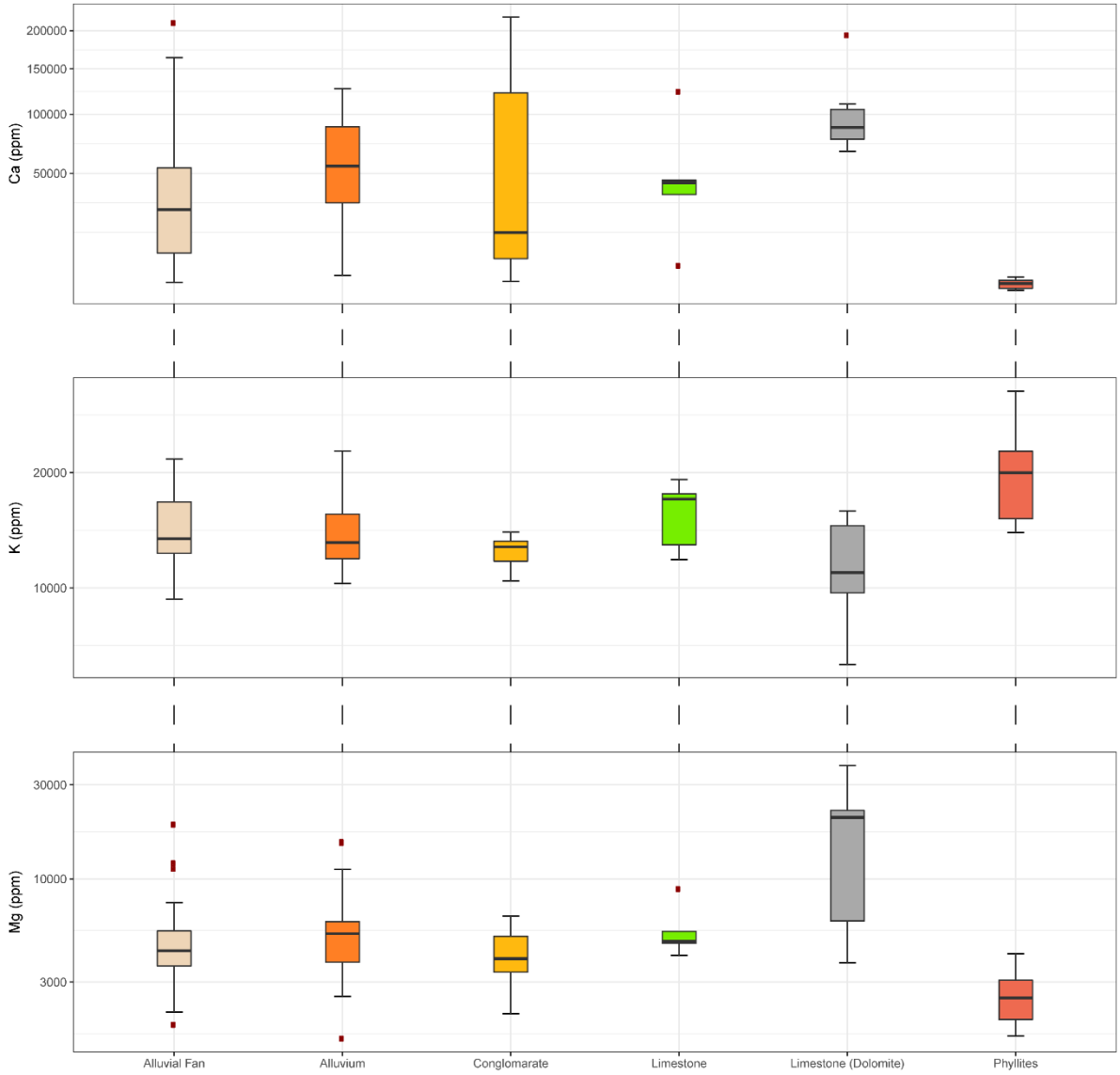

Figure 58: Element concentrations in soils (Ca, K and Mg) of different parent material.

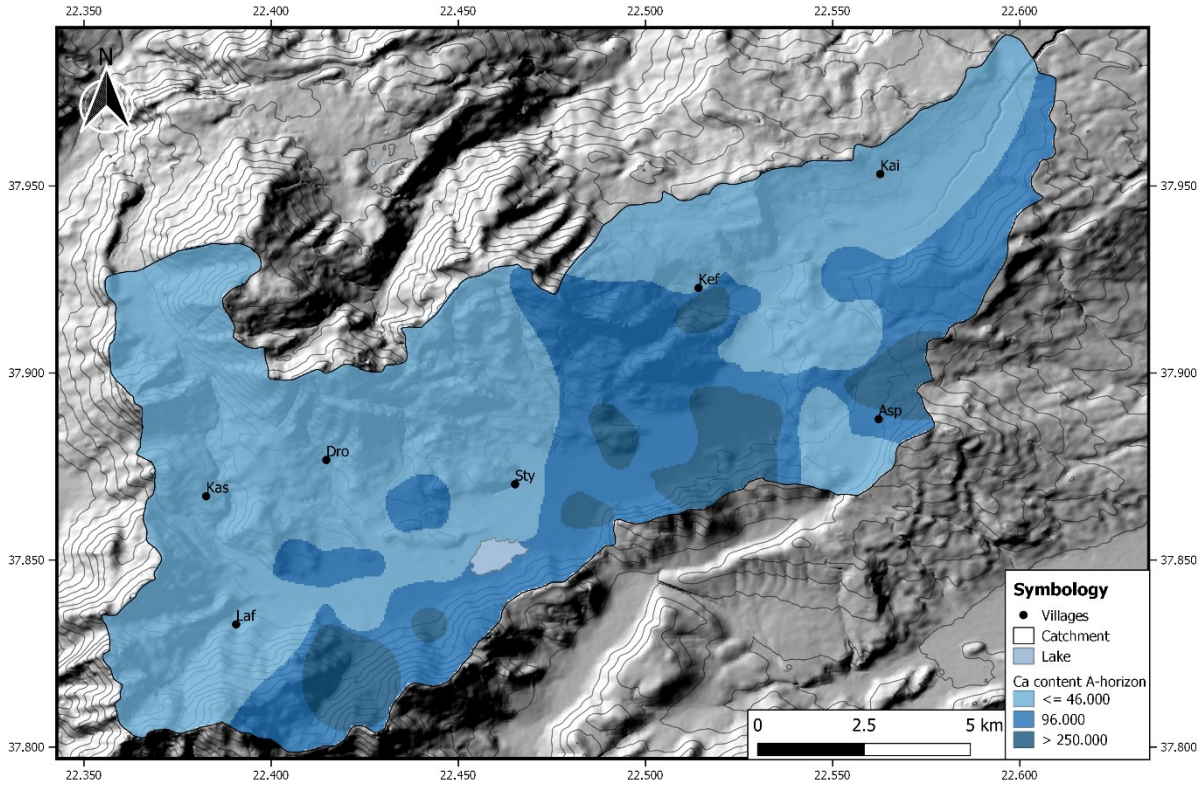

Figure 59: Calcium distribution of the A-horizons in the research area.

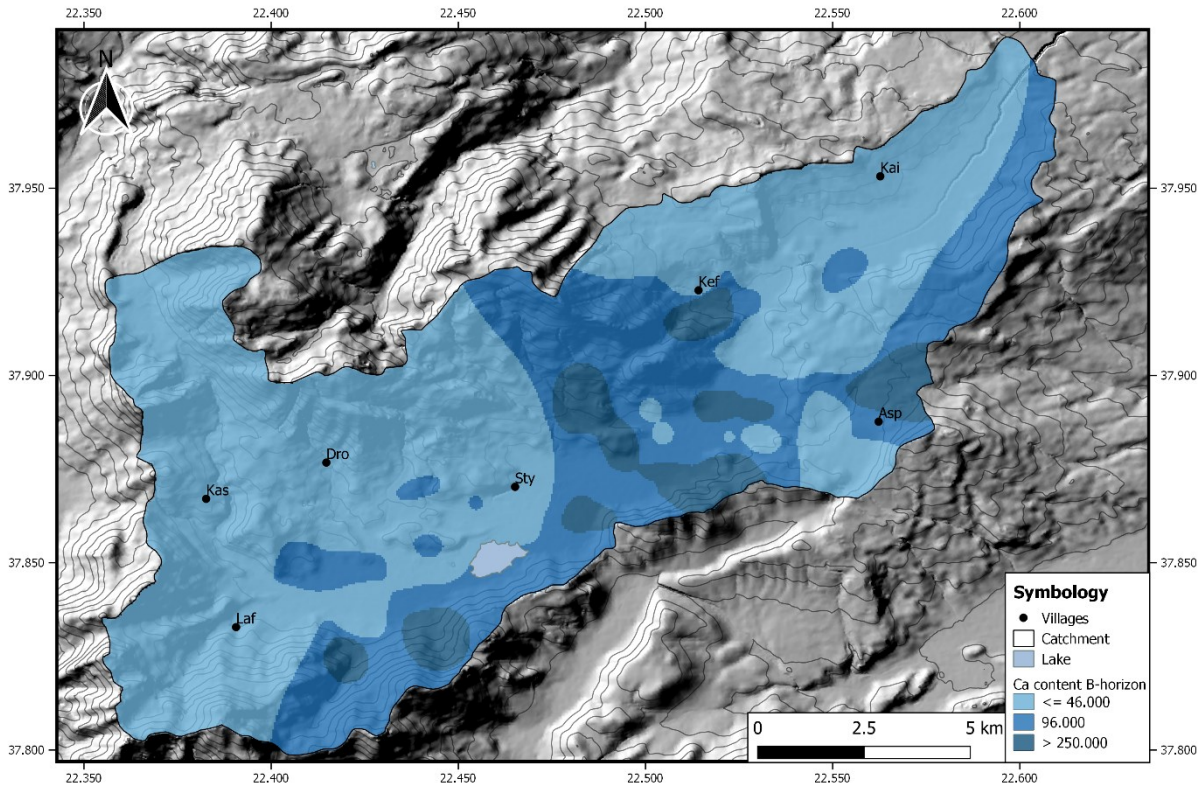

Figure 60: Calcium distribution of the B-horizons in the research area.

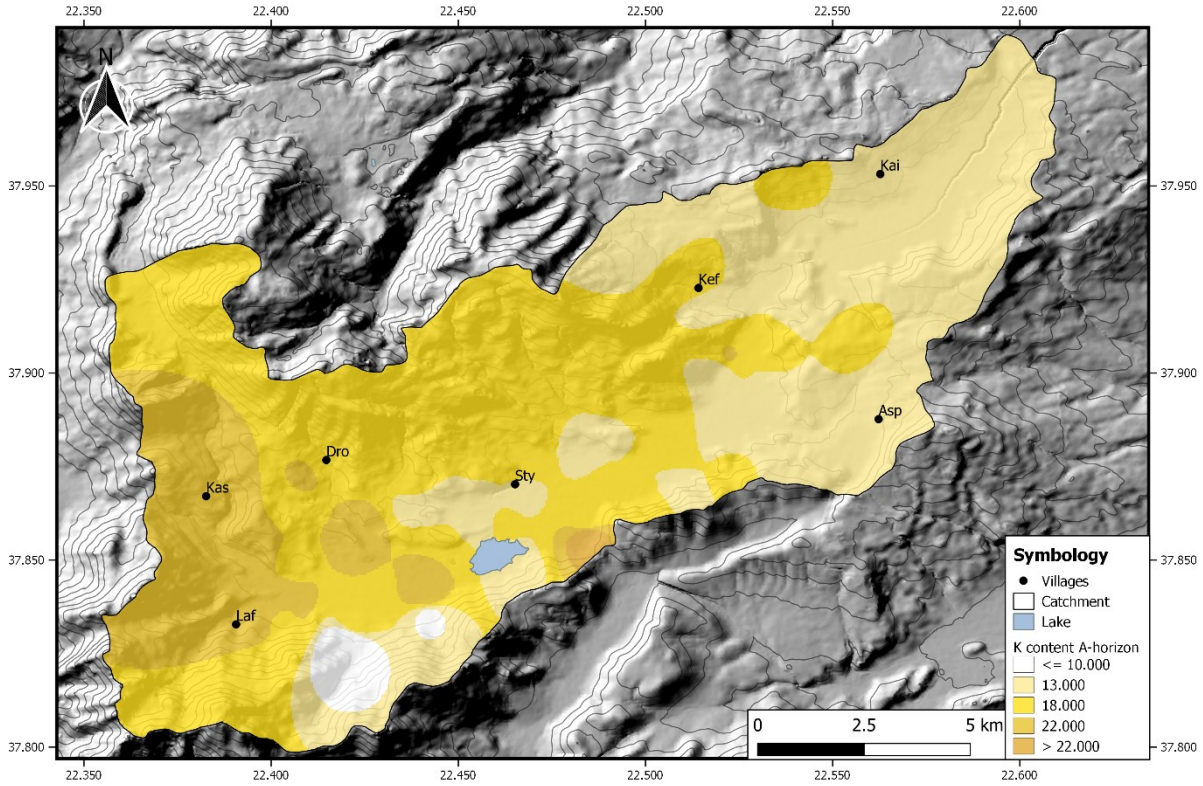

Figure 61: Potassium distribution of the A-horizons in the research area.

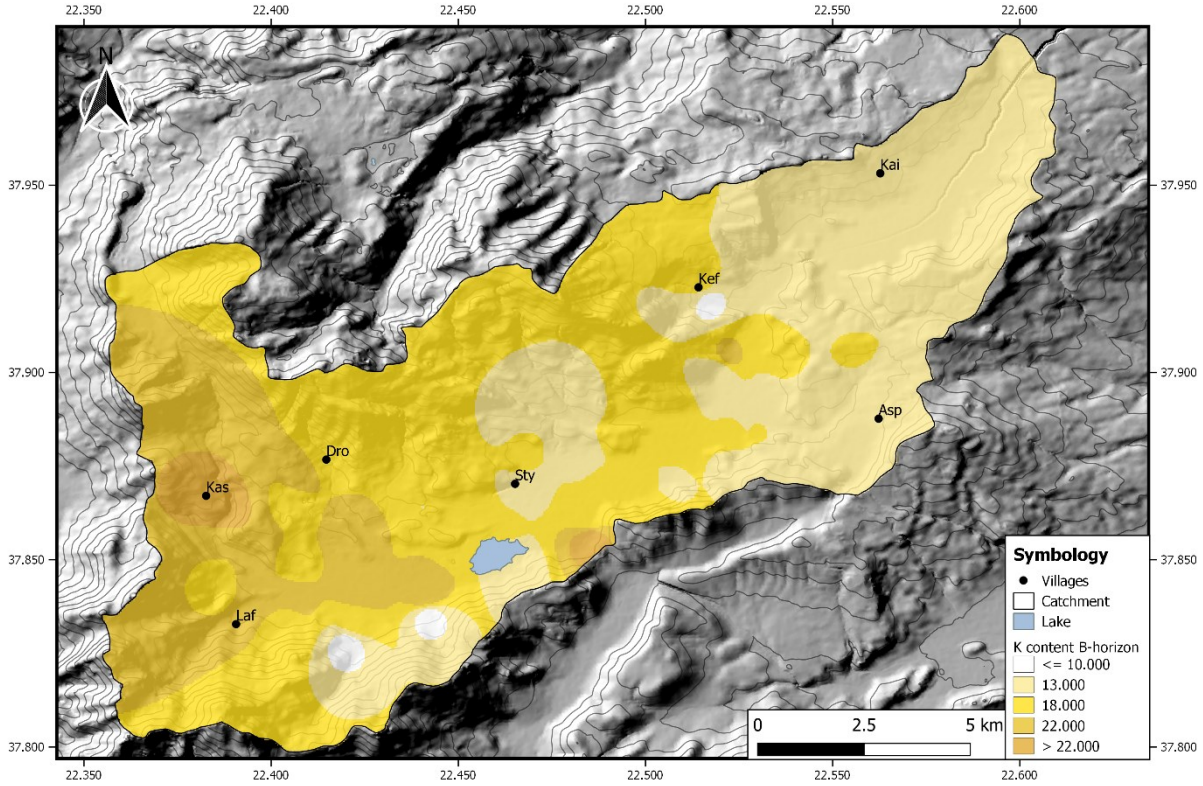

Figure 62: Potassium distribution of the B-horizons in the research area.

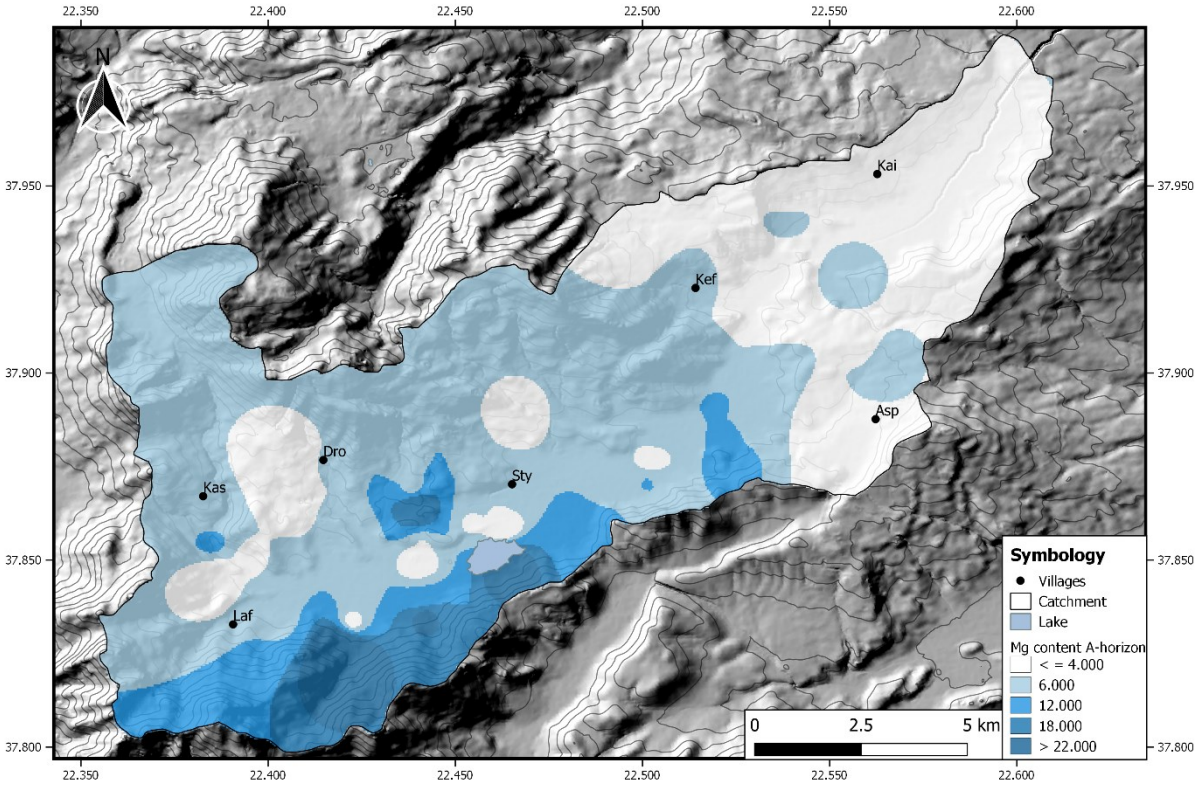

Figure 63: Magnesium distribution of the A-horizons in the research area.

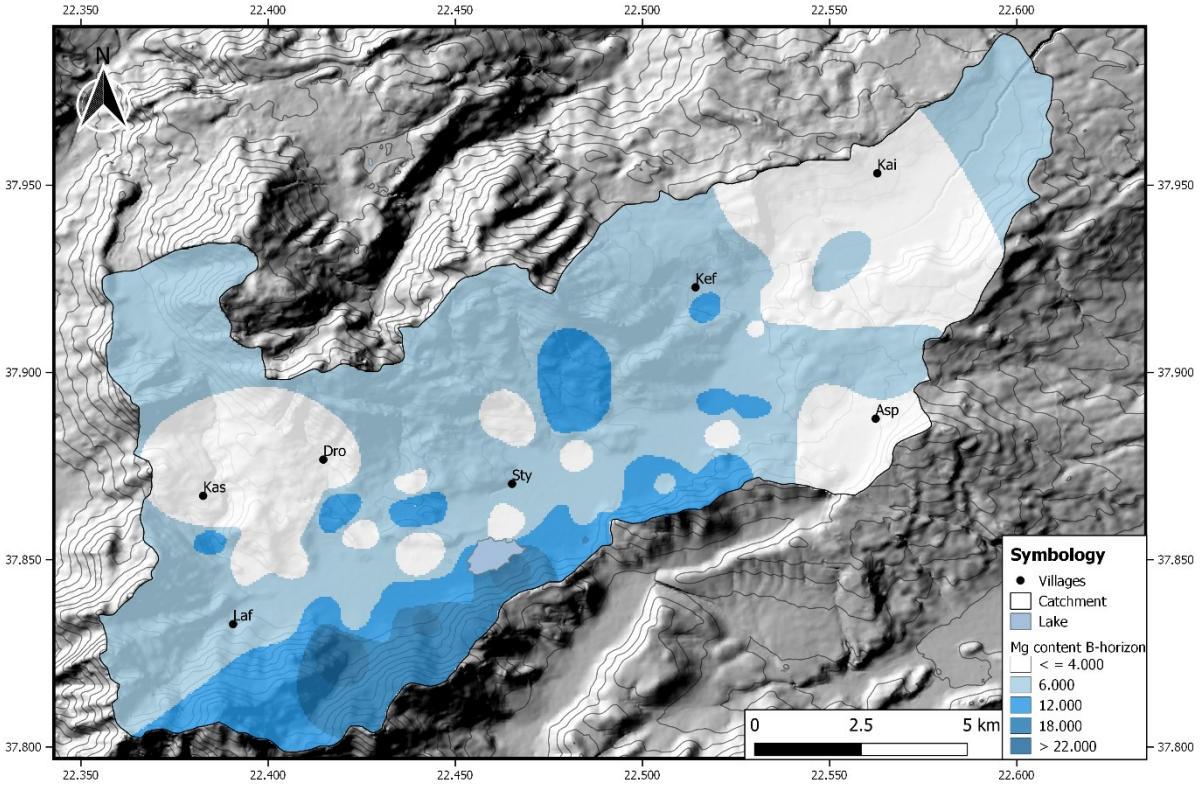

Figure 64: Magnesium distribution of the B-horizons in the research area.

6.2.5 Soil degradation

In general, it can be noted that the polje is and has been used for agricultural purposes to a high degree, which has led to a considerable reduction in the number of soil functions. The intensive cultivation of the soil towards an ideal cultivated plant location displaces functions such as filtering and buffering capacity, the habitat for soil organisms, the archive of cultural and natural history and water storage functionality (Krebs et al., 2017).

Impoverishment processes of the presented soils can be observed in the form of mass losses through erosion. The recording of the site characteristics with regard to the relief shows frequent concave surface forms at sites characterized by agriculture, terraced farming and fallow land. Many sites on the slopes have a high slope inclination, little soil cover, high stone content, i.e. mostly only Leptosols are developed. In addition, there is only a low vegetation cover and is therefore considered to be highly susceptible to erosion. At these sites, both denudation and small linear (groove 10 - 300 cm^2) and large linear forms of erosion (gully erosion, ditch > 40 cm) are common. The mass displacement of the soil is also evident from the colluviums that were found, which at the STY-P 57 site reaching a thickness of up to 72 cm. Long-lasting tillage led to the disturbance of the activity of soil organisms, as indicated by the high C/N ratios in the soil and the destabilization of the soil structure. Through a long lasting fallow the soil fertility and structural stability can be increased again but there are some areas in the polje where the sand content clearly dominates (Deutsches Institut für Fernstudienforschung an der Universität Tübingen, 1997). The grain size as a limiting factor is, as already explained, a decisive factor in semi-arid regions. Furthermore, intensive tillage, i.e. increased ploughing activity, results in mixing of the soil at different depths and across different horizons as well as destruction of the root space and the associated reduction in aggregate stability. Fertilizer input as well as fallow land settling on arable land indicate small deficiencies in the nutrient availability of the macronutrients Ca, K and Mg.

Thus, the degradation tendencies of Stymphalia are caused by the decline of biodiversity, soil loss, depletion of the organic substance (in the polje) and increasing soil acidification (in Isomata and Drosopigi).

6.3 Integrating soil properties for modelled land use scenarios at Archaic and Late Hellenistic times from a geoarchaeological point of view

Three land use types are included for quantifying the environmental footprint of a land use system. These are field crop cultivation, tree crops and woodlot and livestock pasturage. For input parameters of the developed land use model, Weiberg et al. (2019) are using diet, agricultural practices, livestock species and crafting like the iron and bronze metallurgy. In addition to archaeological sources, which provide an insight into the social structure and technological innovations as described in chapter 3.2, historical sources were also included. This provided information on animal husbandry and agricultural production (such as information on pasture rights provided by specific polis and the amount of pastoral production in specific regions)(Hughes et al., 2018; Weiberg et al., 2019). Another aspect that was considered is the fact that ancient societies become increasingly more complex over time. The social development becomes visible archaeologically through the extend of human activates and linked social structures and essentially the range and complexity of observed and recorded material culture. The variability in social complexity is therefore expressed through the social complexity index (SCI) ranges from 1 (low) to 5 (high). This classification is based on the number, distribution and/or extend of archaeological sites and settlements, socio-economic and hierarchical structures, contact networks as well as the range and variety of material culture (Weiberg et al., 2019).

Of particular interest are phases 9 and 10 (Archaic and Hellenistic period) of the Weiberg model in which ancient Stymphalos existed. In Archaic times, a dramatic expansion and intensity of land use is seen on the Peloponnese. The per capita demand increases to 2.9 ha in archaic times and to 3.2 ha in the early Hellenistic period (Weiberg et al., 2019).

Due to the favourable morphological situation of the polje, a land use area of 110 km² can be assumed. Because of the very steep slopes of the catchment (219 km²), 109 km² are not cultivable. Due to lake level fluctuations and related periodic floods, which affect a large part of the cultivated area, a further 10 km² are not

included in the calculation, where crop failures must be expected. Thus a potentially available area for pasturage, field and tree crops of 100 km² in Stymphalia is given (figure 65). Williams (2005) occupies a minimum of 2500 people who lived in ancient Stymphalos in Hellenistic times and about 500 people in the surrounding areas. According to the model calculations, 96 km² are needed to feed such a local population. On the one hand, the size of the town itself, which could not be used as arable land, and on the other hand, the fact that the terraced sites do not provide the amount of cultivable land that would be possible on the plain. Accordingly, both the model calculations and the reconstruction of the number of inhabitants at ancient Stymphalos, based on Williams excavation, fits very well.

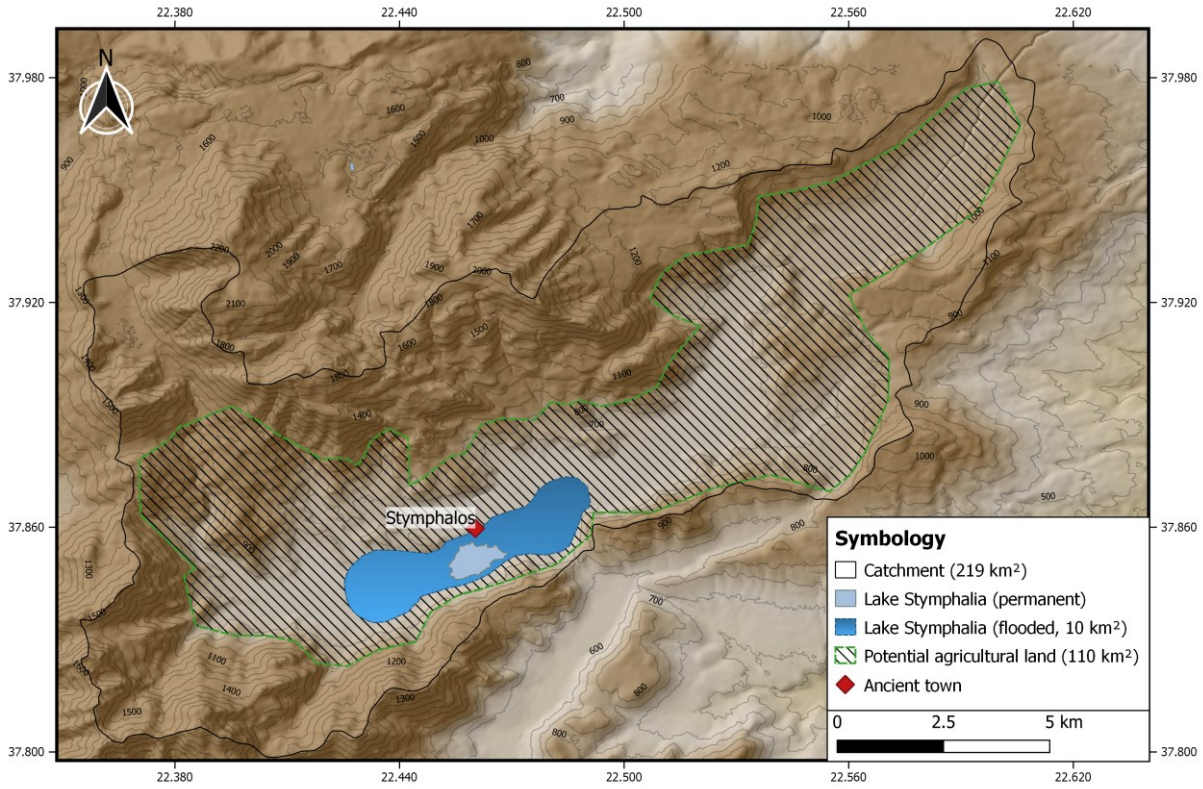

Figure 65: Map of the potential agricultural land in the Stymphalia polje.

The present analysis shows that there are, however, some areas and thus soils that allow only certain crops to be cultivated and also have a poorer soil quality, which can lead to a considerable reduction of the extend of cultivated areas. The areas

with lower soil quality (figure 66 and figure 67) are located at Drosopigi, in the north of the lake and ancient Stymphalos, alluvial fans in the south (e.g. soil profile STY-KEF 4) and in the north (e.g. STY-KEF 2) and large parts in the northern catchment area (e.g. STY-P33).

Due to the location of the ancient town, the nearby cultivated areas on the polje plain were probably used for farming. If a larger area was needed, whether due to floods, crop failures or increasing population, it is conceivable to switch to hillside locations and build field terraces. If the terrace locations on the slopes were no longer sufficient to feed the population, it is also conceivable that small elevated valleys were already used for the cultivation of arable crops in Archaic but certainly in the early Hellenistic period. In the course of the surveys conducted for the present study, two high-lying valleys could be investigated. These are the locations of the soil profiles STY-P 57 and ISO-1. The site at STY-P 57 still shows a very high soil quality and is considered as suitable alternative site due to its location near the ancient city. The location on the Isomata plateau is to be classified differently. The site is not easy to reach, at least in ancient time. The location is characterized by a rather moderate soil quality, which is not least shown by the low pH value. In addition to soil acidification, the soils at the plateau show signs of degradation by cutting off soil horizons.

If one considers a worst-case scenario in which the population of the Hellenistic period was forced to move to the high valleys at the margin of the polje in order to cultivate crops and these soils were degraded to such an extent due to overexploitation, this can have led to considerable consequences. It is also important to note that the cultivation of cereal crops leads to a considerable reduction in nutrient availability and forces a constant change of cultivation, thus increasing land consumption (Deutsches Institut für Fernstudienforschung an der Universität Tübingen, 1997).

Knitter et al. (2019) did a further modelling approach that investigates how much cultivable land was necessary to fulfil the demand of a society. The study investigated to which degree locally available resources of central sites were exploited and the society depends on support for the surroundings and how changing environmental conditions influence the supply. The focus lies on the north-eastern Peloponnese at Mycenaen palace centres of the Late Helladic IIIB

period. To calculate for which site the available space was sufficient they implemented the estimates of Weiberg et al. (2019) cereal based model, settlement data about the population of the archaeological sites and data of land use suitability. They combined the knowledge of land use practices with empirical data of environmental characteristics in a fuzzy rule-based system. The environmental data includes information on slope degrees, precipitation, aquifers and soils (Knitter et al., 2019). The model considers high and medium productive soils such as Fluvisols, Cambisols, Calcisols and Luvisols (Knitter et al., 2019; Yassoglou et al., 2017). In their model, they distinguish between four different types of land use: Agriculture, Arboriculture, Pasture and Wood. Site characteristics such as erosion potential, sufficient rainfall, fertile soils and proximity to water supply are considered for field cultivation. The model does not take into account the cultivation of field terraces, which leads to an underestimation of suitable land (Knitter et al., 2019). The result of the investigations shows that small settlements have sufficient space to ensure the diet of the population. Whereas the large palace centres do not offer enough space regarding field crop cultivation, which can be further aggravated by dry periods. In dry scenarios, also the space for arboriculture products is insufficient at these sites (Knitter et al., 2019). The investigations of the study presented here can help to further refine the models of Weiberg et al. (2019) and Knitter et al. (2019).

The lack of empirical data availability of soil parameters, such as the availability of nutrients on terrace sites, is crucial. The investigations of the present study show, however, that especially the cultivation of terraces is an extremely important factor to cultivate areas. As explained in chapter 5, the terrace sites show a very high soil quality in particular at a depth of more than 20 cm below the ground surface (B-horizons) but also in the topsoils (A-horizons). The soil quality of the terraces exceeds that of the topsoil in the plain.

The study by Seguin et. al. (2019) on the palaeoenvironmental history of the Stymphalia area shows stable conditions with an approximated average sedimentation rate in the lake of 0.2 mm/yr during the Classical-Hellenistic period. In this period, Stymphalia has the highest population density and therefore the highest land use activity. It is possible that the first terraces were built during this period. A large number of terraces in Greece date in the 5th and 4th centuries BC

such as in the area of Attica in the area of ancient deme at Athens and on the Cycladic islands (Delos and Kea)(Dimakopoulos, 2016). As already mentioned, an increase in population and excessive use of soils requires the cultivation of higher situated sites, i.e. hillside locations. The relatively low sedimentation rates recorded in Lake Stymphalia potentially support this assumption, as numerous studies have shown that terrace farming counteracts erosion processes (Frederick & Krahtopoulou, 2000).

To further enhance the existing models of land use of prehistoric societies a more precise few on soil properties must be considered. The pedological analysis in Stymphalia show, that the sites with the soil profiles STY-KEF 2 and STY-KEF 4, which are representative of the reference soil group of Cambisols in this region, have a low soil quality. Within the groups there can also be considerable variations in soil quality. For example, the Luvisols of the different sites show significant differences. While the soil quality is moderate at Kefalari and Isomata, it is very high at site STY-P 57. Therefore, the implementation of soil parameters should be differentiated both within the soil groups as well as site specific.

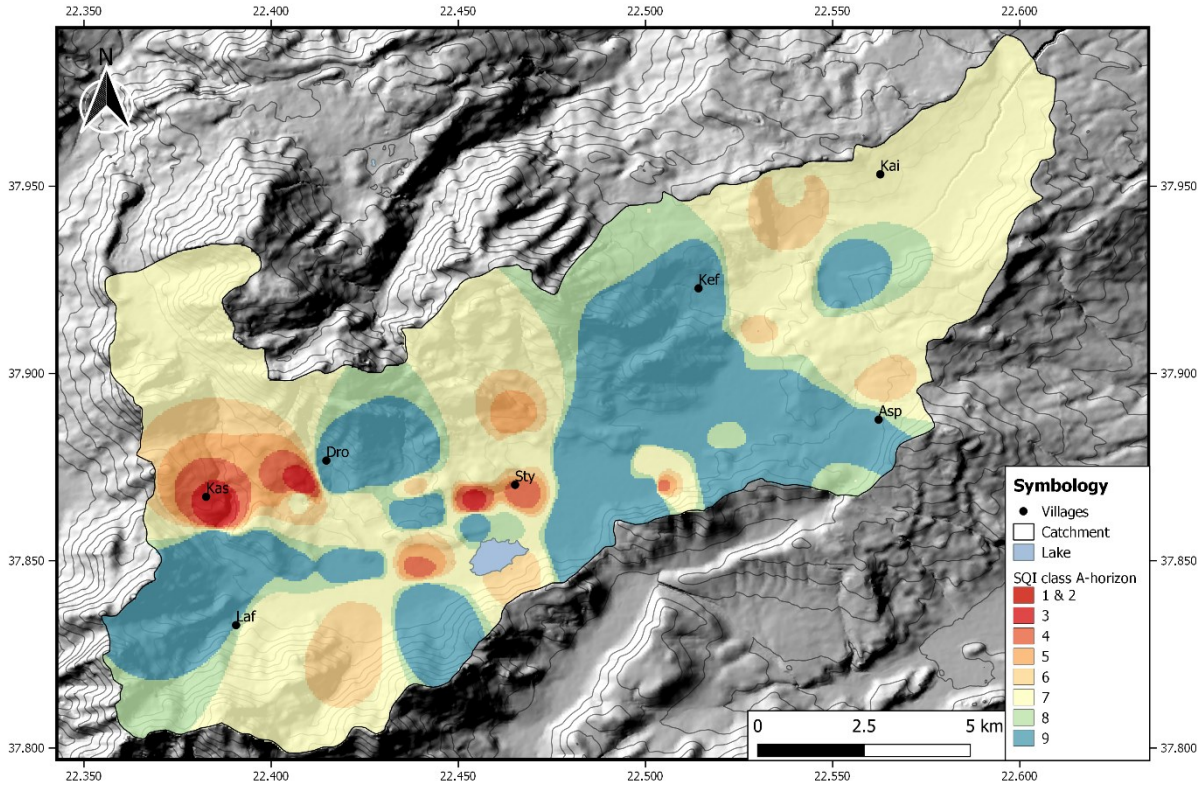

Figure 66: Soil quality index of the A-horizons in the research area.

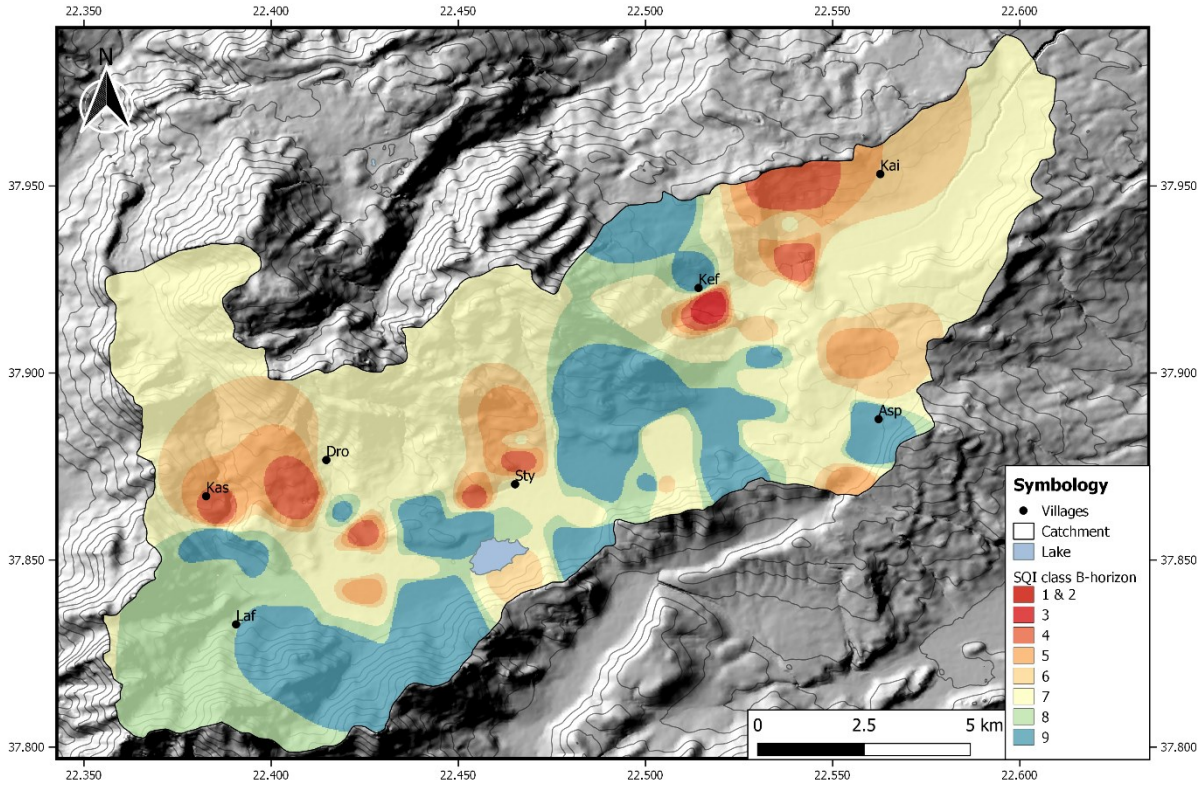

Figure 67: Soil quality index of the B-horizons in the research area.

The distribution maps (figure 66 and 67) show the soil quality index of the A- and B-horizons in the study area. The highest soil quality of the A- and B-horizons is found in the middle of the polje northwest of Asprokampos and southwest of Kefalari. A shift is shown by the alluvial fan south of Kefalari in the B-horizon, which is dominated by coarse stone material due to massive erosion events. Increasing soil degradation with increasing depth is evident in the northern part of the polje south of Kaisari and north of Asprokampos. Significantly low soil quality was observed in the Stymphalia area north of the lake. The poor soil quality may be closely related to the proximity of the former city in Archaic and Hellenistic times. Due to its central location by the lake, this area may have been intensively used for cultivation since Archaic times. Other sites characterized by poor soil quality are located west of Drosopigi and in the area of the small mountain village of Kastania. In the area of the village Lafka, a high soil quality could be recorded which slightly decreases with increasing depth. An increasing decrease in soil

quality is evident in the B-horizons south of the village. East of the village of Lafka, in the area of Transect 1, the soil quality in the plain is poor, while the soil quality on the slopes and especially on the terraces is very high. The study shows a very heterogeneous picture concerning the soil quality on the area.

The question arises what potential the soils of a region like Stymphalia have to produce more than their own demands. Against the background of being able to supply Mycenaean palace centers with goods like grain. According to the current state of research, a settlement in Stymphalia during Mycenaean times is only proven by the detection of some ceramic fragments. There are no clear traces of occupation or settlement at this time. However, since it can be assumed that the palace centers were supplied by surrounding settlements as the above mentioned models show, Stymphalia can be considered as an exemplary region. The topographical situation is an excellent and closed system at least for soil development. For the supply of 3000 inhabitants, the whole area of the polje, the terraces and also the high valleys are used for agriculture due to changes in demand, floods and crop failures. An overproduction seemed unlikely in a time of high population as for example in Hellenistic times.

A clear relationship between population growth and the management of higher lying sites is given by the investigations of Seguin et al. (2019) on a sediment core from Lake Stymphalia and the site at Isomata (ISO-1, chapter 5.2.2.4). The chronological dates of the M-Ap horizon on the Isomata plateau can be connected with unit 69 (dated to ca 1720 - 1850 cal AD) of the Lake Stymphalia core. The dens, compact and clay rich unit shows an abrupt increase in terrigenous elements (Seguin et al., 2019). Furthermore, an increase in Mn, Fe and MS (magnetic susceptibility) points to soil formation processes indicating that the lake has fallen dry during the 19th century. As possible reason the authors refer to the historical evidence that the authorities in the Corinth region reactivated the Hadrian aqueduct in the 1880 to irrigate their local fields (Seguin et al., 2019). During the 19th and early 20th century, the population at the site grew exponentially, which resulted in a strong expand of land use activity and the promotion of agricultural products.

The formation of the colluvium starts more than 150 years ago and shows little or no use of the area as an agricultural site since that time. A low lake level or even

desiccation meant that more land was available for cultivation and there was no need to use the higher-lying plateaus for cultivation. Fluctuations in the lake level have a considerable influence on the amount of land available for cultivation and thus on the supply potential of a stagnating population.

7 Conclusions

The present study on soil development in Stymphalia show how long-term land use can affect soil quality. In order to classify the soil quality of the region, grain size, skeleton content, organic matter, C/N ratio, pH value and element concentrations of Ca, K, and Mg were used as soil parameters. The soils were classified by the soil quality index, showing considerable differences in the quality of the soils. Accordingly, many areas of the polje have already been degraded due to intensive land use. However, this does not include the terraced sites. By using the terraces only temporarily, in contrast to the flattened polje area, which is permanently used for agriculture, the soil is able to recover itself and strengthen its regulatory function.

The soil quality assessment in the study area shows small-scale differences in soil quality according to site specific features. For the creation of modelled scenarios of land use of prehistoric societies, these small regional differences in soil properties can have considerable effects. The potential of the region as a supplier of agricultural products for the support of large palace centres was very limited, at least in the Archaic and Hellenistic period. The investigation of soil quality and the degree of degradation gives an important contribution to the discussion of the multi-causal decline of the palace centres. It is still unclear which factors led to the decline of the Mycenaean palaces. The sea people movement, climatic extremes and political unrest are cited. However, the lack of arable land for the supply of the population must have been a decisive factor. The effects of a worst-case scenario was presented in this thesis. The overexploitation of soils, whose fertility in Greece is strongly supported by water storage capacity, can lead to a considerable reduction of the supply base. The degree of degradation in the form of erosion is evident in the capped soil profiles and colluviums, but is also reflected in intensified land use activity. Despite this considerable human intervention in the natural environment, the quality of the soil at some polje sites is still very high respectively these soils show a very good soil fertility.

Future studies on the soil quality or soil fertility of the region in Archaic and Hellenistic or even Mycenaean times should focus on the dating of the terraces. Terrace agriculture plays a decisive role in the population growth of the region

Stymphalia. The precise dating of the colluvia, which is still lacking, can improve the reconstruction of the land use history. A great challenge is the reconstruction of the soil quality/fertility in earlier times. The soil properties of the subsoil horizons provided the first indications of the soil properties and thus quality. The B-horizons of the soil profiles at Kefalari and Isomata show signs of degradation, i.e. especially the soil physical parameters can be used for the reconstruction of the soil composition in a cultural-historical context. Accordingly, the subsoil horizons already formed the basis for land use practices in Mycenaean times.

The investigations in Tiryns show how important the analysis of environmental archives in combination with archaeological excavations are. The combined examination of archaeological features and finds with the sedimentary stratigraphic sequence allowed us to make concrete statements about the environmental conditions of the Late Bronze Age. An undeveloped cultural horizon from the 14th century BC formed the basis. In this layer both pottery and anthropogenically induced element concentrations could be determined. Periodic slight flooding phases followed. These are interrupted by two layers in which a reduction or shifting of the current line has occurred and the area was used by humans or animals. A first detectable foundation by humans took place to use the former floodplain area. This foundation was eroded by the river, which possibly broke through the Kofini dam. A second, slightly compacted foundation was then constructed for the foundation of the lower town of Tiryns. Contrary to the state of research so far, the investigations of this study show no extreme event challenging Tiryns. The profile shows numerous flood phases, which the people reacted on. The river history is documented form the Late Helladic IIIA1 (approx. 1.400 BC) to the Late Helladic IIIB2 (approx. 1.200 BC) period. The investigated profile, the exact chronological limitation by ceramic fragments under the first fluvial deposits and the first building development above the youngest river gravels, which covers approximately 150 years of river history, is unique for such semi-arid areas. Therefore, the investigated archive represents a valuable event stratigraphy, which helps us to reconstruct the paleoenvironment conditions in the Late Bronze Age. In order to extend the reconstruction of the environmental conditions in Tiryns to the post-palatial period, the dating of the Kofini Dam is necessary. By

knowing when the dam was built, the erosion processes that led to the removal of the foundation layers can be further explained.

In order to obtain further information about the supply of agricultural goods to the palace of Tiryns, besides macro-remain analysis from the excavations and Linear B texts, an approach similar to Stymphalia can be considered. By dating the cultural horizon Y1a, this horizon could provide a first clue to reconstruct the soil quality in Late Helladic times.

References

AG Boden. (2005). Bodenkundliche Kartieranleitung. In *Bundesanstalt für Geowissenschaften und Rohstoffe und den Geologischen Landesämtern in der Bundesrepublik Deutschland Hannover: Vol. 5.*

Alexandrovskaya, E. & Panova, T. (2003). History of the soil, cultural layer, and people in medieval Moscow. *Revista Mexicana de Ciencias Geologicas*, *20*(3), 289–294.

Amacher, M. C., O'Neill, K. P. & Perry, C. H. (2007). Soil vital signs: A new soil quality index (SQI) for assessing forest soil health. *USDA Forest Service - Research Paper RMRS-RP*, *65 RMRS-RP*, 1–14. https://doi.org/10.2737/RMRS-RP-65

Andreae, H., Eickenscheidt, N., Evers, J., Grüneberg, E., Ziche, D., Ahrends, B., Höhle, J., Nagel, H.-D. & Wellbrock, N. (2016). Stickstoffstatus und dessen zeitliche Veränderungen in Waldböden. *Thünen Report*, *43*(Thünen Rep.), 135–180. https://doi.org/10.3220/REP1473930232000

Balcer, J. M. (1974). The Mycenaean Dam at Tiryns. *American Journal of Archaeology*, *78*(2), 141–149. https://doi.org/10.2307/502798

Barsch, H., Ballwitz, K. & Scholz, E. (1984). *Labormethoden der Physischen Geographie*. Gotha, Hermann Haak.

Bevan, A. & Conolly, J. (2011). Terraced fields and Mediterranean landscape structure: An analytical case study from Antikythera, Greece. *Ecological Modelling*, *222*(7), 1303–1314. https://doi.org/10.1016/j.ecolmodel.2010.12.016

Bintliff, J. (2012). *The Complete Archaeology of Greece: From Hunter-Gatherers to the 20th Century A.D.* Oxford, New York, John Wiley & Sons, Ltd.

Blair, T. C. & McPherson, J. G. (1994). Alluvial fans and their natural distinction from rivers based on morphology, hydraulic processes, sedimentary processes, and facies assemblages. *Journal of Sedimentary Research A: Sedimentary Petrology & Processes*, *A64(3)*, 450–489. https://doi.org/10.1306/d4267dde-2b26-11d7-8648000102c1865d

Blume, H.-P., Brümmer, G. W., Horn, R., Kandeler, E., Kögel-Knabner, I., Kretzschmar, R., Stahr, K. & Wilke, B.-M. (2010). *Scheffer/Schachtschabel: Lehrbuch der Bodenkunde*. Springer Berlin Heidelberg. https://doi.org/10.1007/978-3-662-49960-3

Boero, V. & Schwertmann, U. (1989). Iron oxide mineralogy of terra rossa and its genetic implications. *Geoderma*, *44*(4), 319–327. https://doi.org/10.1016/0016-7061(89)90039-6

Brysbaert, A. (2015). "Set in Stone"? Technical, socio-economic and symbolic considerations in the construction of the Cyclopean-style walls of the Late Bronze Age Citadel at Tiryns, Greece. *Analecta Praehistorica Leidensia*, *45*, 69–90.

Calvert, S., Pedersen, T. & Karlin, R. (2001). Geochemical and isotopic evidence for post-glacial palaeoceanographic changes in Saanich Inlet, British Columbia. *Marine Geology*, *174*(1–4), 287–305. https://doi.org/10.1016/S0025-3227(00)00156-0

Calvert, S. E., Bustin, R. M. & Ingall, E. D. (1996). Influence of water column anoxia and sediment supply on the burial and preservation of organic carbon in marine shales. *Geochimica et Cosmochimica Acta*, *60*(9), 1577–1593. https://doi.org/10.1016/0016-7037(96)00041-5

Cline, E. H., ed. (2012). *The Oxford Handbook of the Bronze Age Aegean*. Oxford University Press. https://doi.org/10.1093/oxfordhb/9780199873609.001.0001

Demoule, J.-P. & Pèrles, C. (1993). The Greek Neolithic: A new review. *Journal of World Prehistory*, *7*(4), 355–416. https://doi.org/10.1007/BF00997801

Deutsches Institut für Fernstudienforschung an der Universität Tübingen (DIFF), eds. (1997). *Veränderung von Böden durch anthropogene Einflüsse*. Berlin/Heidleberg, Springer. https://doi.org/10.1007/978-3-642-59222-5

Dimakopoulos, S. (2016). Agricultural Terraces in Classical and Hellenistic Greece. *Multi-, Inter- and Transdisciplinary Research in Landscape Archaeology*, 1–10. https://doi.org/10.5463/lac.2014.37

Dotterweich, M. (2008). The history of soil erosion and fluvial deposits in small catchments of central Europe: Deciphering the long-term interaction between humans and the environment - A review. *Geomorphology*, *101*(1–2), 192–208. https://doi.org/10.1016/j.geomorph.2008.05.023

Drake, B. L. (2012). The influence of climatic change on the Late Bronze Age Collapse and the Greek Dark Ages. *Journal of Archaeological Science*, *39*(6), 1862–1870. https://doi.org/10.1016/j.jas.2012.01.029

Dypvik, H. & Harris, N. B. (2001). Geochemical facies analysis of fine-grained siliciclastics using Th/U, Zr/Rb and (Zr + Rb)/Sr ratios. *Chemical Geology*, *181*(1–4), 131–146. https://doi.org/10.1016/S0009-2541(01)00278-9

Entwistle, J. A., Abrahams, P. W. & Dodgshon, R. A. (2000). The Geoarchaeological Significance and Spatial Variability of a Range of Physical and Chemical Soil Properties from a Former Habitation Site, Isle of Skye. *Journal of Archaeological Science*, *27*(4), 287–303. https://doi.org/10.1006/jasc.1999.0453

Finné, M., Bar-Matthews, M., Holmgren, K., Sundqvist, H. S., Liakopoulos, I. & Zhang, Q. (2014). Speleothem evidence for late Holocene climate variability and floods in Southern Greece. *Quaternary Research (United States)*, *81*(2), 213–227. https://doi.org/10.1016/j.yqres.2013.12.009

Frederick, C. & Krahtopoulou, A. (2000). Deconstructing agricultural terraces: examining the influence of construction method on stratigraphy, dating and archaeological visibility. In *Landscape and land use in postglacial Greece* (1st ed., Issue April 2015, pp. 79–94). Sheffield Academic Press.

French, C. A. I. (2003). *Geoarchaeology in Action : Studies in Soil Micromorphology and Landscape Evolution*. London, Routledge.

Fuchs, M., Lang, A. & Wagner, G. A. (2004). The history of Holocene soil erosion in the Phlious Basin, NE Peloponnese, Greece, based on optical dating. *The Holocene*, *14*(3), 334–345. https://doi.org/10.1191/0959683604hl710rp

Gauss, R. K., Bátora, J., Nowaczinski, E., Rassmann, K. & Schukraft, G. (2013). The Early Bronze Age settlement of Fidvár, Vráble (Slovakia): Reconstructing prehistoric settlement patterns using portable XRF. *Journal of Archaeological Science*, *40*(7), 2942–2960. https://doi.org/10.1016/j.jas.2013.01.029

Halstead, P. (1987). Traditional and ancient rural economy in Mediterranean Europe: plus ça change? *The Journal of Hellenic Studies*, *107*(1987), 77–87. https://doi.org/10.2307/630071

Halstead, P. (1992). Agriculture in the Bronze Age Aegean – Towards a Model of Palatial Economy. In B. Wells (Ed.), *Agriculture in Ancient Greece, Proceedings of the Seventh International Symposium at the Swedish Institute at Athens, 16-17 May 1990* (pp. 105–117).

Hanson, V. D. (1992). Practical Aspects of Grape-Growing and the Ideology of Greek Viticulture. In B. Wells (Ed.), *Agriculture in Ancient Greece, Proceedings of the Seventh International Symposium at the Swedish Institute at Athens, 16-17 May 1990* (pp. 163–166).

Hartge, K. H. & Horn, R. (1992). *Die physikalische Untersuchung von Böden*. Sturrgart, F. Enke.

Haversath, J.-B. (2004). *Griechenland: Raum-zeitlicher Wandel im Süden der Balkanhalbinsel*. Gotha, Klett-Perthes.

Hinojosa, H. (2016). *Local Site Effects in Archaeoseismology: Examples from the Mycenaean Citadels of Tiryns and Midea (Argive Basin , Peloponnese, Greece)*. Universität zu Köln.

Hughes, R. E., Weiberg, E., Bonnier, A., Finné, M. & Kaplan, J. O. (2018). Quantifying land use in past societies from cultural practice and archaeological data. *Land*, *7*(1), 1–21. https://doi.org/10.3390/land7010009

Isager, S. & Skydsgaard, J. E. (1992). *Ancient Greek Agriculture*. London, Routledge. https://doi.org/10.4324/9780203037744

Karkanas, P. & Goldberg, P. (2018). *Reconstructing Archaeological Sites: Understanding the Geoarcheological matrix*. Hoboken, Wiley. https://doi.org/10.1002/9781119016427

Khamnueva, S. (2017). *Landscape development and soil transformation in the former Viking settlement Hedeby*. Universität zu Kiel.

Kilian, K. (1983). Ausgrabungen in Tiryns 1981. Bericht zu den Grabungen. *Archäologisches Anzeiger*, *97*, 392–430.

Kilian, K. (1988). Mycenaeans up to date, trends and changes in recent research. In E. B. French & K. Wardle (Eds.), *Problems in Greek Prehistory*: Papers Presented at the Centenary Conference of the British School of Archaeology at Athens (pp. 112–115). Manchester, Bristol Classical Press.

Knitter, D., Günther, G., Hamer, W. B., Keßler, T., Seguin, J., Unkel, I., Weiberg, E., Duttmann, R. & Nakoinz, O. (2019). Land use patterns and climate change- A modeled scenario of the Late Bronze Age in Southern Greece. *Environmental Research Letters*, *14*(12). https://doi.org/10.1088/1748-9326/ab5126

Kokiasmenou, E., Caliri, C., Kantarelou, V., Germanos Karydas, A., Romano, F. P. & Brecoulaki, H. (2020). Macroscopic XRF imaging in unravelling polychromy on Mycenaean wall-paintings from the Palace of Nestor at Pylos. *Journal of Archaeological Science: Reports*, *29*(October 2019), 102079. https://doi.org/10.1016/j.jasrep.2019.102079

Kokinou, E., Kamberis, E., Vafidis, A., Monopolis, D., Ananiadis, G. & Zelilidis, A. (2005). Deep seismic reflection data from offshore Western Greece: A new crustal model for the Ionian Sea. *Journal of Petroleum Geology*, *28*(2), 185–202. https://doi.org/10.1111/j.1747-5457.2005.tb00079.x

Koutsoyiannis, D., Mamassis, N., Efstratiadis, A., Zarkadoulas N., & Markonis, I. (2012). Floods in Greece. In Z. Kundzewicz (Ed.), *Changes in Flood Risk in Europe* (Issue SPEC. ISS. 10, pp. 293–303). CRC Press.

Krebs, R., Egli, M., Tobias, S. & Schulin, R. (2017). *Bodenschutz in der Praxis*. Stuttgart UTB. https://nbn-resolving.org/urn:nbn:de:101:1-201712085086

Macklin, M. G., Benito, G., Gregory, K. J., Johnstone, E., Lewin, J., Michczyńska, D. J., Soja, R., Starkel, L. & Thorndycraft, V. R. (2006). Past hydrological events reflected in the Holocene fluvial record of Europe. *Catena*, *66*(1–2), 145–154. https://doi.org/10.1016/j.catena.2005.07.015

Macklin, M. G., Fuller, I. C., Lewin, J., Maas, G. S., Passmore, D. G., Rose, J., Woodward, J. C., Black, S., Hamlin, R. H. B. & Rowan, J. S. (2002). Correlation of fluvial sequences in the Mediterranean basin over the last 200 ka and their relationship to climate change. *Quaternary Science Reviews*, *21*(14–15), 1633–1641. https://doi.org/10.1016/S0277-3791(01)00147-0

Manning, S. W. (2010). Chronology and terminology. In E. Cline (Ed.), *The Oxford Handbook of the Bronze Age Aegean (ca. 3000-1000 BC)* (pp. 11–28). Oxford University Press.

Maran, J. (2008). Nach dem Ende: Tiryns - Phönix aus der Asche. In Badisches Landesmuseum Karlsruhe (Ed.), *Zeit der Helden. Die dunklen Jahrhunderte Griechenlands 1200-700 v. Chr.* (p. 400). Badisches Landesmuseum Karlsruhe/Primus Verlag Darmstad.

Maran, J. (2009). The crisis years? : reflections on signs of instability in the last decades of the Mycenaean palaces. *Scienze Dell'Antichità*, *15*(15), 241–262.

Maran, J. & Papadimitriou, A. (2006). Forschungen im Stadtgebiet von Tiryns 1999-2002. *Archaologischer Anzeiger*, 97–169.

Maran, J. & Papadimitriou, A. (2017). Die aktuelle Unterstadt-Grabung und das Erbe palatialer Bauplanung. In D. A. Institut (Ed.), *AtheNea* (pp. 30–42).

Maran, J., Papadimitriou, A., Birndorfer, T., Khamnueva, S., Bork, R., Unkel, I. & Kroll, H. (2019). Tiryns, Griechenland. Die Arbeiten der Jahre 2015 bis 2018. *DAI E-Forschungsberichte*, 68–77. https://publications.dainst.org/journals/efb/2182/6595

Maran, J., Papadimitriou, A. & Hinzen, K. G. (2015). Tiryns, Griechenland. Die Arbeiten der Jahre 2012 bis 2014. *DAI E-Forschungsberichte*, *3*, 1–9.

Maroukian, H., Gaki-Papanastassiou, K. & Piteros, C. (2004). Geomorphological and Archaeological Study of the Broader Area of the Mycenaean Dam of Megalo Rema and Ancient Tiryns , Southeastern Argive Plain , Peloponnesus. *Bulletin of the Geological Society of Greece*, *36*(3), 1154–1163. https://doi.org/10.12681/bgsg.16458

Miall, A. D. (1985). Architectural-Element Analysis: A New Method of Facies Analysis Applied to Fluvial Deposits. *Earth-Science Reviews Elsevier Science Publishers B.V*, *22*, 261–308. https://doi.org/10.1016/0012-8252(85)90001-7

Morfis, A. & Zojer, H. (1986). Karst hydrogeology of the Central and Eastern Peloponnesus (Greece). *Steir. Beitr. Zur Hydrogeologie*, *37/38*, 1–301.

Mühlenbruch, T. (2009). Tiryns - The Settlement and its History in LH III C. In S. Deger-Jalkotzy & A. E. Bächle (Eds.), *LH III C Chronology and Synchronisms III. LH III C Late and the transition to the Early Iron Age* (pp. 313–326).

Mukherjee, A. & Lal, R. (2014). Comparison of Soil Quality Index Using Three Methods. *PLoS ONE*, *9*(8), e105981. https://doi.org/10.1371/journal.pone.0105981

Nakos, G. (1979). Forest soils of Greece: Physical, chemical and biological properties. *Forest Ecology and Management*, *2*, 35–51. https://doi.org/10.1016/0378-1127(79)90035-5

Nguemezi, C., Tematio, P., Yemefack, M., Tsozue, D. & Silatsa, T. B. F. (2020). Soil quality and soil fertility status in major soil groups at the Tombel area, South-West Cameroon. *Heliyon*, *6*(2). e03432. https://doi.org/10.1016/j.heliyon.2020.e03432

Nichols, G. J. & Fisher, J. A. (2007). Processes, facies and architecture of fluvial distributary system deposits. *Sedimentary Geology*, *195*(1–2), 75–90. https://doi.org/10.1016/j.sedgeo.2006.07.004

Nicosia, C. & Stoops, G. R. (2017). Archaeological Soil and Sediment Micromorphology. In C. Nicosia & G. Stoops (Eds.), *Archaeological Soil and Sediment Micromorphology*. New York, John Wiley & Sons, Ltd. https://doi.org/10.1002/9781118941065

Oldfield, F., Wake, R., Boyle, J., Jones, R., Nolan, S., Gibbs, Z., Appleby, P., Fisher, E. & Wolff, G. (2003). The late-Holocene history of Gormire Lake (NE England) and its catchment: a multiproxy reconstruction of past human impact. *The Holocene*, *13*(5), 677–690. https://doi.org/10.1191/0959683603hl654rp

Panagos, P. (2006). The European soil database. *GEO: Connexion*, *5*(7), 32–33.

Papastergiadou, E. S., Retalis, A., Kalliris, P. & Georgiadis, T. (2007). Land use changes and associated environmental impacts on the Mediterranean shallow Lake Stymfalia, Greece. *Hydrobiologia*, *584*(1), 361–372. https://doi.org/10.1007/s10750-007-0606-9

Parker, V. (2014). *A History of Greece. 1300 to 30 BC*. New Yourk, John Wiley & Sons, Ltd.

Perlès, C. & Monthel, G. (2001). The Early Neolithic in Greece. In *University Press* (Vol. 40, Issue 03). Cambridge University Press. https://doi.org/10.1017/CBO9780511612855

Photiades, A. (2017). Geological contribution to the tectoni-stratigraphy of the Nafplio area (NW Argolis, Greece). *Bulletin of the Geological Society of Greece*, *43*(3), 1495–1507. https://doi.org/10.12681/bgsg.11324

Pope, K. O. & van Andel, T. H. (1984). Late quaternary alluviation and soil formation in the southern Argolid: its history, causes and archaeological implications. *Journal of Archaeological Science*, *11*(4), 281–306. https://doi.org/10.1016/0305-4403(84)90012-8

Price, S. & Nixon, L. (2005). Ancient Greek Agricultural Terraces: Evidence from Texts and Archaeological Survey. *American Journal of Archaeology*, *109*(4), 665–694. https://doi.org/10.3764/aja.109.4.665

Roberts, N., Moreno, A., Valero-Garcés, B. L., Corella, J. P., Jones, M., Allcock, S., Woodbridge, J., Morellón, M., Luterbacher, J., Xoplaki, E. & Türkeş, M. (2012). Palaeolimnological evidence for an east–west climate see-saw in the Mediterranean since AD 900. *Global and Planetary Change*, *84–85*, 23–34. https://doi.org/10.1016/j.gloplacha.2011.11.002

Robertson, A. H. F., Clift, P. D., Degnan, P. J. & Jones, G. (1991). Palaeogeographic and palaeotectonic evolution of the Eastern Mediterranean Neotethys. *Palaeogeography, Palaeoclimatology, Palaeoecology*, *87*(1–4), 289–343. https://doi.org/10.1016/0031-0182(91)90140-M

Rodrigue, J. A. & Burger, J. A. (2004). Forest Soil Productivity of Mined Land in the Midwestern and Eastern Coalfield Regions. *Soil Science Society of America Journal*, *68*(3). https://doi.org/10.2136/sssaj2004.0833

Rothwell, R. G. & Croudace, I. W. (2015). Micro-XRF Studies of Sediment Cores. In I. W. Croudace & R. G. Rothwell (Eds.), *Micro-XRF Studies of Sediment Cores: Applications of a non-destructive tool for the environmental sciences* (Vol. 17). Springer Netherlands. https://doi.org/10.1007/978-94-017-9849-5

Ruppenstein, F. (2012). Gesellschaftliche Transformationen und politisch-soziale Krisen im frühen Griechenland. Überlegungen zur Entstehung der mykenischen Palaststaaten. In Sigrid Deger-Jalkotzy & A. Suppan (Eds.), *Krise und Transformation* (Denkschriften der philosophisch-historischen Klasse 441, pp. 37–68). Austrian Academy of Sciences Press.

Schliemann, H. (1886). *Tiryns: Der prähistorische Palast der Könige von Tiryns*. Mannheim, F. A. Brockhaus.

Seguin, J., Bintliff, J. L., Grootes, P. M., Bauersachs, T., Dörfler, W., Heymann, C., Manning, S. W., Müller, S., Nadeau, M. J., Nelle, O., Steier, P., Weber, J., Wild, E. M., Zagana, E. & Unkel, I. (2019). 2500 years of anthropogenic and climatic landscape transformation in the Stymphalia polje, Greece. *Quaternary Science Reviews*, *213*, 133–154. https://doi.org/10.1016/j.quascirev.2019.04.028

Shelmerdine, C. W. (1997). Review of Aegean Prehistory VI: The Palatial Bronze Age of the Southern and Central Greek Mainland. *American Journal of Archaeology*, *101*(3), 537. https://doi.org/10.2307/507109

Tataris, A., Kallergis, G., Kounis, G., Bizon, G. & Christodoulou, G. (1970). *Nafplion sheet in scale 1:50,000. Geological map of Greece.* Institute Research, for Geology and Subsurface.

van Andel, T. H., Runnels, C. N. & Pope, K. O. (1986). Five Thousands Years of Land Use and Abuse in the Southern Argolid, Greece. *Hesperia*, *55*(1), 103. https://doi.org/10.2307/147733

van Andel, T. H., Zangger, E. & Demitrack, A. (1990). Land Use and Soil Erosion in Prehistoric and Historical Greece. *Journal of Field Archaeology*, *17*(4), 379–396. https://doi.org/10.1179/009346990791548628

van Andel, T. H., Zangger, E. & Perissoratis, C. (1990). Quaternary transgressive/regressive cycles in the Gulf of Argos, Greece. *Quaternary Research*, *34*(3), 317–329. https://doi.org/10.1016/0033-5894(90)90044-L

van Breemen, N. & Buurman, P. (2002). *Soil Formation*. Springer Netherlands. https://doi.org/10.1007/978-0-585-31788-5

Vita-Finzi. (1969). *Mediterranean Valleys: Geological Changes in Historical Times*. Cambridge University Press.

Von Lützow, M., Kögel-Knabner, I., Ludwig, B., Matzner, E., Flessa, H., Ekschmitt, K., Guggenberger, G., Marschner, B. & Kalbitz, K. (2008). Stabilization mechanisms of organic matter in four temperate soils: Development and application of a conceptual model. *Journal of Plant Nutrition and Soil Science*, *171*(1), 111–124. https://doi.org/10.1002/jpln.200700047

Vött, A., Brückner, H., M.Zander, A., M.May, S., Athen, I. M., Darmstadt, F. L., Koln, I. F. & Marburg, A. D. (2009). Late Quaternary evolution of mediterranean poljes - The Vatos case study (akarnania, NW greece) based on geo-scientific core analyses and IRSL dating. *Zeitschrift Fur Geomorphologie*, *53*(2), 145–169. https://doi.org/10.1127/0372-8854/2009/0053-0145

Walsh, K., Brown, A. G., Gourley, B. & Scaife, R. (2017). Archaeology, hydrogeology and geomythology in the Stymphalos valley. *Journal of Archaeological Science: Reports*, *15*, 446–458. https://doi.org/10.1016/j.jasrep.2017.03.058

Weiberg, E., Hughes, R. E., Finné, M., Bonnier, A. & Kaplan, J. O. (2019). Mediterranean land use systems from prehistory to antiquity: a case study from Peloponnese (Greece). *Journal of Land Use Science*, *14*(1), 1–20. https://doi.org/10.1080/1747423X.2019.1639836

Williams, H. (2003). *The Exploration of Ancient Stymphalos, 1982 - 2002*. 397–411.

Williams, H. & Gouley, B. (2005). The Fortifications of Stymphalos. *Mouseion: Journal of the Classical Association of Canada*, *5*(3), 213–259. https://doi.org/10.1353/mou.2005.0013

Xoplaki, E., González-Rouco, J. F., Gyalistras, D., Luterbacher, J., Rickli, R. & Wanner, H. (2003). Interannual summer air temperature variability over Greece and its connection to the large-scale atmospheric circulation and Mediterranean SSTs 1950-1999. *Climate Dynamics*, *20*(5), 537–554. https://doi.org/10.1007/s00382-002-0291-3

Xoplaki, E., Luterbacher, J., Burkard, R., Patrikas, I. & Maheras, P. (2000). Connection between the large-scale 500 hPa geopotential height fields and precipitation over Greece during wintertime. *Climate Research*, *14*(2), 129–146. https://doi.org/10.3354/cr014129

Yassoglou, N., Kosmas, C. & Moustakas, N. (1997). The red soils, their origin, properties, use and management in Greece. *CATENA*, *28*(3–4), 261–278. https://doi.org/10.1016/S0341-8162(96)00042-2

Yassoglou, N., Tsadilas, C. & Kosmas, C. (2017). *The Soils of Greece* (World Soils Book Series). Berlin, Springer. https://doi.org/10.1007/978-3-319-53334-6

Zangger, E. (1994). Landscape Changes around Tiryns during the Bronze Age. *American Journal of Archaeology*, *98*(2), 189–212. https://doi.org/10.2307/506635

Zangger, E. (1993). The geoarchaeology of the Argolid (Argolis 2). Berlin, Gebr. Mann.

Appendices

Appendix 1: Sediment properties of the different strata of the profile at Tiryns.

Sample ID	*Sand [%]*	*Silt [%]*	*Clay [%]*	*LOI [%]*	*P [ppm]*	*As [ppm]*	*Zn [ppm]*	*Fe [ppm]*	*Ca [ppm]*	*log (Zr/Rb)*	*Log (Rb/Sr)*
Y1a	24.98	65.83	9.20	2.37	372	10	63	31742	72736	0.375	0.277
Y3	75.05	22.35	2.60	1.44	119	6	31	24275	63215	0.616	0.375
2	91.96	7.12	0.91	1.13	189	6	23	19340	66311	0.512	0.464
3	73.36	23.72	2.93	1.57	306	7	37	24183	66035	0.760	0.487
Y2	39.88	53.51	6.61	2.23	245	11	48	29135	83452	0.432	0.379
5	86.55	12.05	1.39	1.33	699	5	19	17508	68786	0.485	0.513
6	53.51	41.83	4.66	1.37	1714	7	47	25360	73946	0.439	0.427
7	66.36	30.09	3.55	1.73	1576	7	40	24163	76946	0.547	0.497
8	62.91	33.11	3.99	1.67	1613	8	42	23926	71519	0.487	0.440
9	82.14	16.26	1.60	1.37	103	4	24	20588	68661	0.602	0.509
10	56.47	39.67	3.85	1.70	182	7	38	24323	78120	0.584	0.475
11	88.54	10.29	1.17	1.07	182	5	28	20893	64611	0.744	0.543
12	64.76	31.92	3.32	1.40	141	8	42	25228	74784	0.425	0.397
13	45.59	48.59	5.82	2.13	154	7	43	27393	77827	0.448	0.368
14	44.75	49.46	5.79	2.13	285	9	50	29805	76619	0.477	0.362
15	69.21	27.29	3.49	1.60	668	4	38	23936	65868	0.456	0.400
16	95.00	4.61	0.39	0.90	258	5	20	17038	62027	0.508	0.454
17	55.46	39.72	4.82	1.93	210	6	42	25904	71339	0.474	0.341
18	76.88	20.25	2.87	1.60	192	5	39	22835	64051	0.556	0.392
Y1b	32.38	61.11	6.52	2.33	182	7	47	28796	80212	0.477	0.367

Appendix 2: Soil properties of the different soil profiles form the Stymphalia polje.

Soil properties of Profile STY-KEF 1

Sample ID	Unit	Clay [%]	Silt [%]	Sand [%]	Stones [%]	LOI [%]	C/N ratio	pH-value	Zr [ppm]	Fe [ppm]	Ti [ppm]	Ca [ppm]	K [ppm]	Mg [ppm]
STY-K1 0 - 5	Ap	20.85	41.44	37.71	90	9.43	12.42	7.27	160	46999	3708	20973	11017	3496
STY K1 5 - 10	Ap	28.29	70.81	0.90	90	8.04	14.19	7.28	150	46535	4005	32474	10905	5377
STY K1 20 - 25	Bt1	27.59	71.35	1.07	70	6.20	9.38	7.29	179	56791	4514	6607	11403	3513
STY K1 35 - 40	Bt1	28.57	68.35	3.08	70	5.46	8.61	7.20	166	57611	4474	5370	11901	NA
STY K1 55 - 60	Bt1	18.62	36.11	45.27	70	5.00	8.03	7.19	158	56487	4452	5505	10837	2993
STY K1 80 - 85	Bt1	16.85	45.66	37.49	70	4.82	7.58	7.17	143	47400	3204	4282	7155	2154
STY K1 100 – 105	Bt1	16.44	42.01	41.54	40	4.73	7.83	7.17	168	48319	3977	6225	8544	3098
STY K1 125 - 130	Bt2	9.08	31.68	59.24	40	4.40	9.40	7.28	155	35767	2851	6496	8262	NA

Soil properties of Profile STY-KEF 2

Sample ID	Unit	Clay [%]	Silt [%]	Sand [%]	Stones [%]	LOI [%]	C/N ratio	pH-value	Zr [ppm]	Fe [ppm]	Ti [ppm]	Ca [ppm]	K [ppm]	Mg [ppm]
STY-KEF-2 0-6	IAh	16.93	50.42	32.64	95	6.74	43.47	7.35	80	24476	1961	164055	12509	NA
STY-KEF-2 20	IAh	8.36	31.15	60.49	95	2.95	40.10	7.52	54	26795	2558	210680	9401	6295
STY-KEF-2 40	IAh	8.56	32.64	58.81	85	2.46	37.20	7.52	51	24946	2366	202667	9066	6163
STY-KEF-2 200-205	IIBv	33.19	52.87	13.94	85	6.32	54.43	7.43	140	41785	3705	67228	15686	NA
STY-KEF-2 210-220	IIIBv	9.19	37.57	53.24	70	3.70	40.20	7.55	72	15693	1293	192708	9052	NA
STY-KEF-2 245	IIIBv-Cv	7.59	47.81	44.60	70	2.86	49.50	7.64	44	10076	866	255954	6916	NA

Soil properties of Profile STY-KEF 4

Sample ID	Unit	Clay [%]	Silt [%]	Sand [%]	Stones [%]	LOI [%]	C/N ratio	pH-value	Zr [ppm]	Fe [ppm]	Ti [ppm]	Ca [ppm]	K [ppm]	Mg [ppm]
STY-KEF-4 IAh	IIAh	14.07	43.61	42.32	70	4.43	50.41	7.37	95	28659	3079	147437	10570	4219
STY-KEF 4 IBv	IIBv	21.74	53.64	24.61	65	4.44	74.86	7.51	98	32436	3667	143048	12140	5461

Soil properties of Profile ISO-1

Sample ID	Unit	Clay [%]	Silt [%]	Sand [%]	Stones [%]	LOI [%]	C/N ratio	pH-value	Zr [ppm]	Fe [ppm]	Ti [ppm]	Ca [ppm]	K [ppm]	Mg [ppm]
ISO-1 M-Ap	M-Ap	11.52	36.78	51.71	15	6.49	12.91	6.09	234	49406	6023	3711	10611	2540
ISO-1 IBt	IBt	20.50	49.90	29.60	5	6.06	8.11	5.55	172	84906	5185	2921	14848	NA
ISO-1 IBt-Cv	IBt-Cv	21.65	46.15	32.19	5	5.64	5.40	5.43	185	72232	4937	3000	13344	2757
ISO-1 ICv	ICv	15.33	41.47	43.20	10	5.07	7.31	4.86	135	69404	4245	2676	12551	2908

Soil properties of Profile STY-P57

Sample ID	Unit	Clay [%]	Silt [%]	Sand [%]	Stones [%]	LOI [%]	C/N ratio	pH-value	Zr [ppm]	Fe [ppm]	Ti [ppm]	Ca [ppm]	K [ppm]	Mg [ppm]
STY-P57 M-Ap	M-Ap	23.84	58.42	17.74	15	6.52	35.10	7.45	186	33799	4053	66471	11260	15224
STY-P57 M-Bt	M-Bt	28.99	58.18	12.83	7	5.56	12.97	7.49	244	54779	5906	7951	16054	5545
STY-P57 IBt	IBt	30.71	63.02	6.27	2	5.86	7.51	7.29	255	59692	6006	4256	16992	4754
STY-P57 IBht	IBht	34.52	60.06	5.43	2	6.56	6.75	7.11	236	64169	5940	4063	15966	3504

Soil properties of Profile STY-DRO-1

Sample ID	Unit	Clay [%]	Silt [%]	Sand [%]	Stones [%]	LOI [%]	C/N ratio	pH-value	Zr [ppm]	Fe [ppm]	Ti [ppm]	Ca [ppm]	K [ppm]	Mg [ppm]
STY-DRO-1 M-Ap	M-Ap	5.63	46.28	48.09	30	4.47	17.00	5.45	421	23564	5724	2179	19336	1597
STY-DRO-1 M	M	15.77	53.70	30.53	30	4.77	16.60	5.32	327	37808	7345	1799	20639	3196
STY-DRO-1 IBht	IBht	23.17	58.88	17.95	40	5.59	8.34	4.33	275	58282	6272	1874	19952	2544
STY-DRO-1 ICv	ICv	7.81	39.09	53.10	95	2.83	12.94	4.14	416	30555	4427	979	11670	1335

Soil properties of Profile STY-ASP-1

Sample ID	Unit	Clay [%]	Silt [%]	Sand [%]	Stones [%]	LOI [%]	C/N ratio	pH-value	Zr [ppm]	Fe [ppm]	Ti [ppm]	Ca [ppm]	K [ppm]	Mg [ppm]
STY-ASP-1 Ah	Ah	18.19	50.68	31.13	3	10.84	14.25	7.03	174	44507	4729	12770	11620	2077
STY-ASP-1 Bt	Bt	24.00	59.43	16.57	30	5.46	19.50	7.47	188	49263	4892	18099	12246	3302
STY-ASP-1 Cv	Cv	16.65	71.04	12.32	20	3.16	120.25	7.71	53	10548	1836	284771	5818	1636
STY-ASP-1 cC	cC	16.30	74.00	9.70	10	3.26	150.12	7.75	53	8933	1484	305807	5119	1590

Appendix 3: Results of the pedological- and geomorphological mapping in Stymphalia

Sample ID	Altitude a.s.l.	Inclination	Exposition	Curvature vertivcal	Curvature horizontal	Relief type	M. relief 1	M. relief 2	Position	Erosion/deposition	Appearence	Type of use	Vegetation	Geology
STY-P01	862	N6	SW	X	X	H	RR	RR	O	EWL	FE	G	WI	Phyllites
STY-P02	726	N2	NE	V	V	H	RW	RW	U	EWF	T	BA	OV	Alluvial Fan
STY-P03	816	N4	EE	X	X	H	RW	RW	M	EWL	T	G	WI	Alluvial Fan
STY-P4.1	710	N4	SW	X	V	H	RW	RW	M	EWF	T	BA	WI	Alluvial Fan
STY-P4.2	890	N2	SE	V	G	H	RE	RE	M	EWF	T	BA	WI	Phyllites
STY-P05	709	N5	NE	X	X	H	RW	RW	M	EWF	FE	BA	GB	Limestone (Dolomite)
STY-P06	671	N2	NE	X	G	T	RW	RW	T	AWF	FE	BA	OV	Alluvium
STY-P07	692	N2	NE	X	X	H	RE	RE	U	AWF	FE	BA	L	Alluvial Fan
STY-P08	750	N4	WW	X	V	H	RE	RE	M	EWF	T	BA	WI	Alluvial Fan
STY-P09	650	N2	SE	V	V	H	RW	RS	M	EWF	T	BA	L	Alluvial Fan
STY-P10	670	N2	NW	V	V	T	RW	RW	T	EWF	P	BA	L	Alluvial Fan
STY-P11	645	N1	SS	G	G	T	RW	RW	T	AWF	P	BA	L	Alluvium
STY-P12	645	N1	SS	G	G	T	RW	RW	T	AWF	P	A	L	Alluvium
STY-P13	677	N3	EE	X	X	H	RS	RS	M	EWF	FE	BA	L	Alluvial Fan
STY-P14	772	N2	NE	V	X	H	RS	RS	M	EWF	T	F	NW	Limestone (Dolomite)

STY-P15	902	N2	SS?	V	V	H	RW	RW	O	EWF	FE	BA	OV	Conglomarate
STY-P16	741	N3	SS	V	G	H	RE	RE	M	EWF	FE	BA	OV	Alluvial Fan
STY-P17	630	N3	SO	G	X	H	RW	RE	M	EWF	FE	BA	L	Limestone
STY-P18	600	N2	SS	G	G	T	RW	RW	T		P	BA	WI	Alluvium
STY-P20	600	N0	SW	G	G	T	RE	RE	T	AWF	P			Alluvium
STY-P21	615	N3	NW	G	G	H	RW	RS	U	EWF	T	BA	WI	Limestone (Dolomite)
STY-P22	775	N6	SS	X	X	H	RW	RW	M	EWF	T	O	GB	Limestone
STY-P23	775	N4	EE	V	X	H	RW	RW	O	EWF/AWF	T	BA/40a	FP	Conglomarate
STY-P24	615	N2	SS	V	G	T	RE	RE	T	AWF	P	A	L	Alluvium
STY-P25	600	N0	SW	G	G	T	RW	RW	T	EWF	P	A	L	Alluvium
STY-P26	610	N0	SW	X	X	T	RW	RW	T	EWF	P	BA	WI	Alluvium
STY-P27	610	N2	WW	V	X	H	RW	RS	U	EWF	T	BA	WI	Alluvial Fan
STY-P28	625	N4	EE	X	X	H	RE	RW	U	EWF	FE	A	L	Limestone
STY-P29	610	N2	EE	X	X	H	RE	RW	F	EWF	P	A	L	Alluvial Fan
STY-P30	610	N0		G	G	T	RE	RW	T	AWF	P	A	L	Alluvium
STY-P31	615	N0	WW	G	G	T	RE	RE	T		P	A	L	Alluvium
STY-P32	740	N4	NW	V	V	H	RW	RE	U	EWF	T	A	L	Conglomarate
STY-P33	920	N0	SS	V	G	H	RE	RW	M	AY	T	BA/50a	GB	Conglomarate

STY-P34	810	N4	EE	G	G	H	RE	RW	M	EWF	P	A	L	Alluvial Fan
STY-P35	720	N5	WW	V	V	H	RE	RW	M	AY	T	GW	GB/PG	Alluvial Fan
STY-P36	675	N2	EE-SE	X	X	H	RE	RW	U	EWF/AWF	P	A	L	Alluvial Fan
STY-P37	645	N2	NE	X	X	H	RE	RW	U	AWF	P	A	KV	Alluvial Fan
STY-P38	640	N2	WW	G	G	H	RE	RW	U	AWF	FE	BA		Alluvial Fan
STY-P39	640	N2	WW	V	G	H	RE	RW	U		T	A	L	Alluvial Fan
STY-P40	635	N1		G	G	H	RE	RW	U	AWF	P	A	L	Alluvial Fan
STY-P41	615	N0	NW	G	G	T	RE	RW	T	AWF	P	A	L	Alluvium
STY-P42	655	N1		V	G	T	RE	RW	T	AWF	P	A	L	Alluvial Fan
STY-P45	600	N1	NE	G	G	T	RW	RW	T		P	A	L	Alluvium
STY-P46	615	N2	SE	G	G	T	RE	RE	T	EWF	P	A	L	Alluvium
STY-P47	916	N2	NO	V	G	H	RW	RW	O	AWF	T	BA	GB	Conglomarate
STY-P48	715	N0	NW	G	G	T	RW	RE	T	AWF	P	A	L	Alluvial Fan
STY-P49	740	N3	NW	V	G	H	RE	RE	U	EWF/AWF	FE	BA	WI	Conglomarate
STY-P50	790	N3	SS	V	V	H	RW	RW	M	AWF	FE	BA	WI	Conglomarate
STY-P51	770	N4	SW	V	V	H	RW	RW	O	EWF	T	A	L	Conglomarate
STY-P52	720	N3	WW	V	V	H	RW	RW	U	EWF/AWF	T	GW	WI	Alluvial Fan
STY-P53	710	N2	WW	V	G	H	RE	RW	U	EWF	P	A	L	Alluvium

STY-P54	710	N4	NW	V	G	H	RE	RW	M	EWF	T	A	L	Alluvial Fan
STY-P55	810	N2	SW	V	V	H	RW	RW	M	EWF	T	BA	OV	Alluvial Fan
STY-P56	730	N2	SS	V	V	H	RE	RW	M	EWF	T	BA	L	Conglomarate
STY-P57	727	N1	NN	G	X	T	RW	RW	T	AWF	P	A	L	Alluvium
STY-P58	654	N4	SO	G	X	H	RW	RW	M	EWF	FE	G	OV	Alluvium
STY-P59	648	N2	SS	X	X	T	RW	RW	T	AWF	FE	A	L	Alluvium
STY-P60	640	N1	NN	G	G	T	RW	RW	T	AWF	P	A	L	Alluvium
STY-P61	710	N3	NN	V	G	H	RE	RE	M	EWF	FE	BA	GB	Alluvial Fan
STY-P63	680	N4	SW	V	V	H	RW	RE	M	EWF	T	BA	WI	Alluvial Fan
STY-P64	635	N0	SS	X	X	T	RE	RE	T	AWF	FE	A	L	Alluvial Fan
STY-P65	625	N0	SW	G	G	T	RW	RW	T	AWF	FE	A	L	Alluvium
STY-P66	615	N0	SS	G	G	T	RW	RE	T	AWF	P	A	L	Alluvium
STY-P67	650	N4	NW	X	X	H	RW	RW	M	EWF	FE	A	L	Alluvial Fan

Inclination: N0 = not inclined, N1 = very slightly inclined, N2 = weakly inclined, N3 = medium inclined, N4 = strongly inclined, N5 = very strongly inclined, N6 = steep;
Curvature: G = stretched, X = convex, V = concave;
Relief type: T = depth range, H = slope;
Micro relief: RE = smooth, RR = groove, RS = stepped, RW = wavy;
Position: O = upper slope, M = middle slope, U = lower slope, T = depth location;
Erosion/deposition: AWF = accumulation through denudation, EWF = surface soil erosion by water, AY = anthropogenic accumulation
Appearance: FE = alluvial fan, P = plain, T = terrace;
Type of use: A = arable land, BA = fallow land, GW = grassland and rotation farming, F = forest, G = grassland;
Vegetation: FP = fodder plants, GB = bush, shrub and herbaceous plants, L = agricultural use, PG = plant communities on permanent grassland, WI = meadow, OV = open landscape, NW = coniferous forest;

Appendix 4: Soil properties of transect 1.

Sample ID	Clay	Silt	Sand	Soil type	Color	Stones [%]	LOI [%]	C/N ratio	pH-value	Ca [ppm]	K [ppm]	Mg [ppm]	SQI [%]	Class
P55A	16.23	51.75	32.02	Uls	2.5YR2.5/4	20	6.80	10.71	6.87	8137	15776	4907	79.17	9
P55B	15.55	49.76	34.70	Slu	2.5YR2.5/4	20	5.28	8.49	7.13	8422	15416	4135	62.50	7
P56A	11.81	49.43	38.76	Slu	7.5YR3/4	75	4.51	12.81	7.46	53667	14553	5266	50.00	5
P56B	15.72	59.44	24.84	Uls	10YR3/4	75	4.91	20.72	7.46	66085	17003	3282	54.17	6
P57A	21.79	55.18	23.03	Lu	7.5YR4/6	15	7.24	22.16	7.38	63637	11616	15372	75.00	9
P57B	19.83	57.52	22.65	Lu	5YR4/4	10	6.28	31.66	7.52	59300	12014	11156	66.67	8
P58A	32.40	65.09	2.51	Tu4	5YR3/3	50	18.11	16.33	7.19	39096	16414	3967	50.00	5
P58B	34.88	61.35	3.77	Tu3	5YR3/3	80	15.01	9.00	7.25	50818	15484	3115	70.83	8
P59A	11.47	41.36	47.17	Slu	7.5YR3/4	60	5.83	12.17	7.27	8312	19133	3005	41.67	3
P59B	14.09	50.83	35.08	Uls	7.5YR3/4	50	5.57	12.70	7.17	9348	18893	3584	58.33	6
P60A	7.63	65.90	26.47	Us	10YR3/4	5	5.00	17.06	7.38	55191	21783	6042	70.83	8
P60B	7.72	67.13	25.15	Us	10YR3/4	0	4.86	32.97	7.39	55164	21884	7309	70.83	8
P61A	22.90	58.05	19.05	Lu	2.5YR2.5/3	15	14.33	22.85	7.23	101821	9128	18833	79.17	9
P61B	21.60	57.05	21.35	Lu	2.5YR2.5/3	15	7.50	38.08	7.36	129809	9014	18809	79.17	9

Appendix 5: Soil properties of transect 2.

Sample ID	Clay	Silt	Sand	Soil type	Color	Stones [%]	LOI [%]	C/N ratio	pH-value	Ca [ppm]	K [ppm]	Mg [ppm]	SQI [%]	Class
P28A	26.67	59.37	13.95	Lu	7.5YR2.5/2	90	7.22	7.47	7.50	43636	18170	4098	70.83	8
P28B	30.23	58.35	11.42	Tu3	7.5YR2.5/2	60	8.89	10.10	7.41	36181	19404	4822	62.50	7
P29A	17.01	50.91	32.08	Lu	5YR3/3	25	6.01	21.28	7.37	78449	11407	4914	70.83	8
P29B	14.35	50.53	35.12	Uls	5YR3/3	30	5.04	25.56	7.37	80570	10726	5667	62.50	7
P63A	27.01	60.62	12.37	Lu	5YR3/3	80	10.16	10.77	7.47	49403	17828	4634	66.67	8
P63B	25.19	55.94	18.87	Lu	5YR3/3	70	8.19	9.66	7.06	45445	17482	4630	62.50	7
P23A	17.23	58.86	23.91	Lu	10YR3/3	50	6.90	13.52	7.44	141375	13018	4752	75.00	9
P23B	18.89	59.12	21.99	Lu	10YR3/3	50	5.58	10.94	7.24	120644	14485	5142	70.83	8
P24A	19.75	63.18	17.06	Lu	10YR3/2	5	6.89	14.89	7.43	64787	12535	4312	79.17	9
P24B	17.08	61.77	21.15	Lu	10YR3/2	5	6.76	9.30	7.32	64844	12360	3777	75.00	9
P18A	13.43	48.80	37.77	Slu	10YR3/4	65	5.64	12.12	7.41	42325	12686	5123	41.67	3
P18B	13.83	50.70	35.47	Uls	10YR3/3	65	5.93	14.02	7.42	34858	12354	4322	58.33	6
P45A	23.04	64.17	12.78	Lu	5YR3/4	20	7.73	12.95	7.28	31534	12899	3823	70.83	8
P45B	24.04	64.56	11.40	Lu	5YR3/4	10	6.63	14.02	7.41	24307	15290	5419	79.17	9

Appendix 6: Soil properties of transect 3.

Sample ID	Clay	Silt	Sand	Soil type	Color	Stones [%]	LOI [%]	C/N ratio	pH-value	Ca [ppm]	K [ppm]	Mg [ppm]	SQI [%]	Class
P33A	15.49	41.91	42.61	Slu	2.5YR3/4	30	6.93	14.44	7.17	7304	13708	3758	54.17	6
P33B	13.77	45.74	40.49	Slu	2.5YR3/4	50	5.58	12.04	7.12	12606	13488	3831	37.50	3
P34A	14.20	38.68	47.12	Sl4	2.5YR3/4	20	5.31	13.43	7.41	21497	13279	4232	50.00	5
P34B	17.41	47.26	35.33	Ls2	2.5YR3/4	20	4.58	27.69	7.38	43907	13066	3094	54.17	6
P35A	14.62	38.50	46.88	Sl4	2.5YR3/4	20	6.63	9.98	6.07	4527	13071	1818	54.17	6
P35B	14.01	45.45	40.54	Slu	2.5YR3/4	5	5.80	12.30	6.52	4491	13419	3186	37.50	3
P38A	12.47	42.95	44.58	Slu	7.5YR3/3	30	5.20	10.59	7.36	31178	15328	3366	50.00	5
P38B	11.59	39.81	48.60	Sl3	7.5YR3/3	30	4.44	11.34	7.31	29345	15461	3983	50.00	5
P39A	13.47	43.38	43.15	Slu	5YR3/3	10	4.63	7.97	7.36	7923	13826	4345	62.50	7
P39B	13.07	43.29	43.64	Slu	7.5YR5/6	5	4.20	12.99	7.47	8454	14275	5094	70.83	8
P31A	12.67	58.70	28.63	Uls	10YR3/4	5	4.37	22.55	7.50	98531	12539	6076	62.50	7
P31B	14.40	59.41	26.19	Uls	10YR3/4	2	4.17	10.71	7.32	45838	13990	3314	66.67	8
P32A	17.12	57.00	25.88	Lu	7.5YR3/4	40	5.13	11.22	7.44	127589	13690	6474	79.17	9
P32B	18.92	61.61	19.47	Lu	7.5YR3/4	30	4.13	14.04	7.54	132195	13227	6414	70.83	8

Appendix 7: Profiles of the geoarchive at Tiryns.

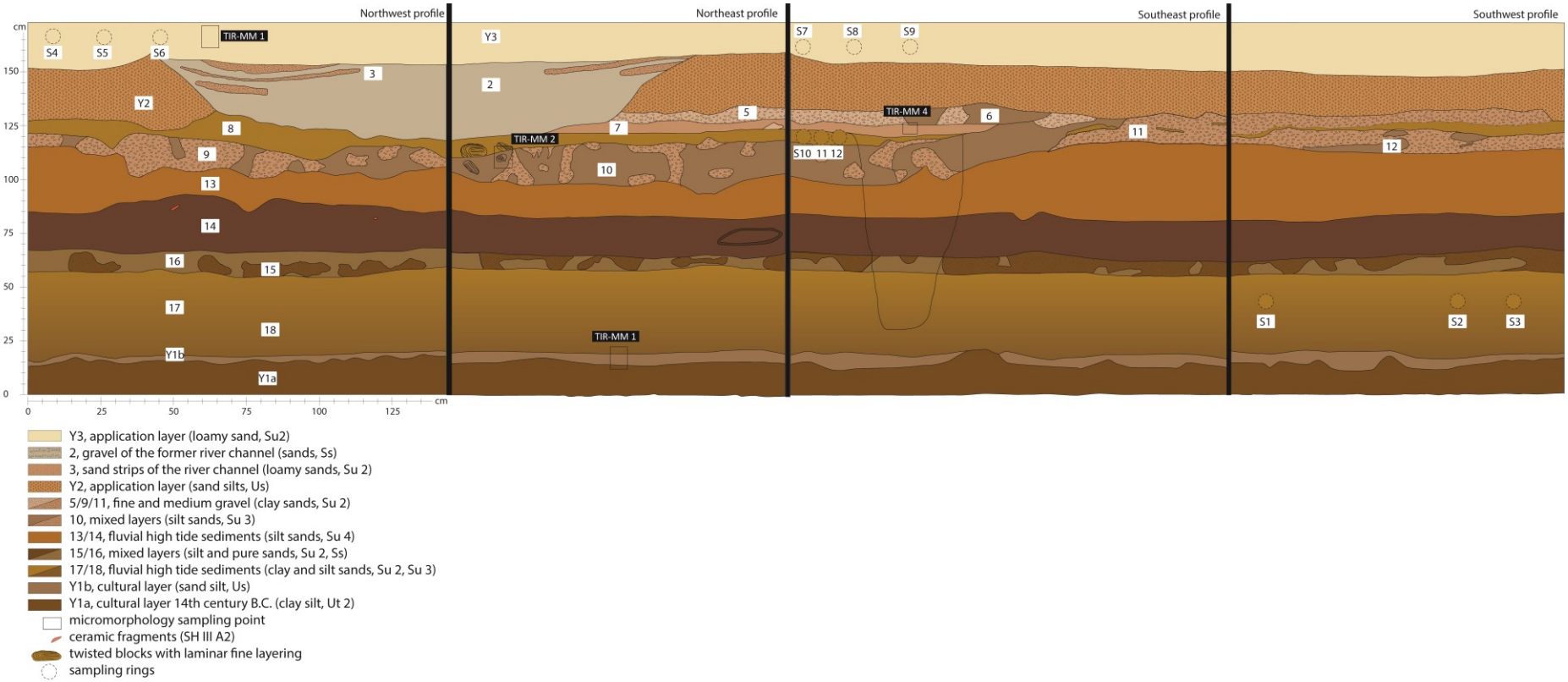

Appendix 8: Statistics of the different classified soil quality indexes.

Class 1	*mean*	*sd*	*median*	*trimmed*	*mad*	*min*	*max*	*range*	*skew*	*kurtosis*	*se*
Sand	50.59	3.54	50.59	50.59	3.71	48.09	53.10	5.01	0.00	-2.75	2.50
Silt	42.69	5.08	42.69	42.69	5.33	39.09	46.28	7.18	0.00	-2.75	3.59
Clay	6.72	1.54	6.72	6.72	1.62	5.63	7.81	2.18	0.00	-2.75	1.09
LOI	3.65	1.16	3.65	3.65	1.22	2.83	4.47	1.64	0.00	-2.75	0.82
C/N ratio	14.97	2.87	14.97	14.97	3.01	12.94	17.00	4.06	0.00	-2.75	2.03
pH-value	4.80	0.93	4.80	4.80	0.97	4.14	5.45	1.31	0.00	-2.75	0.66
Gravel	62.50	45.96	62.50	62.50	48.18	30.00	95.00	65.00	0.00	-2.75	32.50
Ca	1579	848	1579	1579	889	979	2179	1199	0.00	-2.75	599
K	15503	5420	15503	15503	5682	11670	19336	7666	0.00	-2.75	3833
Mg	1466	185	1466	1466	194	1335	1597	262	0.00	-2.75	131

Class 2	*mean*	*sd*	*median*	*trimmed*	*mad*	*min*	*max*	*range*	*skew*	*kurtosis*	*se*
Sand	58.10	2.60	58.76	58.10	1.32	54.40	60.49	6.10	-0.52	-1.79	1.30
Silt	35.07	5.17	33.25	35.07	2.02	31.15	42.65	11.50	0.65	-1.75	2.58
Clay	6.82	2.63	7.89	6.82	0.84	2.96	8.56	5.60	-0.67	-1.75	1.31
LOI	4.34	2.14	3.86	4.34	1.71	2.46	7.19	4.73	0.35	-2.03	1.07
C/N ratio	27.64	12.78	27.29	27.64	15.80	15.89	40.10	24.21	0.01	-2.41	6.39
pH-value	7.16	0.72	7.51	7.16	0.01	6.08	7.52	1.45	-0.75	-1.69	0.36
Gravel	82.50	10.41	82.50	82.50	11.12	70.00	95.00	25.00	0.00	-1.96	5.20
Ca	114388	10774	121909	114388	125670	3054	210679	207625	-0.04	-2.39	53870
K	13266	6176	10866	13266	2420	9065	22265	13200	0.63	-1.78	3088
Mg	5500	970	5762	5500	692	4182	6294	2112	-0.41	-1.98	485

Class 3	*mean*	*sd*	*median*	*trimmed*	*mad*	*min*	*max*	*range*	*skew*	*kurtosis*	*se*
Sand	36.13	12.42	40.52	37.33	6.98	9.70	48.09	38.39	-1.06	-0.34	3.32
Silt	51.19	10.58	46.91	50.11	6.75	41.36	74.00	32.64	1.06	-0.33	2.83
Clay	12.68	3.96	13.89	13.11	2.46	3.58	16.65	13.07	-1.21	0.19	1.06
LOI	4.93	0.92	5.17	5.00	0.96	3.16	5.86	2.69	-0.68	-0.94	0.25
C/N ratio	24.50	29.40	14.99	17.95	4.22	7.31	120.25	112.94	2.47	5.10	7.86
pH-value	6.76	1.00	7.32	6.84	0.44	4.86	7.75	2.89	-0.75	-1.20	0.27
Gravel	41.07	29.43	40.00	40.83	40.77	0.00	85.00	85.00	0.02	-1.67	7.87
Ca	63783	105352	10458	48794	12965	1628	305807	304178	1.46	0.46	28156
K	14525	5841	13610	14265	3130	5118	27061	21942	0.34	-0.44	1561
Mg	3391	1363	3191	3342	1420	1590	5785	4195	0.32	-1.20	364

Class 4	mean	sd	median	trimmed	mad	min	max	range	skew	kurtosis	se
Sand	34.70	17.84	37.74	34.70	4.16	1.61	55.71	54.11	-0.78	-0.70	7.28
Silt	49.82	10.98	46.99	49.82	3.70	40.38	71.30	30.91	1.11	-0.45	4.48
Clay	15.10	7.51	15.42	15.10	3.56	3.90	27.10	23.19	0.12	-1.09	3.07
LOI	5.34	1.07	5.18	5.34	0.89	3.84	6.98	3.14	0.17	-1.40	0.44
C/N ratio	13.21	3.75	13.37	13.21	3.32	7.58	18.34	10.76	-0.13	-1.52	1.53
pH-value	6.93	0.60	7.10	6.93	0.06	5.72	7.36	1.64	-1.27	-0.22	0.24
Gravel	38.33	24.22	45.00	38.33	22.24	5.00	70.00	65.00	-0.17	-1.75	9.89
Ca	13009	12194	7915	13009	4587	4281	36386	32105	1.05	-0.67	4978
K	13657	4585	13305	13657	711	7154	21513	14359	0.36	-0.89	1871
Mg	3774	1219	3494	3774	1299	2153	5326	3172	0.13	-1.79	497

Class 5	mean	sd	median	trimmed	mad	min	max	range	skew	kurtosis	se
Sand	30.91	18.19	39.22	31.88	12.99	2.51	48.60	46.09	-0.53	-1.62	5.04
Silt	52.44	15.04	44.56	51.43	8.71	37.05	78.85	41.81	0.62	-1.39	4.17
Clay	16.66	5.58	15.06	15.69	2.46	11.59	32.40	20.81	1.63	2.06	1.55
LOI	7.07	4.55	5.06	6.40	1.63	3.40	18.11	14.71	1.22	0.10	1.26
C/N ratio	24.25	18.86	16.33	20.89	7.40	10.59	74.86	64.27	1.51	1.24	5.23
pH-value	7.34	0.17	7.36	7.35	0.21	6.97	7.58	0.61	-0.55	-0.62	0.05
Gravel	49.62	23.49	50.00	49.09	29.65	20.00	85.00	65.00	0.07	-1.86	6.52
Ca	88555	76811	53666	83442	47694	13905	219448	205543	0.64	-1.36	21303
K	12600	3395	12140	13093	1975	3365	16413	13048	-1.29	1.49	941
Mg	9385	10442	4436	7365	1052	3365	37630	34265	1.63	1.38	2896

Class 6	mean	sd	median	trimmed	mad	min	max	range	skew	kurtosis	se
Sand	31.47	13.29	33.69	32.22	12.11	1.20	56.59	55.39	-0.48	-0.33	2.39
Silt	51.98	9.04	50.70	51.58	12.13	38.50	69.33	30.82	0.32	-1.10	1.62
Clay	16.43	6.12	15.49	16.15	4.60	3.96	34.39	30.43	0.62	0.96	1.10
LOI	6.17	1.40	5.97	6.06	1.37	4.10	10.45	6.35	0.87	0.76	0.25
C/N ratio	13.59	4.51	13.36	13.22	3.84	5.40	27.69	22.29	0.96	1.25	0.81
pH-value	7.11	0.75	7.36	7.30	0.22	4.33	7.64	3.31	-2.38	4.86	0.13
Gravel	41.71	28.62	40.00	41.40	44.48	0.00	90.00	90.00	0.12	-1.42	5.14
Ca	33320	28088	31124	29671	32127	1873	118411	116537	1.12	0.90	5044
K	14849	2884	14143	14783	2652	8544	21176	12632	0.26	-0.55	518
Mg	3900	1082	3833	3909	1106	1818	5746	3928	-0.048	-0.904	194

Class 7	mean	sd	median	trimmed	mad	min	max	range	skew	kurtosis	se
Sand	30.62	14.85	32.89	31.20	14.67	3.21	52.83	49.61	0.31	-0.86	3.32
Silt	51.53	10.71	51.85	51.94	11.70	28.75	70.55	41.80	0.32	-0.85	2.39
Clay	17.77	7.32	14.90	17.08	6.20	9.73	32.10	22.38	0.71	-1.00	1.64
LOI	6.40	1.67	5.63	6.20	1.10	4.37	10.29	5.92	0.88	-0.43	0.37
C/N ratio	13.20	5.11	12.66	12.49	5.49	7.97	25.56	17.59	0.88	-0.26	1.14
pH-value	7.12	0.51	7.30	7.22	0.25	5.66	7.56	1.90	1.56	1.39	0.11
Gravel	38.50	30.78	25.00	36.25	25.95	5.00	90.00	85.00	0.37	-1.61	6.88
Ca	30311	28882	21493	26291	23003	2768	98531	95762	0.91	-0.45	6458
K	14633	3404	13866	14301	3843	10611	21315	10703	0.56	-0.91	761
Mg	4565	1264	4488	4594	1436	2112	7077	4965	0.12	-0.78	282

Class 8	mean	sd	median	trimmed	mad	min	max	range	skew	kurtosis	se
Sand	20.16	10.25	22.32	20.23	11.85	1.76	43.64	41.88	0.04	-0.85	1.87
Silt	60.23	8.24	60.15	59.80	8.76	43.29	79.83	36.54	0.33	-0.05	1.51
Clay	19.61	6.65	18.91	19.35	4.73	7.63	34.88	27.25	0.39	-0.22	1.21
LOI	7.42	5.18	5.94	6.35	1.96	4.13	31.89	27.75	3.57	13.80	0.95
C/N ratio	14.81	7.27	12.97	13.88	3.50	0.00	32.97	32.97	0.99	0.95	1.33
pH-value	7.33	0.28	7.38	7.37	0.15	6.03	7.65	1.62	3.41	13.52	0.05
Gravel	24.23	30.85	8.50	19.88	12.60	0.00	90.00	90.00	1.11	-0.48	5.63
Ca	57887	41441	52990	55609	52499	4256	132195	127939	0.37	-1.20	7566
K	14445	3223	13888	14137	2995	9155	21883	12728	0.73	-0.15	588
Mg	5668	3803	5004	5062	2261	1549	22347	20797	2.79	9.63	694

Class 9	mean	sd	median	trimmed	mad	min	max	range	skew	kurtosis	se
Sand	18.80	8.17	18.96	18.76	10.53	4.80	33.32	28.52	0.12	-1.06	1.54
Silt	59.96	6.68	60.20	59.62	5.53	48.03	76.51	28.49	0.47	-0.04	1.26
Clay	21.24	5.23	20.41	21.07	5.01	11.11	34.52	23.41	0.44	-0.22	0.99
LOI	7.50	1.94	6.98	7.34	0.82	4.50	14.33	9.83	1.46	3.22	0.37
C/N ratio	14.67	7.83	11.90	13.42	3.16	6.75	38.08	31.33	1.79	2.17	1.48
pH-value	7.30	0.20	7.39	7.32	0.10	6.75	7.59	0.84	1.15	0.40	0.04
Gravel	32.46	31.92	15.00	30.79	19.27	0.00	90.00	90.00	0.52	-1.54	6.03
Ca	65193	42623	64815	64292	57461	4063	141374	137311	0.19	-1.18	8055
K	15305	4162	14376	15001	4348	9014	25655	16641	0.70	0.01	786
Mg	7093	4678	5322	6498	1617	2128	18833	16705	1.42	0.69	884

Eidesstattliche Erklärung

Hiermit erkläre ich, dass ich die von mir angefertigte Dissertation selbstständig verfasst wurde und abgesehen von der Beratung durch meinen Betreuer keine anderen als die angegebenen Hilfsmittel und Quellen benutzt habe. Die vorliegende Dissertation wurde nicht und auch nicht zum Teil an einer anderen Fakultät oder Universität im Rahmen eines Prüfungsverfahrens vorgelegt, veröffentlicht oder zur Veröffentlichung eingereicht. Die Dissertation wurde unter Einhaltung der Regeln guter wissenschaftlicher Praxis der Deutschen Forschungsgemeinschaft erstellt. Es wurde kein akademischer Grad je entzogen.

Kiel, den

Thomas Birndorfer